

Imperial College of Science, Technology and Medicine
Department of Physics

Causal Structure and Quantum Gravity

Ian Jubb

Supervised by
Prof. H. F. Dowker

Submitted in part fulfilment of the requirements for the degree of
Doctor of Philosophy in Physics of Imperial College London and
the Diploma of Imperial College, December 2, 2017

Abstract

In this thesis we will investigate the problem of quantum gravity from a variety of directions. Each avenue we explore begins at the quantum gravity path integral, and throughout our investigations the notion of spacetime causal structure will frequently appear.

After a brief introduction to the path integral for quantum gravity we will present several of the concepts behind Causal Set Theory — an approach to quantum gravity in which the continuum spacetime is replaced by a discrete structure.

We will then familiarise ourselves with the gravitational action that appears in the path integral, and its necessary boundary terms, in preparation for our discussion of the analogous quantities in Causal Set Theory. In particular, we will focus on the boundary terms in the causal set action and propose causal set expressions for the case of a spacelike boundary. We will then formulate causal set expressions to encode other boundary geometry, and conclude our discussion of the causal set action by investigating what boundary terms, if any, are present in the current proposal for the bulk causal set action.

Finally, we will return to the continuum quantum gravity path integral and explore whether the sum over spacetimes should include spacetimes which exhibit spatial topology change. To attempt to answer this question we will focus our attention on the simple case of the trousers spacetime, and use the Sorkin-Johnston formalism to study a scalar quantum field theory living on the spacetime.

Contents

Abstract	1
Contents	3
List of Figures	6
Copyright Declaration	9
Declaration of Originality	10
Acknowledgements	12
1 Introduction	13
1.1 Causal Set Theory	15
2 Boundary Terms in the Gravitational Action	17
2.1 Introduction	17
2.2 Mathematical Preliminaries	19
2.2.1 Boundary Geometry	19
2.2.2 Joint Signatures	21
2.2.3 Introduction to Tetrads	22
2.3 The Tetrad Formalism	24
2.3.1 The Einstein-Hilbert Action	24
2.3.2 Varying the Action	26
2.3.3 The Boundary Term	28
2.3.4 Gauge Transformation of the Boundary Term	31
2.3.5 Corner Terms	32
2.3.6 Creases	38

2.4	Summary	38
3	Boundary Terms and Related Geometry in Causal Set Theory	42
3.1	Introduction	42
3.2	Volume of a Small Causal Cone	44
3.2.1	The Setup	44
3.2.2	Leading Order Correction to Small Volume	45
3.2.3	Definitions for Higher Order Terms	50
3.2.4	All Possible Contributions	51
3.2.5	Intrinsic Curvature Terms	54
3.2.6	Extrinsic Curvature Terms	55
3.3	Use In Causal Set Theory	57
3.3.1	The Mean of \mathbf{P}_k and \mathbf{F}_k	57
3.3.2	Use of the Cone Volume Expansion	60
3.4	Causal Set Expressions	62
3.4.1	The Boundary Terms	62
3.4.2	The Surface Volume Family	65
3.4.3	Higher Order Causal Set Expressions	66
3.4.4	Finite ρ and Fluctuations	69
3.4.5	Normal Derivatives of a Scalar Field	72
3.5	The Causal Set Action for a Flat Alexandrov Interval	77
3.6	Summary	83
4	Topology Change in Quantum Gravity	85
4.1	Introduction	85
4.2	Background and Setup	87
4.2.1	The SJ Formalism	87
4.2.2	The Trousers Spacetime	89
4.2.3	The Pair of Diamonds	90
4.2.4	Isometries of the Pair of Diamonds	93
4.3	Green Functions	94
4.3.1	1 + 1 dimensional Minkowski	94

4.3.2	The Pair of Diamonds	96
4.3.3	A One-Parameter Family of Green Functions	98
4.4	Eigenfunctions of the Pauli-Jordan Operator	100
4.4.1	The Norm of the Pauli-Jordan Function	101
4.4.2	Isometries and the Pauli-Jordan Function	102
4.4.3	“Copy” Eigenfunctions	102
4.4.4	The Other Eigenfunctions	103
4.4.5	$p = \frac{1}{2}$	104
4.4.6	$p \neq \frac{1}{2}$	106
4.5	Energy momentum in the SJ State	108
4.5.1	$p = \frac{1}{2}$	110
4.5.2	$p \neq \frac{1}{2}$	111
4.6	From the Pair of Diamonds to the Infinite Trousers	111
4.6.1	The Discontinuous Modes in the Infinite Trousers	112
4.6.2	Wightman function	113
4.6.3	Energy Density in the SJ State in the Infinite Trousers	113
4.7	Propagation and Nonunitarity	115
4.7.1	Propagation	115
4.7.2	Nonunitarity	117
4.8	Summary	119
5	Conclusions and Future Directions	122
	Bibliography	126
A		133
A.1	Zero Eigenvalue Eigenfunctions Are Not Solutions	133
A.2	Sum of Squares of Eigenvalues	134
A.2.1	$p \neq \frac{1}{2}$	134
A.2.2	$p = \frac{1}{2}$	136

List of Figures

- 2.1 An illustration of how the normal covectors and normal vectors would be orientated on a patch of $1+1$ Minkowski spacetime whose boundary is a circle. We have also included the transverse covector/vector, l_a/l^a , for when the normal is null. We also note that we are visualising both the covectors and vectors with arrows, and that the arrows only illustrate the direction, not the magnitude. 20
- 2.2 An illustration (in 3D spacetime) of a join \mathcal{J}_{ij} between a spacelike boundary component Σ_i and a timelike component Σ_j . The two adapted tetrad 1-forms, $e_{(i)}^\mu$ and $e_{(j)}^\mu$, are also shown, and one can see that $e_{(i)}^{0'}/e_{(j)}^{1'}$ is the normal on Σ_i/Σ_j . The diagram also illustrates how we can choose our tetrads such that $e_{(i)}^{2'} = e_{(j)}^{2'}$ on \mathcal{J}_{ij} , and choose $e_{(i)}^{1'}$ to be outward pointing with respect to Σ_i when evaluated on the join. Σ_δ is the region on $\Sigma_i \cup \Sigma_j$ between the dotted lines, and $\Sigma_{i,\delta}/\Sigma_{j,\delta}$ is the region of Σ_i/Σ_j outside of Σ_δ . Again we note that we have used arrows to visualise the covectors. 34
- 3.1 A illustration of a causal cone in 3 dimensions of spacetime. 45
- 3.2 A 3-dimensional representation of the region \mathcal{X}_q in RNCs. The hat, T_q , of $\partial\mathcal{X}_q$ can be approximated as a flat cone, and the base, B_q , intersects T_q at a radial coordinate, $r_{max}(\phi)$, which will in general be a function of the angles ϕ (in 3 dimensions there is one angle ϕ). This function is found by projecting down from the intersection to the \bar{t} plane. . . 48

- 3.3 An illustration of a sprinkling into a spacetime partitioned by a spacelike hypersurface. Black points correspond to causal set elements and links (irreducible causal relations) between elements are shown as thin black lines. The maximal (\mathcal{F}_0) elements in \mathcal{C}^- and the minimal (\mathcal{P}_0) elements in \mathcal{C}^+ have been highlighted with white filling. The shaded areas illustrate the regions whose volumes are V_{\blacktriangle} and V_{\blacktriangledown} . In this sketch $P_0[\mathcal{C}^+] = 11$ and $F_0[\mathcal{C}^-] = 5$ (with time flowing upwards). 58
- 3.4 A plot of the standard deviation in samples of 100 of $\mathbf{S}_0^{(d)}$ for a flat ($K = 0$) surface bisecting a $d = 2, 3$ and 4-dimensional unit cube in Minkowski space for different values of $N = \rho$. Black dots, blue triangles and red squares correspond to the simulation results in $d = 2, 3$ and 4 dimensions, respectively. The corresponding black, blue and red lines have gradients $\frac{1}{4}$, 0 and $-\frac{1}{8}$ and best-fit intercepts of order 1. 70
- 3.5 Base-2 log-log plot of the standard deviation of \mathbf{I}_a against $\langle \mathbf{N} \rangle$. In the graph these quantities have been denoted by σ and N respectively. From top to bottom the data and the corresponding best fit lines are for dimensions $d = 3, 4, 5$ and 6 respectively. 72
- 3.6 The Alexandrov interval $I(p, q)$. The boundary consists of the null sections B^\pm and the spatial sphere S^{d-2} at their joint. 78
- 4.1 The trousers spacetime is shown on the left. The flat two-dimensional representation of the trousers on the right is obtained by cutting along the dotted lines and unwrapping the trousers on the left. The arrows indicate the respective identifications in the trunk and in the left and right legs. The crosses are identified and mark the location of x_c , the singularity. The dashed lines on the right form the boundary of a neighbourhood of x_c which we call the pair of diamonds. 89

- 4.2 The pair of diamonds in more detail. Diamond A is on the left and diamond B is on the right. The arrows in regions 1 and 5 indicate the topological identifications inherited from the trousers. The dashed lines are the past and future lightcones from the singularity. 91
- 4.3 The pair of diamonds on the trousers. The numbers illustrate the different regions of the pair of diamonds. 91
- 4.4 The pair of diamonds on the trousers, as “viewed from above”. The numbers correspond to the same 8 regions as before. The arrows represent the direction of time in each region. Isometry \mathfrak{P} is reflection in the dotted horizontal line, labelled P . Isometry \mathfrak{T} is reflection about the dotted line at 45° to the horizontal, labelled T 93
- 4.5 A causal interval or causal diamond not containing the singularity. . . 97
- 4.6 Example of a double diamond containing the singularity. 97
- 4.7 The Minkowski retarded Green function $G_{\text{Mink}}(x, y) = -\frac{1}{2}\chi_{>}(x, y)$ in the pair of diamonds, drawn as a function of y for fixed x where x is in the causal future of the singularity. The dashed contour corresponds to the boundary of a double diamond, DD , centred on the singularity. 98
- 4.8 An ansatz for the retarded Green function $G(x, y)$ for fixed $x \in R_1$. If $\beta_1 + \beta_2 = 1$, then $\mathfrak{E}_y^{DD}G(x, y) = 0$ for any double diamond, DD , around the singularity. 99
- 4.9 The retarded Green function $G_p(x, y)$ for fixed y in R_3 as a function of x 100
- 4.10 The Pauli-Jordan function $\Delta_p(x, y)$ in the pair of diamonds as a function of y , with the first argument x fixed in the causal future of the singularity. Here $q = 1 - p$ 101
- 4.11 The $\hat{f}_k^{(\frac{1}{2})}$ mode for the lowest k satisfying (4.40). On the top we have plotted the absolute value of the mode across the pair of diamonds. In the middle we have plotted its real part, and at the bottom its imaginary part. The discontinuity across the line of $X = 0$ for $T > 0$ is not a discontinuity in the mode. It is simply a consequence of how we have set up the identifications on the pair of diamonds. 105

4.12	Illustration of the $\Gamma_0(x)$ function. The function is zero in the white regions.	117
4.13	Illustration of the $\Gamma(x)$ function. The function is zero in the white regions.	118
4.14	The double diamond for equation (4.73).	119
4.15	The double diamond for equation (4.74).	120

Copyright Declaration

The copyright of this thesis rests with the author and is made available under a Creative Commons Attribution Non-Commercial No Derivatives licence. Researchers are free to copy, distribute or transmit the thesis on the condition that they attribute it, that they do not use it for commercial purposes and that they do not alter, transform or build upon it. For any reuse or redistribution, researchers must make clear to others the licence terms of this work.

Declaration of Originality

I declare that this work is entirely my own, except where otherwise stated. Most of the work in Chapters 2, 3, and 4 has been published in [1], ([2, 3]), and [4] respectively.

Ian Jubb

December 2, 2017

Acknowledgements

For teaching me so much about physics over the last four years (and politics too) I would like to thank my supervisor, Fay Dowker. Through the high standards you set for yourself and those you work with, and your unending passion for understanding, you have inspired me to new heights as a physicist. You have been the perfect mentor, a good friend, and it has been a pleasure to do physics with you.

For the many wonderful and insightful discussions I would like to thank Rafael Sorkin, Sumati Surya, and all those involved in Causal Set Theory. I am honoured to have worked alongside such kind-hearted and welcoming people.

I would also like to thank Michel Buck, for being a great research colleague over the past four years, and for all the laughs we've had along the way (albeit at effectively the same joke).

Thank you so much to all of my friends in the Theory Group (current and past members). Thank you for listening and engaging with me every time I asked questions blindly into the office air, and thank you for your insightful responses to those questions, your help throughout has been invaluable. And thank you most of all for all the laughter and joy you've given me. You've honestly made this Ph.D the best time of my life, and I love you all.

Thank you to Laura Sumner. You were around all the way back in undergrad when I realised this physics-thing was going to be an important part of my life, and I thank you for enduring your fair share of one-sided discussions. Thank you for being with me for all those years, and making me feel like I could do anything.

To my family, my parents Pamela and Dave, you have always believed in me, and supported me in whatever I've done. I cannot thank you enough for the aeons of time spent driving me to squash training whilst I hurriedly tried to finish homework in the car, or for the maths discussions that sparked my interests more than a decade ago (even to this day we're still discussing maths!). Thank you for making all this possible, I could not have done it without you.

Lastly, with all that I have, I would like to thank Carrie. You've stuck with me through all the tough times in the last two years and been so understanding and supportive through it all, and I really don't know what I've done to deserve you. You've injected so much happiness into each day I've spent with you, and you've never failed to encourage one of my physics rants. You are, without question, the light that has reignited my life. I love you.

Chapter 1

Introduction

Our current understanding of the physical world rests on two great pillars of theoretical physics: Einstein's theory that gravity is a consequence of spacetime curvature (General Relativity), and the quantum theory of matter (Quantum Field Theory). Despite their tremendous successes in their respective regimes, they resist a peaceful merger when we consider extremely high energy densities, e.g. the Planck mass in a region of diameter roughly equal to the Planck length. Such situations arise inside black holes, or far enough back in time towards the Big Bang. It is this incompatibility that has motivated a nearly century long search for a consistent theory that can describe gravity in a quantum regime. We call this hypothetical theory *Quantum Gravity*.

The quest for quantum gravity has seen many proposals attempt to solve the problem, but the lack of experimental evidence has made it extremely difficult to verify a given theory. Moreover, the proposed theories themselves have not yet been fully understood even in a theoretical sense. One might think that quantising gravity is simply a matter of writing down a quantum gravity path integral, that mirrors the quantisation of matter:

$$Z_g = \int \mathcal{D}g_{\mu\nu} e^{iS[g_{\mu\nu}]}, \quad (1.1)$$

where the integral symbolically represents a sum over different spacetimes, and $S[g_{\mu\nu}]$ is the classical action for a given spacetime. The integral in (1.1) turns out to be extremely complicated, both technically and conceptually. There is still no consensus on what exactly the sum over spacetimes should include, an issue we will return to later. Solving the problem of quantum gravity may require more than just evaluating this integral; we may have to make creative leaps from our current foundations to an entirely new conception of the physical world ((1.1) may still be

relevant at an effective level in this new theory). In formulating a new theory of quantum gravity one must decide which fundamental principles are to be retained, and which should be cast aside. This is not straightforward, and there are many conflicting ideas, as can be seen by attempted resolutions of Hawking's black hole information paradox [5–7].

Causal Set Theory attempts to solve the problem of quantum gravity, while retaining certain principles from General Relativity and quantum theory, namely the causal structure and the path integral respectively. The theory hypothesises that spacetime is fundamentally discrete at the Planck scale, and this discreteness, married with causal order, results in the proposal that the fundamental structure of spacetime is a *causal set* (to be defined shortly). The quantum dynamics is then described by a path integral over causal sets:

$$Z_{\mathcal{C}} = \sum_{\mathcal{c}} e^{iS[\mathcal{c}]} , \quad (1.2)$$

where the discreteness has turned the usual integral into a well defined sum over causal sets, and where $S[\mathcal{C}]$ is the action of the causal set \mathcal{C} ¹.

There are still open questions surrounding (1.2), and one that we will investigate in this thesis is *what is the causal set action $S[\mathcal{C}]$* ? One requirement we would like to impose on the causal set action is that it reproduces the action of a continuum spacetime in an appropriate limit. The continuum action will be introduced in Chapter 2 and we will derive its associated boundary terms, which are a necessary addition to the action in order to obtain a consistent variational principle. In Chapter 3 we will then propose a causal set counterpart to the boundary terms of the continuum action, and investigate what boundary terms, if any, are present in the recently proposed bulk causal set action in [9–11]. In Chapter 4 we will return to the continuum path integral, (1.1), and investigate the open question of what the sum over spacetimes in (1.1) actually includes. More specifically, we will investigate whether the sum should include spacetimes that undergo spatial topology change. An example of this would be a spacetime in which two black holes are pair produced. Causal structure will again play an important role, and we shall see that it helps us extend the framework of curved spacetime Quantum Field Theory to include spacetimes that exhibit topology change².

¹Within Causal Set Theory there exists another approach to causal set dynamics that envisages the causal set as a growing network [8]. This approach does not, at present, involve a path integral such as (1.2).

²It should be noted that there are a few differences in conventions between the chapters, but this should not be a cause for concern since the chapters themselves are sufficiently self-contained.

Before confronting these questions regarding spacetime causal structure and its place in quantum gravity, let us first introduce the main concepts behind Causal Set Theory.

1.1 Causal Set Theory

The discreteness of Causal Set Theory is motivated by the somewhat troubling infinities that arise when describing physics on a continuum background. The first, and least troubling, infinity is encountered in Quantum Field Theory, and is usually dealt with via renormalisation, although this is not always possible. The second infinity arises in General Relativity, at singularities where the curvature of spacetime blows up. The third and final infinity occurs when considering black hole entropy. Specifically, we obtain an infinite result for the entropy of a black hole when trying to enumerate the degrees of freedom of the horizon [12].

These infinities all occur around the Planck length, and hence we might hope to resolve them using a fundamental cut-off around that scale. The continuum manifold would then be replaced by a “discrete manifold”, and in 1854 Riemann had already noted that such a discrete manifold could contain its own metric relations, in contrast to a continuum manifold that must be supplemented with a metric. The volume of any region of this discrete manifold is then determined by simply counting the discrete elements that make it up.

A causal set is a particular discrete structure with an order relation that mirrors the causal order (or structure) of a continuum spacetime. The motivation for the link between this order relation and causal order derives from results by Malament, Levichev, and Hawking *et al* [13–15] that together show that one can recover the metric up to a conformal (or volume) factor from the causal structure alone³. Since a causal set is a discrete structure it contains its own volume information, and so together with the order relation one might expect it to encode *all* the geometric information about a spacetime, on scales much larger than the discreteness scale.

All of the above has led to a causal set being defined as a locally finite partial order. Specifically, a causal set is a pair (\mathcal{C}, \preceq) , where \mathcal{C} is a set, and $\forall x, y, z \in \mathcal{C}$, \preceq is an order relation that is

1. Reflexive: $x \preceq x$
2. Acyclic: $x \preceq y \preceq x \Rightarrow x = y$

³Technically speaking, when the spacetime is *distinguishing* [16], the causal structure allows one to determine the differential structure, the topology, and the metric up to a conformal factor.

3. Transitive: $x \preceq y \preceq z \Rightarrow x \preceq z$
4. Locally finite: $|I(x, y)| < \infty$

where $|I(x, y)|$ is the cardinality of the interval $I(x, y) = \{z \mid z \in \mathcal{C}, x \preceq z \preceq y\}$. The first three conditions resemble the requirements of a causal order on a continuum spacetime (provided we are discussing spacetimes that do not contain closed timelike curves for which the acyclic condition fails), while the final condition encodes the discreteness of the causal set, since an interval in a continuum spacetime would contain an uncountably infinite number of points. A causal set can be represented by a directed graph, where the vertices are the elements of the causal set, and the directed edges represent the causal relations.

We now turn to the question of how to relate a given causal set to a spacetime, and vice versa. This is done via a *sprinkling*, which is a random process for generating a causal set from a given spacetime. In a sprinkling the elements of the causal set are generated using a Poisson process to select points from the spacetime manifold at some density, ρ , such that the expected number of points in a spacetime region of volume V is given by ρV . The selected points are said to be “sprinkled” into the manifold, and the probability of sprinkling k points into a spacetime region of volume V is

$$\mathbb{P}(k \text{ points in region of volume } V) = \frac{(\rho V)^k}{k!} e^{-\rho V}. \quad (1.3)$$

The order relations amongst the elements of the causal set are then induced from their causal order within the continuum spacetime⁴. The correspondence between causal sets and spacetimes is then as follows: a causal set, \mathcal{C} , is well approximated by a spacetime, \mathcal{M} , if \mathcal{C} is generated, with relatively high probability, by sprinkling into \mathcal{M} .

We will return to causal sets in Chapter 3 where we will discuss proposals for the action of a causal set, but before then let us first introduce the continuum action and its boundary terms.

⁴It should be noted that the process of sprinkling is purely kinematical, and is unrelated to any dynamical processes that generate causal sets, such as *sequential growth models* [8].

Chapter 2

Boundary Terms in the Gravitational Action

2.1 Introduction

The action of a spacetime in the continuum is usually taken to be the Einstein-Hilbert (EH) action. This action depends on the metric and its first and second derivatives. Indeed, the dependence on second derivatives is forced on us by the principle of general covariance, since there is no local coordinate scalar that can be formed from the metric and its first derivatives.

While the EH Lagrangian does depend on the second derivatives of the metric, the dependence is rather innocuous since, as it turns out, the equations of motion are second order in metric derivatives, rather than fourth order, as one might naively expect. One can remove the dependence on second derivatives by adding a total divergence to the EH Lagrangian, which integrates to a boundary term. The appropriate action for general relativity is therefore the EH action with this boundary term. This makes the action first order in the metric derivatives: the second derivative term $\partial\partial g$ present in the Einstein Hilbert Lagrangian is replaced by a term of the form $(\partial g)^2$. All of this has been known for a while [17, 18].

The action principle for General Relativity is important when we consider the path integral approach to quantum gravity. In summing over histories, we would like the quantum amplitudes to have the “folding” property, which we write symbolically as:

$$K(X_1, X_3) = \int dX_2 K(X_1, X_2) K(X_2, X_3), \quad (2.1)$$

where X_1 and X_3 are initial and final states respectively and X_2 is an intermediate state which is summed over. In the metric representation X_1, X_3 represent the metrics

on an initial and final spatial hypersurface $\Sigma_{1,3}$ and (Σ_2, X_2) , an intermediate spatial geometry. We would clearly like the action to be additive under a decomposition of spacetime into pieces. There is a close relation between additivity of the action and having a first order Lagrangian. This can be clearly seen in a particle mechanics analogy. Consider the amplitude for a particle to go from x_0 at time t_0 to x_N at time $T = t_N$, $K(x_0, t_0; x_N, T)$. Introducing time slices at $t_k = k\epsilon = kT/N$, we have the skeletonised version of the path integral

$$K(x_0, t_0; x_N, T) = \int dx_1 \dots dx_{N-1} K(x_0, t_0; x_1, t_1) \dots K(x_{N-1}, t_{N-1}; x_N, T), \quad (2.2)$$

If the Lagrangian is first order, i.e. if L depends only on x and \dot{x} , the additivity of the action is immediate. One writes the short time propagator replacing \dot{x} in the Lagrangian by $(x_{k+1} - x_k)/\epsilon$. This results in nearest neighbour couplings on the time lattice with the sites labelled by k . Decomposing the lattice into two parts separated by t_j gives us the folding property Eqn (2.1). However, for a second order Lagrangian $L(x, \dot{x}, \ddot{x})$, one needs *three* time steps in order to define \ddot{x} . E.g $\ddot{x}_k = (x_{k+1} + x_{k-1} - 2x_k)/\epsilon^2$. This brings in *next* nearest neighbour couplings on the time lattice, which spoils the additivity of the action.

A related point stems from the tensor nature of the gravitational field, which is not captured in the simple particle analogy above. In summing over histories that go from X_1 to X_3 via X_2 we allow all spacetime geometries, which on pullback agree with X_2 . No further restriction needs to be placed on the metric. In particular, the components of the metric in directions transverse to the spacelike surfaces need not be held fixed. Textbook treatments (see [19, 20] for example) however hold *all* components of the metric fixed on the boundary, which is a stronger requirement. In a path integral, one typically sums over all paths without requiring continuity of all components of the metric across Σ_2 . All we need is that the pullback of the four-metric to Σ_2 agrees with X_2 .

Another reason for investigating the action principle is to explore boundaries of different signatures. A region in spacetime may have boundaries with components which are spacelike, timelike and null. There may also be corners where components of the boundary join. We present a formalism in which all these cases are derived in a transparent manner. The role of boundaries in gravitational physics has been increasing in recent years. Ideas relating bulk and boundary degrees of freedom have been discussed in the context of black hole entropy, and hence one of the possible applications of this work is in black hole physics.

The need for adding a total divergence to the Einstein-Hilbert action was re-

alised very early in the history of General Relativity[21]. The required boundary counterterm was given a geometric interpretation by York[17] and this line of thought was carried further by Gibbons and Hawking in their work on black hole thermodynamics. When the boundary has corners, there is a need for additional corner terms. These were first discussed by Sorkin and Hartle [22, 23], and subsequently by Hayward[24], Brill and Hayward[25] for timelike and spacelike boundaries. The need for a treatment of null boundaries was recognised by Parattu et al [26, 27]. There are also several contributions by Neiman[28–31] and Epp[32]. Very recently Lehner et al [33] have given a detailed account of this problem. The work in this chapter will differ from these in a few respects. We postpone a discussion of the differences to the concluding section.

Our treatment uses the tetrad formulation to give us a unified approach to the different boundary signatures. If one has a good understanding of the tetrad formalism of General Relativity then this simplifies the calculation of the boundary terms considerably. In Section 2.2 we review some of the mathematical preliminaries. In Section 2.3 we present the tetrad formulation, which brings out the need for the corner terms and their explicit forms. Section 2.4 contains a discussion and some open questions.

2.2 Mathematical Preliminaries

Let the orientable spacetime manifold (\mathcal{M}, g_{ab}) be described by a Lorentzian metric g_{ab} of signature $(-+++)$, and take x^a to be coordinates on the spacetime, with the spacetime index $a = 0, 1, 2, 3$. We begin with the Einstein-Hilbert action

$$S_{EH} = \frac{1}{2} \int_{\mathcal{M}} d^4x \sqrt{-g} R \quad (2.3)$$

for a spacetime (\mathcal{M}, g_{ab}) , where the boundary of the manifold, $\partial\mathcal{M} = \cup_i \Sigma_i$, can have several piecewise C^2 components Σ_i whose normal covectors $n_{i\ a}$ are everywhere either timelike, spacelike or null. We have chosen units in which $8\pi G$ has been set to 1.

2.2.1 Boundary Geometry

Consider a single component of the boundary $\Sigma \subset \partial\mathcal{M}$. We define the normal covector, n_a , using a function $S(x)$ that increases going from the inside to the

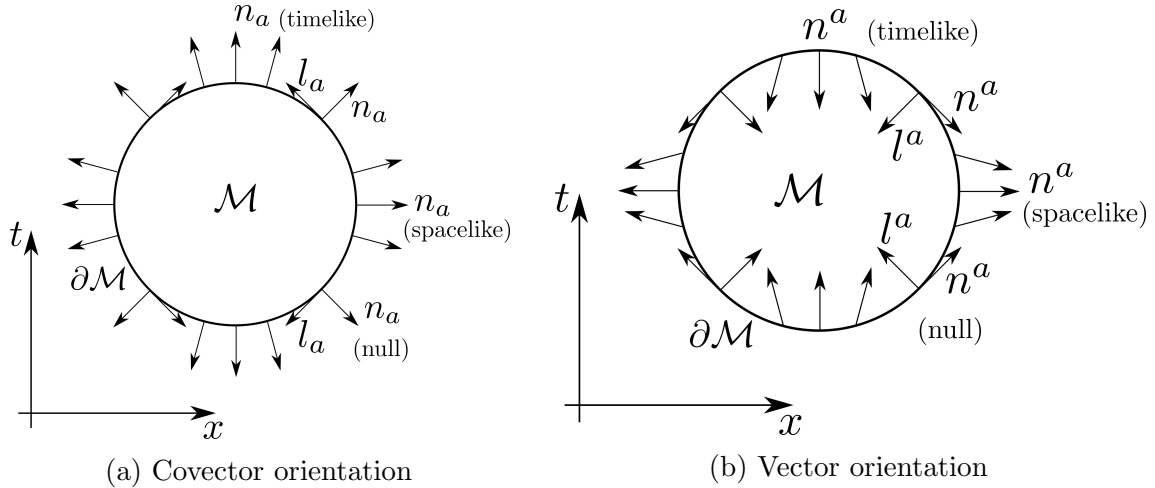


Figure 2.1: An illustration of how the normal covectors and normal vectors would be orientated on a patch of 1 + 1 Minkowski spacetime whose boundary is a circle. We have also included the transverse covector/vector, l_a/l^a , for when the normal is null. We also note that we are visualising both the covectors and vectors with arrows, and that the arrows only illustrate the direction, not the magnitude.

outside of \mathcal{M} (when \mathcal{M} is embedded in some larger spacetime), and that satisfies $S(x)|_{x \in \Sigma} = 0$. The normal covector is then defined as

$$\begin{aligned} n_a &= (\epsilon g^{bc} \partial_b S \partial_c S)^{-1/2} \partial_a S && \text{(Non - Null)} \\ n_a &= \partial_a S && \text{(Null)}. \end{aligned} \quad (2.4)$$

When Σ is non-null, the unit normal n_a satisfies $n^a n_a = \epsilon$ where $\epsilon \equiv \pm 1$ depending on whether Σ is timelike or spacelike respectively. When Σ is null, n_a is null ($n^a n_a = 0$). The normal in this case is not unique, as we could always scale it by some factor, and for each n_a there is an equivalence class of null vectors l^a which satisfy $n_a l^a = -1$. See Figure 2.1 to better understand how these vectors and covectors are orientated for different components of the boundary. We define the transverse parts of the metric in the non-null and null cases as

$$\begin{aligned} h_{ab} &= g_{ab} - \epsilon n_a n_b && \text{(Non - Null)} \\ \sigma_{ab} &= g_{ab} + l_a n_b + n_a l_b && \text{(Null)} \end{aligned} \quad (2.5)$$

The transverse parts satisfy $h_{ab} n^b = 0$, and $\sigma_{ab} n^b = \sigma_{ab} l^b = 0$.

For a non-null Σ with coordinates y^i , where $i = 1, 2, 3$, the induced metric is defined as

$$h_{ij} = g_{ab} \frac{\partial x^a}{\partial y^i} \frac{\partial x^b}{\partial y^j}. \quad (2.6)$$

One can then show that $h^{ab} = h^{ij} \frac{\partial x^a}{\partial y^i} \frac{\partial x^b}{\partial y^j}$, where $h^{ab} = g^{ac} g^{bd} h_{cd}$ and h^{ij} is the inverse of h_{ij} .

When Σ is null we find that the surface is ruled by the null geodesics generated by the null normal vector n^a . This normal vector can be written as $n^a = \frac{dx^a}{d\lambda}$, where λ is the parameter along the geodesic (this parameter is not necessarily affine). We take our coordinates on Σ to be $y^i = (\lambda, \theta^A)$, where $A = 2, 3$ and θ^A are spatial coordinates that label the different ruling null geodesics. The induced metric on the spatial sections of Σ is then defined as

$$\sigma_{AB} = g_{ab} \frac{\partial x^a}{\partial \theta^A} \frac{\partial x^b}{\partial \theta^B}. \quad (2.7)$$

Given some choice of coordinates θ^A we can pick a unique null vector l^a from the class of those satisfying $n_a l^a = -1$ by imposing that $l_a \frac{\partial x^a}{\partial \theta^A} = 0$. One can then show that $\sigma^{ab} = \sigma^{AB} \frac{\partial x^a}{\partial \theta^A} \frac{\partial x^b}{\partial \theta^B}$, where $\sigma^{ab} = g^{ac} g^{bd} \sigma_{cd}$ and σ^{AB} is the inverse of σ_{AB} .

2.2.2 Joint Signatures

The ‘‘joins’’ or intersections $\mathcal{J}_{ij} = \Sigma_i \cap \Sigma_j$ of $\partial\mathcal{M}$ are allowed to be discontinuous in the sense that n_i^a and n_j^a differ at \mathcal{J}_{ij} . The \mathcal{J}_{ij} are of codimension two and, like the boundary components, may also be timelike, spacelike or null.

To determine the signature of \mathcal{J}_{ij} , given the signatures of Σ_i and Σ_j , we can first pick a point $p \in \mathcal{J}_{ij}$. Any curve $\gamma \in \mathcal{J}_{ij}$ passing through p must have a tangent vector that is orthogonal to the vectors n_i and n_j at p . Thus, the signature of \mathcal{J}_{ij} is given by the signature of the part of the tangent space that is orthogonal to the span of n_i and n_j .

Using the letter S/T/N to denote spacelike/timelike/null, the six different possibilities for the two surfaces Σ_i and Σ_j are TT, TS, TN, SS, SN, NN. The corresponding normals are SS, ST, SN, TT, TN, NN. The signature of the plane spanned by n_i and n_j can be inferred from the determinant of the metric induced on this plane, which we denote by $g'_{IJ} := g_{ab} n_i^a n_j^b$, where $I, J = i$ or j . The determinant, $g' := \det(g'_{IJ})$, is positive/negative/zero when the plane is S/T/N. From the signature of the plane we can determine the signature of its orthogonal subspace, which is the signature of \mathcal{J}_{ij} . For any pair of normals n_i and n_j we have that $g' = n_i^2 n_j^2 - (n_i \cdot n_j)^2$, where $n_i^2 = g_{ab} n_i^a n_i^b$ and $n_i \cdot n_j = g_{ab} n_i^a n_j^b$. We will now go through each of the signature possibilities for Σ_i and Σ_j , and find the resulting signature of \mathcal{J}_{ij} :

TT: Normals are SS, so $n_i^2 = n_j^2 = 1$, and hence $g' = 1 - (n_i \cdot n_j)^2$.

If $(n_i \cdot n_j) > 1$, $g' < 0$, the plane of the normals is T, and \mathcal{J}_{ij} is S.

If $(n_i \cdot n_j) = 1$, $g' = 0$, the plane of the normals is N, and \mathcal{J}_{ij} is N.

If $(n_i \cdot n_j) < 1$, $g' > 0$, the plane of the normals is S, and \mathcal{J}_{ij} is T.

TS: Normals are ST, so $n_i^2 = -n_j^2 = 1$, and hence $g' = -(1 + (n_i \cdot n_j)^2)$. Therefore, $g' < 0$, and the plane of the normals is T, and \mathcal{J}_{ij} is S.

TN: Normals are SN, so $n_i^2 = 1$ and $n_j^2 = 0$, and hence $g' = -(n_i \cdot n_j)^2$.

If $(n_i \cdot n_j) = 0$, $g' = 0$, the plane of the normals is N, and \mathcal{J}_{ij} is N.

If $(n_i \cdot n_j) \neq 0$, $g' < 0$, the plane of the normals is T, and \mathcal{J}_{ij} is S.

SS: Normals are TT, so $n_i^2 = n_j^2 = -1$, and hence $g' = 1 - (n_i \cdot n_j)^2$. One can verify that $g' < 0$, and hence the plane of the normals is T, and \mathcal{J}_{ij} is S.

SN: Normals are TN, so $n_i^2 = -1$ and $n_j^2 = 0$, and hence $g' = -(n_i \cdot n_j)^2$. $n_i \cdot n_j$ cannot be zero, hence $g' < 0$, the plane of the normals is T, and \mathcal{J}_{ij} is S.

NN: Normals are NN, so $n_i^2 = n_j^2 = 0$, and hence $g' = -(n_i \cdot n_j)^2$. One can verify that $g' < 0$ ($g' = 0$ only if the normals are proportional to one another, which cannot happen), and hence the plane of the normals is T, and \mathcal{J}_{ij} is S.

2.2.3 Introduction to Tetrads

In Section 2.3 we use the Cartan tetrad formalism. This has the significant advantage offered by differential forms which can be integrated over manifolds without reference to a metric or its signature. It also has the advantage of giving us a fiducial Minkowski vector space as a reference. Given a metric g_{ab} on \mathcal{M} we choose an orthonormal frame such that $g_{ab} = e_a^\mu e_b^\nu \eta_{\mu\nu}$. The tetrad e_a^μ maps a vector $X \in T_p \mathcal{M}$ to a point in $(\mathcal{M}_0, \eta_{\mu\nu})$

$$e_a^\mu : X \rightarrow e^\mu(X) = e_a^\mu X^a = X^\mu \in \mathcal{M}_0, \quad (2.8)$$

where $(\mathcal{M}_0, \eta_{\mu\nu})$ is a fixed fiducial Minkowski vector space, with a the spacetime index and μ the frame index ranging over $0', 1', 2', 3'$ (the primes allow us to more easily distinguish whether a tetrad has the fixed spacetime/frame indices up or down, e.g. $e_1^{0'}$ has the frame/spacetime index up/down). The map Eqn (2.8) is invertible, since we assume that the metric is non-degenerate, and its inverse is given by $e_\mu^a = g^{ab} \eta_{\mu\nu} e_b^\nu$. Frame indices μ, ν are raised and lowered with $\eta_{\mu\nu}$. There is an $O(1, 3)$ gauge freedom in the choice of the e_a^μ . Associated with the e_a^μ are the connection 1-forms $A_a^{\mu\nu} = e_b^\mu \nabla_a e^{\nu b}$ where ∇_a is the metric compatible Christoffel

connection. $A^{\mu\nu}$ takes values in the Lie Algebra of $O(1,3)$ and is antisymmetric in the frame indices: $A^{\mu\nu} = -A^{\nu\mu}$. $A^{\mu\nu}$ is compatible with frames and satisfies Cartan's equation

$$de^\mu + A^\mu{}_\nu \wedge e^\nu = 0, \quad (2.9)$$

where d is the exterior derivative, and the wedge product, \wedge , is with respect to the spacetime indices. We can write this more succinctly by defining a covariant derivative, D_a , compatible with the Christoffel connection and $A_a^{\mu\nu}$. Some examples of the action of D_a are:

$$\begin{aligned} D_a e_b^\mu &= \partial_a e_b^\mu + A_{a\nu}^\mu e_b^\nu - \Gamma_{ab}^c e_c^\mu \\ D_a A_b^{\mu\nu} &= \partial_a A_b^{\mu\nu} + A_{a\rho}^\mu A_b^{\rho\nu} + A_{a\rho}^\nu A_b^{\mu\rho} - \Gamma_{ab}^c A_c^{\mu\nu} \\ D_a \eta_{\mu\nu} &= -A_{a\mu}^\rho \eta_{\rho\nu} - A_{a\nu}^\rho \eta_{\mu\rho} = 0, \end{aligned} \quad (2.10)$$

and it is straight forward to generalise its action to tensors with more frame and spacetime indices. In the last line we have used the asymmetry of $A^{\rho\lambda}$ to deduce that $D_a \eta_{\mu\nu} = 0$. We can use D_a to define an exterior derivative on a p -form $X^{\mu\dots\nu}$ (with some number of frame indices) as

$$DX^{\mu\dots\nu} = D_a X_{a_1\dots a_p}^{\mu\dots\nu} dx^a \wedge dx^{a_1} \wedge \dots \wedge dx^{a_p}. \quad (2.11)$$

D satisfies a graded product rule just as d does, and its action on a tensor with no frame indices is the same as the action of d . Finally, we can now rewrite (2.9) more compactly as $De^\mu = 0$.

Written explicitly in the spacetime indices, the 2-form field strength of $A^{\mu\nu}$ is

$$F_{ab}^{\mu\nu} = \partial_a A_b^{\mu\nu} - \partial_b A_a^{\mu\nu} + A_{a\rho}^\mu A_b^{\rho\nu} - A_{b\rho}^\nu A_a^{\mu\rho} = R_{abcd} e^{\mu c} e^{\nu d}, \quad (2.12)$$

where R_{abcd} is the usual Riemann tensor. This can be more succinctly expressed using form notation as $F^{\mu\nu} = dA^{\mu\nu} + A^\mu{}_\rho \wedge A^{\rho\nu}$.

2.3 The Tetrad Formalism

2.3.1 The Einstein-Hilbert Action

We will now show that the Einstein-Hilbert action can be written as

$$\frac{1}{4} \int_{\mathcal{M}} \varepsilon_{\mu\nu\rho\lambda} e^\mu \wedge e^\nu \wedge F^{\rho\lambda}, \quad (2.13)$$

where $\varepsilon_{\mu\nu\rho\sigma}$ is the Levi-Civita symbol. From now on, unless otherwise stated, we will use the ε symbol, followed by r spacetime or frame indices to stand for the r -dimensional Levi-Civita symbol. (2.13) is an integral over the 4-form $L = \frac{1}{4!} L_{abcd} dx^a \wedge dx^b \wedge dx^c \wedge dx^d = \varepsilon_{\mu\nu\rho\lambda} e^\mu \wedge e^\nu \wedge F^{\rho\lambda}$, and the integral of such a top form can be defined as

$$\int_{\mathcal{M}} L = \int_{\mathcal{M}} d^4x L_{0123}. \quad (2.14)$$

One finds that the component L_{0123} is

$$L_{0123} = \frac{4!}{2} e^\mu_{[0} e^\nu_{1} F_{34]}^{\rho\lambda} \varepsilon_{\mu\nu\rho\lambda} = \frac{1}{2} e^\mu_a e^\nu_b F_{cd}^{\rho\lambda} \varepsilon_{\mu\nu\rho\lambda} \varepsilon^{abcd}, \quad (2.15)$$

where the square brackets denote anti-symmetrisation of the enclosed indices. From the defining relation for the tetrads, $g_{ab} = e^\mu_a e^\nu_b \eta_{\mu\nu}$, one can see that $g := \det(g_{ab}) = -\det(e^\mu_a)^2$, and therefore that $e := \det(e^\mu_a) = \pm\sqrt{-g}$. The $+/-$ sign means the tetrad has the same/opposite orientation as the coordinate system. That is, there is a linear transformation between the tetrad and the coordinate vectors, ∂_a , which has positive/negative determinant. We can fix the tetrad to have the same orientation by taking the canonical volume form, $\Omega = \sqrt{-g} dx^0 \wedge dx^1 \wedge dx^2 \wedge dx^3$, and imposing that $\Omega = e^{0'} \wedge e^{1'} \wedge e^{2'} \wedge e^{3'}$. This then ensures that $e = \sqrt{-g}$.

The determinant of the tetrad can be written using the Levi-Civita symbol as

$$e \varepsilon_{abcd} = \varepsilon_{\mu\nu\rho\sigma} e^\mu_a e^\nu_b e^\rho_c e^\sigma_d, \quad (2.16)$$

from which we find that

$$\varepsilon_{\mu\nu\rho\sigma} e^\mu_a e^\nu_b = e \varepsilon_{abcd} e^c_\rho e^d_\sigma. \quad (2.17)$$

We can use this relation in (2.15) to find that

$$L_{0123} = \frac{e}{2} \varepsilon^{abcd} \varepsilon_{abef} e^e_\rho e^f_\lambda F_{cd}^{\rho\lambda}. \quad (2.18)$$

Using the relation $\varepsilon^{abcd} \varepsilon_{abef} = 4\delta^c_{[e} \delta^d_{f]}$ and the definition of $F_{cd}^{\rho\lambda}$ from (2.12) in terms

of the Riemann tensor we arrive at

$$L_{0123} = 2\sqrt{-g}R, \quad (2.19)$$

where R is the Ricci scalar. Thus, we have that

$$\frac{1}{4} \int_{\mathcal{M}} \varepsilon_{\mu\nu\rho\lambda} e^\mu \wedge e^\nu \wedge F^{\rho\lambda} = \frac{1}{2} \int_{\mathcal{M}} d^4x \sqrt{-g} R, \quad (2.20)$$

which is the same as S_{EH} above ¹.

The tetrad form of S_{EH} is invariant under local gauge transformations that preserve the orientation of the tetrad. That is, it is independent of our choice of tetrad, provided we maintain the same orientation. To see this, define a new tetrad $e'^{\mu'}_a = \Lambda^{\mu'}_\mu(x) e^\mu_a$, where $\Lambda^{\mu'}_\mu(x)$ is the local gauge, or Lorentz, transformation that leaves the frame metric unchanged. Under this transformation we get that $F'^{\mu'\nu'} = \Lambda^{\mu'}_\mu \Lambda^{\nu'}_\nu F^{\mu\nu}$, and hence

$$\varepsilon_{\mu'\nu'\rho'\lambda'} e'^{\mu'} \wedge e'^{\nu'} \wedge F'^{\rho'\lambda'} = \varepsilon_{\mu'\nu'\rho'\lambda'} \Lambda^{\mu'}_\mu \Lambda^{\nu'}_\nu \Lambda^{\rho'}_\rho \Lambda^{\lambda'}_\lambda e^\mu \wedge e^\nu \wedge F^{\rho\lambda} \quad (2.21)$$

The first part on the right can be rewritten as the determinant of $\Lambda^{\mu'}_\mu$ using the Levi-Civita symbol as

$$\det(\Lambda^{\mu'}_\mu) \varepsilon_{\mu\nu\rho\lambda} = \varepsilon_{\mu'\nu'\rho'\lambda'} \Lambda^{\mu'}_\mu \Lambda^{\nu'}_\nu \Lambda^{\rho'}_\rho \Lambda^{\lambda'}_\lambda, \quad (2.22)$$

but since we have preserved the tetrad orientation we have that $\det(\Lambda^{\mu'}_\mu) = 1$, and hence the form of S_{EH} is unchanged. If we had changed orientation then we would have that $\det(\Lambda^{\mu'}_\mu) = -1$, and hence we would have an additional minus sign in front of S_{EH} . This minus sign would then be cancelled by another minus sign that would appear in the relationship between the determinant of the tetrad and $\sqrt{-g}$. Thus, one would still obtain the original EH action. To avoid having to deal with these extra minus signs we will stick to tetrads of the same orientation.

When we take the variation of S_{EH} we will get a bulk term (which yields the equations of motion) and a boundary term. The boundary term will be expressed as the variation of a boundary action $-S_B$, which gives us a counterterm to be added to the action. The total gravitational action is therefore

$$S_G = S_{EH} + S_B \quad (2.23)$$

¹Note that we do not regard this tetrad formalism as a first order Palatini action, since $A_a^{\mu\nu}$ is a function of e_a^μ determined by Eqn (2.9) and is not independent.

where S_B in the non-null case is the usual Gibbons-Hawking-York (GHY) term. From its definition, the boundary term S_B is only defined up to terms that have zero variation. Certain imaginary terms that have been discussed before in the literature are of this variety. We will ignore them for the most part and comment on them in the conclusion. When the boundary is only piecewise C^2 the boundary contribution includes “corner” terms. We will now derive the various boundary contributions in the tetrad formalism.

2.3.2 Varying the Action

We will now vary the action S_{EH} with respect to the metric, and hold fixed the pullback of the metric to the boundary. The metric and the tetrad are related through $g_{ab} = e^\mu_a e^\nu_b \eta_{\mu\nu}$, and hence the variation of the metric induces a variation on the tetrad. Varying the tetrad form of the action S_{EH} we find

$$\delta S_{EH} = \frac{1}{4} \left(2 \int_{\mathcal{M}} \varepsilon_{\mu\nu\rho\lambda} \delta e^\mu \wedge e^\nu \wedge F^{\rho\lambda} + \int_{\mathcal{M}} \varepsilon_{\mu\nu\rho\lambda} e^\mu \wedge e^\nu \wedge \delta F^{\rho\lambda} \right). \quad (2.24)$$

The first term gives us Einstein’s vacuum equations. To see this we define the 4-form $X = \varepsilon_{\mu\nu\rho\lambda} \delta e^\mu \wedge e^\nu \wedge F^{\rho\lambda}$, so that

$$\int_{\mathcal{M}} \varepsilon_{\mu\nu\rho\lambda} \delta e^\mu \wedge e^\nu \wedge F^{\rho\lambda} = \int_{\mathcal{M}} X = \int_{\mathcal{M}} d^4x X_{0123}. \quad (2.25)$$

The component X_{0123} is

$$X_{0123} = \frac{1}{2} \varepsilon_{\mu\nu\rho\lambda} \varepsilon^{abcd} \delta e^\mu_a e^\nu_b R_{cd}{}^{ef} e^\rho_e e^\lambda_f. \quad (2.26)$$

Using (2.16) we have that $\varepsilon_{\mu\nu\rho\lambda} e^\nu_b e^\rho_e e^\lambda_f = e \varepsilon_{gbcf} e_\mu^g$, and hence

$$X_{0123} = \frac{1}{2} \varepsilon_{gbcf} \varepsilon^{abcd} e_\mu^g \delta e^\mu_a R_{cd}{}^{ef}. \quad (2.27)$$

We can now perform the contractions on the Levi-Civita symbols using the relation $\varepsilon_{gbcf} \varepsilon^{abcd} = 3! \delta_{[g}^a \delta_e^c \delta_f^d]$. We also note that, for any symmetric tensor S^{ab} , we have that $e_\mu^b \delta e^\mu_a S^a_b = \frac{1}{2} S^{ab} \eta_{\mu\nu} \delta(e^\mu_a e^\nu_b) = \frac{1}{2} S^{ab} \delta g_{ab}$. With these relations one finds that

$$X_{0123} = -e \delta g_{ab} (R^{ab} - \frac{1}{2} g^{ab} R) = -e \delta g_{ab} G^{ab}, \quad (2.28)$$

where G^{ab} is the Einstein tensor. Thus,

$$\int_{\mathcal{M}} \varepsilon_{\mu\nu\rho\lambda} \delta e^\mu \wedge e^\nu \wedge F^{\rho\lambda} = - \int_{\mathcal{M}} d^4x \sqrt{-g} \delta g_{ab} G^{ab}. \quad (2.29)$$

The second term in (2.24) reduces to a boundary contribution. This can be seen by first noting that $\varepsilon_{\mu\nu\rho\lambda} \delta F^{\rho\lambda} = \varepsilon_{\mu\nu\rho\lambda} D \delta A^{\rho\lambda}$. The exterior derivative, D , can then be pulled out to the front of the integrand using the graded product rule, the fact that $D e^\mu = 0$ from (2.9), and that $D \varepsilon_{\mu\nu\rho\lambda} = 0$:

$$\int_{\mathcal{M}} \varepsilon_{\mu\nu\rho\lambda} e^\mu \wedge e^\nu \wedge \delta F^{\rho\lambda} = \int_{\mathcal{M}} \varepsilon_{\mu\nu\rho\lambda} e^\mu \wedge e^\nu \wedge D \delta A^{\rho\lambda} = \int_{\mathcal{M}} D(\varepsilon_{\mu\nu\rho\lambda} e^\mu \wedge e^\nu \wedge \delta A^{\rho\lambda}). \quad (2.30)$$

D is now acting on a scalar with respect to the frame indices, and hence it acts as d , and we can use Stokes' theorem to reduce this to a boundary integral:

$$\int_{\mathcal{M}} D(\varepsilon_{\mu\nu\rho\lambda} e^\mu \wedge e^\nu \wedge \delta A^{\rho\lambda}) = \int_{\partial\mathcal{M}} \varepsilon_{\mu\nu\rho\lambda} e^\mu \wedge e^\nu \wedge \delta A^{\rho\lambda}. \quad (2.31)$$

In using Stokes' theorem we must remember that the orientation of the coordinates on \mathcal{M} induces an orientation on the boundary coordinates y^i . This fact will be important when it comes to rewriting our tetrad boundary term in the usual GHY format.

To fix the orientation of the boundary coordinates we introduce coordinates $x'^{a'} = (S, y^i)$ in some spacetime neighbourhood of Σ , where S is the function used above to define the surface Σ , and the coordinates y^i act as coordinates on Σ when $S = 0$. The orientation of the y^i coordinates is then fixed by requiring that the determinant of the transformation matrix is positive, i.e. that $\det\left(\frac{\partial x^a}{\partial x'^{a'}}\right) > 0$.

A more covariant way to define the boundary orientation uses the canonical volume form Ω , which defines an orientation on \mathcal{M} . In a similar manner a top-form, $\tilde{\Omega}$, on Σ can define an orientation on Σ . To fix this orientation we require that, for any three vectors $V_{1,2,3} \in T\Sigma$ ($T\Sigma$ is the tangent space of Σ), the action of $\tilde{\Omega}$ on these vectors satisfies $\tilde{\Omega}(V_1, V_2, V_3) = \Omega(\partial_S, V_1, V_2, V_3)$, where the vector $\partial_S = \frac{\partial}{\partial S}$ has components $\frac{dx^a}{dS}$. Given the coordinates $x'^{a'}$ above one can then show that $\tilde{\Omega} = \sqrt{-g'} dy^1 \wedge dy^2 \wedge dy^3$, where g' is the determinant of the metric written in $x'^{a'}$ coordinates and evaluated at $S = 0$, i.e. on Σ .

When performing the integral on the right hand side of (2.31) we must pullback the 3-form from \mathcal{M} to the boundary manifold. Above we stated that the pullback of δg_{ab} to the boundary vanishes, that is $\delta g_{ab} \frac{\partial x^a}{\partial y^i} \frac{\partial x^b}{\partial y^j} = 0$. This condition imposes certain constraints on the variation of the tetrad, δe^μ_a , since $\delta g_{ab} = \eta_{\mu\nu} (\delta e^\mu_a e^\nu_b + e^\mu_a \delta e^\nu_b)$.

These constraints afford us 6 free parameters when choosing δe_a^μ , and one can always pick δe_a^μ such that its pullback vanishes. With this choice of δe_a^μ we can pull the variation outside of the integral and write it as

$$\int_{\partial\mathcal{M}} \varepsilon_{\mu\nu\rho\lambda} e^\mu \wedge e^\nu \wedge \delta A^{\rho\lambda} = \delta \left(\int_{\partial\mathcal{M}} \varepsilon_{\mu\nu\rho\lambda} e^\mu \wedge e^\nu \wedge A^{\rho\lambda} \right). \quad (2.32)$$

We then define the general boundary term to be

$$S_B = -\frac{1}{4} \int_{\partial\mathcal{M}} \varepsilon_{\mu\nu\rho\lambda} e^\mu \wedge e^\nu \wedge A^{\rho\lambda}, \quad (2.33)$$

so that $\delta S_G = \delta S_{EH} + \delta S_B$ only contains bulk term involving G^{ab} .

2.3.3 The Boundary Term

Our derivation so far is independent of the type of boundary $\partial\mathcal{M}$. We will now show that this expression is the GHY term written in a universal form, by looking at the three types of boundaries: spacelike, timelike and null. Let us denote the 3-form in the integrand of (2.33) as $B = \varepsilon_{\mu\nu\rho\lambda} e^\mu \wedge e^\nu \wedge A^{\rho\lambda}$. To evaluate the boundary integral we must pullback B to $\partial\mathcal{M}$, and we denote this pullback as \tilde{B} . The components of B are $B_{abc} = \varepsilon_{\mu\nu\rho\lambda} 3! e_{[a}^\mu e_b^\nu A_{c]}^{\rho\lambda}$. If x^a are our coordinates on \mathcal{M} , and y^i are coordinates on the boundary $\partial\mathcal{M}$ ($i = 1, 2, 3$), then the components of \tilde{B} are

$$\tilde{B}_{ijk} = \varepsilon_{\mu\nu\rho\lambda} 3! e_{[a}^\mu e_b^\nu A_{c]}^{\rho\lambda} \frac{\partial x^a}{\partial y^i} \frac{\partial x^b}{\partial y^j} \frac{\partial x^c}{\partial y^k} = \varepsilon_{\mu\nu\rho\lambda} 3! \tilde{e}_{[i}^\mu \tilde{e}_{j}^\nu \tilde{A}_{k]}^{\rho\lambda}, \quad (2.34)$$

where $\tilde{\cdot}$ denotes the pullback, so for example $\tilde{e}_i^\mu = e_a^\mu \frac{\partial x^a}{\partial y^i}$. The integral is then

$$\int_{\partial\mathcal{M}} \varepsilon_{\mu\nu\rho\lambda} e^\mu \wedge e^\nu \wedge A^{\rho\lambda} = \int_{\partial\mathcal{M}} d^3 y \tilde{B}_{123}. \quad (2.35)$$

where $\tilde{B}_{123} = \varepsilon_{\mu\nu\rho\lambda} \tilde{e}_i^\mu \tilde{e}_j^\nu \tilde{A}_k^{\rho\lambda} \varepsilon^{ijk}$.

First, let us treat the case where Σ is spacelike. It will be convenient to pick a tetrad that is adapted to Σ , which we do by choosing $e_a^{0'} = n_a$. We then have that $\tilde{e}_i^{0'} = e_a^{0'} \frac{\partial x^a}{\partial y^i} = N \partial_a(S) \frac{\partial x^a}{\partial y^i} = N \frac{\partial S}{\partial y^i} = 0$, where N is the normalisation factor $(\varepsilon g^{bc} \partial_b S \partial_c S)^{-1/2}$ in the definition of the normal (2.4). The fact that $\tilde{e}_i^{0'} = 0$ means that the indices μ and ν in \tilde{B}_{123} cannot be $0'$, which simplifies the component to

$$\tilde{B}_{123} = -2 \varepsilon_{i'j'k'} \tilde{e}_i^{i'} \tilde{e}_j^{j'} \tilde{A}_k^{k'0'} \varepsilon^{ijk}, \quad (2.36)$$

where $i' = 1', 2', 3'$, and we have used the fact that $\varepsilon_{0'i'j'k'} = \varepsilon_{i'j'k'}$.

The pulled-back tetrad \tilde{e}^i satisfies $h_{ij} = \delta_{i'j'} \tilde{e}^{i'} \tilde{e}^{j'}$, and hence the determinant of the pulled-back tetrad $\tilde{e} = \pm \sqrt{h}$. The sign in this relationship is fixed by the orientation of the boundary. This can be seen by first recalling the expression for the volume form in terms of the tetrads, $\Omega = e^{0'} \wedge \dots \wedge e^{3'}$. One can then show that the top-form on Σ is given in terms of the pulled-back tetrad as $\tilde{\Omega} = N \tilde{e}^{1'} \wedge \tilde{e}^{2'} \wedge \tilde{e}^{3'}$, and using the expression for the determinant of the tetrad one finds that $\tilde{\Omega} = \pm N \sqrt{h} dy^1 \wedge dy^2 \wedge dy^3$. If we compare this expression with the previous expression for $\tilde{\Omega}$, one finds that $\pm N \sqrt{h}$ must equal $\sqrt{-g}$, and hence the plus sign must be chosen for consistency. We can now write the relationship between the tetrad determinant and \sqrt{h} as

$$\sqrt{h} \varepsilon_{ijk} = \varepsilon_{i'j'k'} \tilde{e}^{i'} \tilde{e}^{j'} \tilde{e}^{k'}, \quad (2.37)$$

from which we can derive the relation $\sqrt{h} \varepsilon_{ijk} \tilde{e}^k = \varepsilon_{i'j'k'} \tilde{e}^{i'} \tilde{e}^{j'}$, where the indices of the pulled-back tetrad are raised and lowered with h_{ij} and $\delta_{i'j'}$. From this relation, and the fact that $\tilde{A}_k^{k'0'} = e_a^{k'} \nabla_b (e^{0'a}) \frac{\partial x^b}{\partial y^k} = e_a^{k'} \nabla_b (n^a) \frac{\partial x^b}{\partial y^k}$, we can show that

$$\tilde{B}_{123} = -2\sqrt{h} \varepsilon_{ijl} \varepsilon^{ijk} \tilde{e}_k^l e_a^{k'} \nabla_b (n^a) \frac{\partial x^b}{\partial y^k}. \quad (2.38)$$

Using the relations $\varepsilon_{ijl} \varepsilon^{ijk} = 2\delta_l^k$ and $\tilde{e}_k^l = \delta_{k'l'} h^{lm} \frac{\partial x^a}{\partial y^m} e_a^{l'}$, we can rewrite the component as

$$\tilde{B}_{123} = -4\sqrt{h} \delta_{i'j'} e_c^{i'} e_a^{j'} \nabla_b (n^a) h^{ij} \frac{\partial x^c}{\partial y^i} \frac{\partial x^b}{\partial y^j}. \quad (2.39)$$

We then have that $\delta_{i'j'} e_c^{i'} e_a^{j'} = \eta_{\mu\nu} e_c^\mu e_a^\nu + e_c^{0'} e_a^{0'} = g_{ca} + n_c n_a = h_{ca}$, and that $h^{ij} \frac{\partial x^c}{\partial y^i} \frac{\partial x^b}{\partial y^j} = h^{cb}$. This allows us to write $\tilde{B}_{123} = -4\sqrt{h} h_{ac} h^{bc} \nabla_b (n^a)$, which is equal to $-4\sqrt{h} h^{ab} \nabla_a n_b$ since $h_{ac} h^{bc} = (g_{ac} + n_a n_c) h^{bc} = g_{ac} h^{bc}$. The extrinsic curvature is defined as $K = h^{ab} \nabla_a n_b$, and hence we have our desired result that the boundary term can be written in GHY format as

$$S_B = \int_{\Sigma} d^3y \sqrt{h} K. \quad (2.40)$$

When Σ is timelike the derivation of the boundary term in GHY form is similar, so we will not reproduce all the details. The first important difference is that we choose $e_a^{1'} = n_a$ in our adapted tetrad. The pullback of this tetrad covector vanishes, i.e. $\tilde{e}_i^{1'} = 0$, and hence the indices μ and ν cannot be $1'$ in \tilde{B}_{123} . The component in this case can be written as

$$\tilde{B}_{123} = 2\varepsilon_{i'j'k'} \tilde{e}^{i'} \tilde{e}^{j'} \tilde{A}_k^{k'1'} \varepsilon^{ijk}, \quad (2.41)$$

where $i' = 0', 2', 3'$. Another important difference is that the top-form on Σ in terms of the pulled-back tetrad is $\tilde{\Omega} = -N\tilde{e}^{0'} \wedge \tilde{e}^{2'} \wedge \tilde{e}^{3'}$, and hence the determinant of the pulled-back tetrad is $\tilde{e} = -\sqrt{-h}$. This means that the pulled-back tetrad has opposite orientation to the coordinates y^i on Σ .

The other steps in the timelike calculation are almost identical to the spacelike case, so we will just state the final result for the boundary term:

$$S_B = \int_{\Sigma} d^3y \sqrt{-h} K. \quad (2.42)$$

When Σ is null we make the following choice for our adapted tetrad: $e_a^+ = n_a$ and $e_a^- = l_a$, with $e_a^\pm = (e_a^{0'} \pm e_a^{1'})/\sqrt{2}$. Recall that our coordinates on Σ are $y^i = (\lambda, \theta^A)$, where $n^a = \frac{dx^a}{d\lambda}$. The pulled-back tetrad then satisfies $\tilde{e}_i^+ = 0$, $\tilde{e}_i^- = (-1, 0, 0)$, $\tilde{e}_i^{A'} = (0, \tilde{e}_i^{A'})$, and $\sigma_{AB} = \delta_{A'B'} \tilde{e}_A^{A'} \tilde{e}_B^{B'}$, where $A' = 2', 3'$.

The canonical volume form can be written as $\Omega = e^- \wedge e^+ \wedge e^{2'} \wedge e^{3'}$, and the orientation of the θ^A coordinates on the spatial slices of Σ (slices of constant λ) is fixed by a particular 2-form, $\tilde{\Omega}$, defined on those surfaces. The definition of $\tilde{\Omega}$ follows a similar procedure to what was done for non-null surfaces Σ . Specifically, for any two vectors $V_{1,2}$, belonging to the tangent spaces of these spatial slices, we require that $\tilde{\Omega}(V_1, V_2) = \Omega(\partial_S, \partial_\lambda, V_1, V_2)$, where the vector $\partial_\lambda = \frac{\partial}{\partial \lambda}$ has components n^a . One then finds that $\tilde{\Omega} = \sqrt{-g'} d\theta^2 \wedge d\theta^3$, where g' is the determinant of the metric written in the coordinates $x'^{a'} = (S, \lambda, \theta^A)$. $\tilde{\Omega}$ can be written in terms of the pulled-back tetrad as $\tilde{\Omega} = \tilde{e}^{2'} \wedge \tilde{e}^{3'}$, and hence, using the relation $\sigma_{AB} = \delta_{A'B'} \tilde{e}_A^{A'} \tilde{e}_B^{B'}$, we have that $\sqrt{\sigma} \varepsilon_{AB} = \varepsilon_{A'B'} \tilde{e}_A^{A'} \tilde{e}_B^{B'}$.

We can now write the component \tilde{B}_{123} as

$$\tilde{B}_{123} = \varepsilon_{\mu\nu\rho\lambda} \tilde{e}_i^\mu \tilde{e}_j^\nu \tilde{A}_k^{\rho\lambda} \varepsilon^{ijk} = 2\varepsilon_{A'B'} \varepsilon^{AB} \tilde{e}_A^{A'} \left(\tilde{e}_B^{B'} \tilde{A}_1^{-+} - 2\tilde{A}_B^{B'+} \right). \quad (2.43)$$

The first term on the far right, $2\varepsilon_{A'B'} \varepsilon^{AB} \tilde{e}_A^{A'} \tilde{e}_B^{B'} \tilde{A}_1^{-+}$, can be simplified, using $\sqrt{\sigma} \varepsilon_{AB} = \varepsilon_{A'B'} \tilde{e}_A^{A'} \tilde{e}_B^{B'}$, to the expression $2\sqrt{\sigma} \varepsilon_{AB} \varepsilon^{AB} \tilde{A}_1^{-+} = 4\sqrt{\sigma} \tilde{A}_1^{-+}$, where we have used the relation $\varepsilon_{AB} \varepsilon^{AB} = 2$. We also have that $\tilde{A}_1^{-+} = e_a^- \nabla_b (e^{+a}) \frac{\partial x^b}{\partial y^1} = l_a \nabla_b (n^a) n^b$, using the fact that $\frac{\partial x^b}{\partial y^1} = \frac{dx^b}{d\lambda} = n^b$ along the null geodesics on Σ . This can be simplified further using the definition of the surface gravity, κ , which measures the failure of n^a to be affinely parameterised. Specifically, κ is defined by the geodesic equation for the null generators, $n^a \nabla_a (n^b) = \kappa n^b$. If we contract this with l_b we get $\tilde{A}_1^{-+} = l_a \nabla_b (n^a) n^b = -\kappa$, and hence the first term on the far right above is simply $-4\sqrt{\sigma} \kappa$.

The second term on the far right, $-4\varepsilon_{A'B'} \varepsilon^{AB} \tilde{e}_A^{A'} \tilde{A}_B^{B'+}$, can be simplified using the relation $\sqrt{\sigma} \varepsilon_{AB} \tilde{e}_B^{B'} = \varepsilon_{A'B'} \tilde{e}_A^{A'}$, where we raise and lower the A and A' indices

with σ_{AB} and $\delta_{A'B'}$. We also have that $\tilde{A}_B^{B'+} = e_a^{B'} \nabla_b (e^{+a}) \frac{\partial x^b}{\partial \theta^B} = e_a^{B'} \nabla_b (n^a) \frac{\partial x^b}{\partial \theta^B}$. Using these results, and following similar steps to the spacelike case, one finds that the second term can be written as $-4\sqrt{\sigma} \sigma^{ab} \nabla_a (n_b)$, which is simply $-4\sqrt{\sigma} \Theta$, using the definition of the null expansion $\Theta = \sigma^{ab} \nabla_a (n_b)$.

Thus, the entire component can be written as $\tilde{B}_{123} = -4\sqrt{\sigma} (\Theta + \kappa)$, and the boundary term is

$$S_B = \int_{\Sigma} d^2\theta d\lambda \sqrt{\sigma} (\Theta + \kappa). \quad (2.44)$$

The boundary term in the null case differs from the non-null case in that it depends on the choice of coordinates, specifically the choice of parameter λ . This means that the boundary term is not geometrical, which at first glance appears to be an issue. In fact, as we will discuss more in the conclusion of this chapter, the unphysical dependence on the parameter will drop out when deriving physical probabilities using a double path integral, or a Schwinger-Keldysh formalism of quantum mechanics. Similarly, it will drop out when considering the more physical equations of motion, since a variation of this boundary term will not depend on the parameter λ .

Note that we have made no assumption above regarding extending the normal n_a off the boundary. The normal is only defined at points on the boundary and we only use its tangential derivatives.

2.3.4 Gauge Transformation of the Boundary Term

The boundary term Eqn (2.33) is not gauge invariant under $O(1,3)$ transformations (although its variation is), unlike the tetrad form of the bulk action S_{EH} . This is because $A^{\rho\lambda}$ transforms inhomogeneously under local transformations of the tetrad such as

$$e'^{\mu'} = \Lambda^{\mu'}_{\mu}(x) e^{\mu}. \quad (2.45)$$

Using the definition of $A^{\rho\lambda}$ we can derive how it transforms:

$$A'^{\rho'\lambda'} = \Lambda^{\rho'}_{\rho} \Lambda^{\lambda'}_{\lambda} A^{\rho\lambda} + \eta^{\rho\lambda} \Lambda^{\rho'}_{\rho} d\Lambda^{\lambda'}_{\lambda}, \quad (2.46)$$

with the result that

$$S'_B = S_B - \frac{1}{4} \int_{\partial\mathcal{M}} \varepsilon_{\mu\nu\rho\lambda} e^{\mu} \wedge e^{\nu} \wedge \mathbf{g}^{\rho\lambda} \quad (2.47)$$

where $\mathbf{g}^{\rho\lambda} = \Lambda_{\lambda'}^{\lambda} d\Lambda^{\lambda'\rho}$ is in the Lie Algebra of $O(1,3)$, where the μ (μ') indices are raised and lowered with $\eta_{\mu\nu}$ ($\eta_{\mu'\nu'}$) and its inverse, and where we have restricted

ourselves to orientation preserving transformations. The variation of the second term on the right hand side above vanishes since the gauge transformation does not depend on the spacetime geometry and the pullback of δe_a^μ vanishes. This ensures that the variation of S_B is gauge invariant, i.e. that it is independent of the choice of frame e_a^μ .

We note that in the adapted tetrads there is a residual gauge freedom in the little group H , which preserves the normal. The little group is given by $H = O(3)$ for timelike, $H = O(1,2)$ for spacelike and $H = E(2)$ for null normals. It is easily checked that the adapted boundary term *is* invariant under gauge transformations of the little group. In fact for $\Lambda \in H$, $\mathbf{h}^{\rho\lambda} = \Lambda_{\chi'}^\lambda d\Lambda^{\lambda\rho}$ satisfies $\mathbf{h}^{\hat{\alpha}\lambda} = \mathbf{h}^{\rho\hat{\alpha}} = 0$ for $\hat{\alpha}$ a fixed index labelling the normal, i.e. when the normal is timelike/spacelike/null $\hat{\alpha} = 0'/1'/+$. The change in S_B under such a gauge transformation,

$$\Delta S_B = S'_B - S_B = -\frac{1}{4} \int_{\partial\mathcal{M}} \varepsilon_{\mu\nu\rho\lambda} e^\mu \wedge e^\nu \wedge \mathbf{h}^{\rho\lambda}, \quad (2.48)$$

vanishes entirely. One can see this by noting that the Levi-Civita symbol and the fact that $\mathbf{h}^{\hat{\alpha}\lambda} = \mathbf{h}^{\rho\hat{\alpha}} = 0$, means that the tetrads must take on the frame index $\hat{\alpha}$. Evaluation of the integral requires us to pullback the tetrads to the surface and under this pullback, $e^{\hat{\alpha}}$ vanishes. Hence, $\Delta S_B = 0$.

Let \mathfrak{D} be four discrete elements of $O(1,3)$ corresponding to each of the connected components of the group. They are the elements: \mathfrak{I} for identity, \mathfrak{P} for parity, \mathfrak{T} for time-reversal, and \mathfrak{PT} for parity and time-reversal. Since these are constant matrices, the connection $A^{\rho\lambda}$ transforms homogeneously and the boundary term Eqn (2.33) is invariant under such transformations, up to a sign determined by the determinant of the transformation matrix (S_{EH} is also determined up to a sign in the same way).

2.3.5 Corner Terms

The fact that the boundary term Eqn (2.33) is not gauge invariant can be exploited to identify the corner terms. By adapting our frame to the normal we have been able to derive the forms Eqns (2.40),(2.42),(2.44) of the boundary GHY terms for all signatures of the boundary. When there is a join of two boundary components, the adapted frames will not, in general, agree at the join. In order to pass from one frame to the other we will use the following procedure. By means of a gauge transformation in the little group H , we will ensure that two of the frame fields from each boundary component are tangent to the join and *agree* with each other at the join (they may not agree but are related by a constant orientation preserving

transformation using the discrete elements \mathfrak{D}). With these choices, the relation between the two frames is a Lorentz transformation in the 2-dimensional plane of the normals. The change in the boundary term Eqn (2.33) under this $O(1,3)$ gauge transformation gives us the corner terms. Crucially, the variation of this corner term will *not* vanish like additional piece in (2.47), since the gauge transformation will depend on the spacetime geometry, in the sense that the amount we need to rotate between frames depends on the spacetime. Therefore, the corner term is a necessary addition to the gravitational action.

This transformation between tetrads will have to happen discontinuously in order to have adapted tetrads on both boundary components. This is not strictly permitted, since the tetrad should be twice differentiable if the tetrad form of S_{EH} is to make sense. To overcome this technical difficulty we will take a limit of a smooth transformation of the tetrads across the join.

For a spacelike join \mathcal{J}_{ij} between two boundary components Σ_i and Σ_j we can use transformations in the little group to arrange that $e_{(i)}^{2'} = e_{(i)}^{2'}$, and $e_{(i)}^{3'} = e_{(i)}^{3'}$ on the join, and that both of these are orthogonal to the timelike plane of normals. When Σ_i is spacelike/timelike we will choose the tetrad vector $e_{(i)}^{1'a}/e_{(i)}^{0'a}$ to be outward pointing with respect to Σ_i , while $e_{(i)}^{0'a}/e_{(i)}^{1'a}$ still corresponds to the normal vector. When Σ_i is null $e_{(i)a}^+$ is still the normal covector, and $e_{(i)a}^-$ is fixed to be l_a , which is outward(inward) pointing with respect to Σ_i when λ decreases(increases) towards the join. See Figure 2.2 for an example of how we choose our adapted tetrads.

In any of the above cases the two frames $e_{(i)}^\mu$ and $e_{(j)}^\mu$ are related by a Lorentz boost in the timelike plane of $e_a^{0'}$ and $e_a^{1'}$,

$$e_{(j)}^\mu = \Lambda_{(ij)}{}^\mu{}_\nu e_{(i)}^\nu . \quad (2.49)$$

In some cases the frames might need an additional transformation using orientation preserving discrete elements to relate them, but this will not affect the form of the boundary terms (since it preserves orientation) and hence we can ignore it. We also note that the frames $e_{(i)}^\mu$ and $e_{(j)}^\mu$ are defined throughout the entire spacetime.

Let Σ_δ be a thin neighbourhood of \mathcal{J}_{ij} within the union of the two boundary components $\Sigma_i \cup \Sigma_j$, and let $\Sigma_{i,\delta}$ ($\Sigma_{j,\delta}$) be the points in Σ_i (Σ_j) that are not in the interior of Σ_δ . When we take the $\delta \rightarrow 0$ limit we will take $\Sigma_\delta \rightarrow \mathcal{J}_{ij}$, $\Sigma_{i,\delta} \rightarrow \Sigma_i$, and $\Sigma_{j,\delta} \rightarrow \Sigma_j$. See Figure 2.2 for an illustration of these regions.

We now define the gauge transformation $\lambda \in O(1,1)$ that is the identity on $\Sigma_{i,\delta}$, $\Lambda_{(ij)}$ on $\Sigma_{j,\delta}$, and interpolates between the two in Σ_δ :

$$\lambda^\mu{}_\nu = (\exp[\eta K \Theta_\delta^{(H)}])^\mu{}_\nu , \quad (2.50)$$

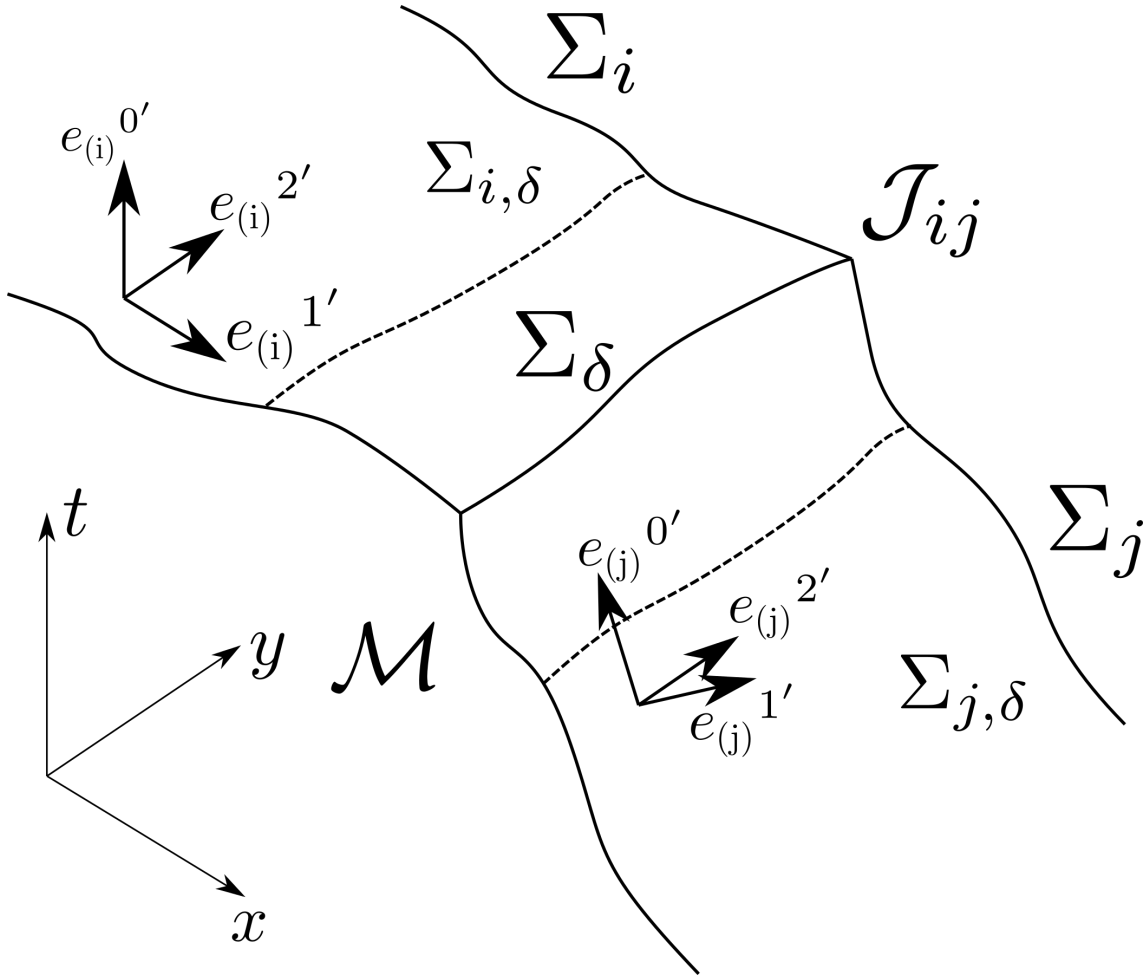


Figure 2.2: An illustration (in 3D spacetime) of a join \mathcal{J}_{ij} between a spacelike boundary component Σ_i and a timelike component Σ_j . The two adapted tetrad 1-forms, $e^{(i)\mu'}$ and $e^{(j)\nu'}$, are also shown, and one can see that $e^{(i)0'}/e^{(j)1'}$ is the normal on Σ_i/Σ_j . The diagram also illustrates how we can choose our tetrads such that $e^{(i)2'} = e^{(j)2'}$ on \mathcal{J}_{ij} , and choose $e^{(i)1'}$ to be outward pointing with respect to Σ_i when evaluated on the join. Σ_δ is the region on $\Sigma_i \cup \Sigma_j$ between the dotted lines, and $\Sigma_{i,\delta}/\Sigma_{j,\delta}$ is the region of Σ_i/Σ_j outside of Σ_δ . Again we note that we have used arrows to visualise the covectors.

where $\Theta_\delta^{(H)}$ is a smooth approximation of the Heaviside function over the spacetime with the requirement that it takes the value 0 on $\Sigma_{i,\delta}$, 1 on $\Sigma_{j,\delta}$, and interpolates between the two in Σ_δ . η is some function over the spacetime satisfying the condition that its values on \mathcal{J}_{ij} match the rapidity of the boost to take you from frame $e_{(i)}^\mu$ to frame $e_{(j)}^\mu$ (η may be a function of position within the join). K is the boost generator in the plane of normals. The only non vanishing components of the boost generator are $K^{0'_{1'}} = K^{1'_{0'}} = 1$, and hence $K^{0'1'} = -K^{1'0'} = 1$ are the only non vanishing components with the frame indices up.

We define a new frame as $e'^\mu = \lambda^\mu_\nu e_{(i)}^\nu$, so that $e'^\mu = e_{(i)}^\mu$ for $x \in \Sigma_{i,\delta}$, and $e'^\mu = e_{(j)}^\mu$ for $x \in \Sigma_{j,\delta}$. This frame transformation is smooth for any finite δ , and in the limit of $\delta \rightarrow 0$ it corresponds to a discontinuous transformation between the adapted frames across the join. Since the tetrad form of S_{EH} is undefined for a discontinuous transformation, we will define the bulk part of the action by taking the $\delta \rightarrow 0$ limit of S_{EH} calculated for finite δ . For finite δ the tetrad form of S_{EH} is the usual EH action, and hence this is obtained in the $\delta \rightarrow 0$ limit.

The boundary integral over $\Sigma_i \cup \Sigma_j$ can be written in terms of the e'^μ frame as

$$\begin{aligned}
S_B &= -\frac{1}{4} \int_{\Sigma_i \cup \Sigma_j} \varepsilon_{\mu\nu\rho\lambda} e'^\mu \wedge e'^\nu \wedge A'^{\rho\lambda} \\
&= -\frac{1}{4} \int_{\Sigma_{i,\delta}} \varepsilon_{\mu\nu\rho\lambda} e'^\mu \wedge e'^\nu \wedge A'^{\rho\lambda} - \frac{1}{4} \int_{\Sigma_{j,\delta}} \varepsilon_{\mu\nu\rho\lambda} e'^\mu \wedge e'^\nu \wedge A'^{\rho\lambda} \\
&\quad - \frac{1}{4} \int_{\Sigma_\delta} \varepsilon_{\mu\nu\rho\lambda} e'^\mu \wedge e'^\nu \wedge A'^{\rho\lambda} \\
&= -\frac{1}{4} \int_{\Sigma_{i,\delta}} \varepsilon_{\mu\nu\rho\lambda} e_{(i)}^\mu \wedge e_{(i)}^\nu \wedge A_{(i)}^{\rho\lambda} - \frac{1}{4} \int_{\Sigma_{j,\delta}} \varepsilon_{\mu\nu\rho\lambda} e_{(j)}^\mu \wedge e_{(j)}^\nu \wedge A_{(j)}^{\rho\lambda} \\
&\quad - \frac{1}{4} \int_{\Sigma_\delta} \varepsilon_{\mu\nu\rho\lambda} e'^\mu \wedge e'^\nu \wedge A'^{\rho\lambda}.
\end{aligned} \tag{2.51}$$

When we take the limit $\delta \rightarrow 0$ the two integrals on the 2nd last line will tend to the usual GHY boundary terms on Σ_i and Σ_j . The integral on the last line will give us the corner term in the $\delta \rightarrow 0$ limit, and we denote this by $S_{\mathcal{J}_{ij}}$:

$$S_{\mathcal{J}_{ij}} = \lim_{\delta \rightarrow 0} -\frac{1}{4} \int_{\Sigma_\delta} \varepsilon_{\mu\nu\rho\lambda} e'^\mu \wedge e'^\nu \wedge A'^{\rho\lambda}. \tag{2.52}$$

By using our definition of the new frame, $e'^\mu = \lambda^\mu_\nu e_{(i)}^\nu$, and the gauge transformation in (2.47) we have that

$$S_{\mathcal{J}_{ij}} = \lim_{\delta \rightarrow 0} -\frac{1}{4} \int_{\Sigma_\delta} \varepsilon_{\mu\nu\rho\lambda} e_{(i)}^\mu \wedge e_{(i)}^\nu \wedge A_{(i)}^{\rho\lambda} - \frac{1}{4} \int_{\Sigma_\delta} \varepsilon_{\mu\nu\rho\lambda} e_{(i)}^\mu \wedge e_{(i)}^\nu \wedge \mathbf{g}^{\rho\lambda}. \tag{2.53}$$

where $\mathbf{g}^{\rho\sigma} = -K^{\rho\sigma}d(\eta\Theta_\delta^{(H)})$, and the first term goes to zero as $\delta \rightarrow 0$. Using the fact that $d(\eta\Theta_\delta^{(H)}) = D(\eta\Theta_\delta^{(H)})$, and that $DK^{\rho\lambda} = 0$, we can pull the exterior derivative out to the front and write $S_{\mathcal{J}_{ij}}$ as

$$\begin{aligned} S_{\mathcal{J}_{ij}} &= \lim_{\delta \rightarrow 0} \frac{1}{4} \int_{\Sigma_\delta} d(\varepsilon_{\mu\nu\rho\lambda} e_{(i)}^\mu \wedge e_{(i)}^\nu \wedge K^{\rho\sigma} \eta \Theta_\delta^{(H)}) \\ &= \lim_{\delta \rightarrow 0} \frac{1}{4} \int_{\partial\Sigma_\delta} \varepsilon_{\mu\nu\rho\lambda} e_{(i)}^\mu \wedge e_{(i)}^\nu \wedge K^{\rho\sigma} \eta \Theta_\delta^{(H)}. \end{aligned} \quad (2.54)$$

In using Stokes' theorem we must remember to inherit the orientation of the coordinates on $\partial\Sigma_\delta$ from the orientation of the coordinates on Σ_δ . The boundary $\partial\Sigma_\delta$ is a disjoint union of a part in Σ_i , which we denote by $C_{i,\delta}$, and a part in Σ_j , denoted by $C_{j,\delta}$. The integral over $C_{i,\delta}$ vanishes since $\Theta_\delta^{(H)} = 0$ there. $\Theta_\delta^{(H)} = 1$ on $C_{j,\delta}$ and hence we can write

$$S_{\mathcal{J}_{ij}} = \lim_{\delta \rightarrow 0} \frac{1}{4} \int_{C_{j,\delta}} \varepsilon_{\mu\nu\rho\lambda} e_{(i)}^\mu \wedge e_{(i)}^\nu \wedge K^{\rho\sigma} \eta. \quad (2.55)$$

As $\delta \rightarrow 0$ we have that $C_{j,\delta} \rightarrow \mathcal{J}_{ij}$. Since the only non-zero components of $K^{\rho\lambda}$ are when $\rho, \lambda = 0', 1'$, the frame indices of the tetrads must be $2'$ or $3'$. In the $\delta \rightarrow 0$ limit the two tetrads $e_{(i)}^\mu$ and $e_{(j)}^\mu$ agree for $\mu = 2', 3'$, and hence we can drop the subscript (i) in the limit. Taking the limit results in the corner term

$$S_{\mathcal{J}_{ij}} = \frac{1}{4} \int_{\mathcal{J}_{ij}} \varepsilon_{\mu\nu\rho\sigma} e^\mu \wedge e^\nu K^{\rho\sigma} \eta. \quad (2.56)$$

Putting in the value $K^{0'1'} = -K^{1'0'} = 1$ we get

$$S_{\mathcal{J}_{ij}} = \int_{\mathcal{J}_{ij}} e^{2'} \wedge e^{3'} \eta, \quad (2.57)$$

The join \mathcal{J}_{ij} is part (or possibly all) of the boundary $\partial\Sigma_i$, and the orientation induced on the coordinates over \mathcal{J}_{ij} is the same as the orientation induced on the coordinates over $\partial\Sigma_i$ from the orientation of the coordinates y^i on Σ_i . Explicitly, we pick coordinates $z^i = (Z, z^A)$ on Σ_i , where Z is some function on Σ_i that increases towards the join where it vanishes, and where the other two coordinates z^A act as coordinates on \mathcal{J}_{ij} when $Z = 0$. The orientation is then fixed by requiring that $\det\left(\frac{\partial y^i}{\partial z^j}\right) > 0$. This particular orientation will determine whether the pullback of the 2-form $e^{2'} \wedge e^{3'}$ to \mathcal{J}_{ij} will give plus or minus the joint area element $\sqrt{\sigma}$, where σ is the determinant of $\sigma_{AB} = g_{ab} \frac{\partial x^a}{\partial z^A} \frac{\partial x^b}{\partial z^B}$. The correct sign can be derived in a similar manner to what was done in the derivation of the GHY boundary terms, and hence

we will just state the results.

When Σ_i is spacelike(timelike), or null with λ increasing(decreasing) in the direction of \mathcal{J}_{ij} :

$$S_{\mathcal{J}_{ij}} = \pm \int_{\mathcal{J}_{ij}} d^2z \sqrt{\sigma} \eta, \quad (2.58)$$

where one recalls that η is the boost parameter to go from frame $e_{(i)}^\mu$ to frame $e_{(j)}^\nu$.

For timelike joins, the argument is very similar, and from 2.2.2 we know that Σ_i and Σ_j must timelike in order for \mathcal{J}_{ij} to be timelike. We can, by gauge transformations in the little group, arrange that $e_{(i)}^{0'} = e_{(i)}^{0'}$ and $e_{(i)}^{3'} = e_{(i)}^{3'}$, and that both of these are orthogonal to the spacelike plane of normals (again we may require an additional action with the discrete elements \mathfrak{D} to relate the frames, but this will not alter the form of the boundary terms). $e_{(i)}^{1'}$ and $e_{(i)}^{1'}$ are still the respective normals for the two surfaces, and we take $e_{(i)}^{2'}$ to be outward pointing with respect to Σ_i . The two frames $e_{(i)}^\mu$ and $e_{(j)}^\mu$ are now related by a rotation in the spacelike plane of normals

$$e_{(j)}^\mu = \Lambda_{(ij)}^\mu{}_\nu e_{(i)}^\nu. \quad (2.59)$$

Again, we define a little neighbourhood about the join and a gauge transformation $\lambda \in O(2)$ that interpolates between the two frames as you move from Σ_i to Σ_j :

$$\lambda^\mu{}_\nu = (\exp[\eta J \Theta_\delta^{(H)}])^\mu{}_\nu, \quad (2.60)$$

where η is now the rotation angle and J the rotation generator in the plane of normals. $-J_{2'}^{1'} = J_{1'}^{2'} = 1$ are the only non-zero components of the generator, and hence its only non-zero components with indices up are $-J^{1'2'} = J^{2'1'} = 1$. In the $\delta \rightarrow 0$ limit the boundary term again gives rise to a contribution from the join

$$S_{\mathcal{J}_{ij}} = \frac{1}{4} \int_{\mathcal{J}_{ij}} \varepsilon_{\mu\nu\rho\sigma} e^\mu \wedge e^\nu J^{\rho\sigma} \eta. \quad (2.61)$$

Since the nonvanishing components of J are $-J^{1'2'} = J^{2'1'} = 1$, we have the form of the corner term:

$$S_{\mathcal{J}_{ij}} = - \int_{\mathcal{J}_{ij}} e^{0'} \wedge e^{3'} \eta. \quad (2.62)$$

Defining coordinates z^A on \mathcal{J}_{ij} , with the correct orientation as before, we find that

$$S_{\mathcal{J}_{ij}} = - \int_{\mathcal{J}_{ij}} d^2z \sqrt{-\sigma} \eta. \quad (2.63)$$

A salient difference between this case and the spacelike join is that the angles are

only defined modulo 2π . This arises because the group $SO(1,1)$ is simply connected ($\pi_1(SO(1,1)) = 0$), while the group $SO(2)$ is multiply connected ($\pi_1(SO(2)) = \mathbb{Z}$). This ambiguity does not however affect the variation.

Null joins differ in that the plane of normals and the tangent space to the join share a one dimensional, null subspace. If n_i is spacelike and n_j is null (with $n_i \cdot n_j = 0$), n_j belongs *both* to the span of normals and the tangent space to the join. It is possible to adapt a null Lorentz frame to both Σ_i and Σ_j as follows: $e_{(i)}^+ = e_{(j)}^+ = n_j$, $e_{(i)}^{3'} = e_{(j)}^{3'} = n_i$ and $e_{(i)}^{2'} = e_{(j)}^{2'}$, $e_{(i)}^- = e_{(j)}^-$. Since $e_{(i)}^\mu = e_{(j)}^\mu$, we have $\Lambda_{(ij)}$ equal to the identity and $\eta = 0$. The corner term therefore vanishes, and the same can be shown when both normals are spacelike and the join is null.

2.3.6 Creases

A physically interesting situation covered by the above analysis occurs when one of the boundaries of spacetime is the event horizon of a dynamically evolving black hole. In this case the horizon does not remain smooth when new generators enter or leave the horizon. Suppose that we are interested in the boundary of a future set (the case of past sets is similar). The boundary of a future set is ruled by null generators. However, when these null generators cross because of gravitational focussing effects, they leave the boundary and enter into the interior of the future set. The horizon then develops a caustic, generically a spacetime region of codimension-2, where the normal to the wavefront is discontinuous. When this happens, we have a ‘‘crease’’ which separates regions of the null surface with different normal vectors. Locally, this is no different from a null-null join discussed above. From the analysis already presented we would expect a boundary term to appear as an integral along the crease of the rapidity parameter. This crease would be the join of two null surfaces, and hence it would be spacelike from our analysis in section 2.2.2. Thus, it would contribute a joint term equal to that which we saw in the spacelike join case treated above.

2.4 Summary

The main new advance of this work is the realisation that the tetrad formulation of Einstein’s theory permits a unified approach to boundaries of all signatures. The calculations are considerably simplified and the use of differential forms permits us to integrate over boundary manifolds regardless of their signature. Additionally, our

derivation of the corner terms is extremely simple when one sticks to the tetrads. The complications arise when one tries to relate the expressions back to more standard geometric objects. The methods used are complementary to [26, 27, 33] and the perspective is somewhat different. The differential form version of the boundary term also makes manifest the fact that the boundary corrected action is additive. In any splitting of a spacetime into pieces, the boundary term S_B , Eqn (2.33), appears twice on the shared boundary with opposite orientation, due to our application of Stokes' theorem, and so cancels out.

We have worked within the Dirichlet formalism for gravity in which the pullback metric, h_{ij} , is held fixed on the boundary during the variation. One can also conceive of “Neumann gravity” in which the conjugate variable is held fixed. For example if the boundary is spacelike, the quantity $\sqrt{\hbar}(K^{ij} - 1/2Kh^{ij})$ related to the extrinsic curvature is conjugate to the three-metric. There has been recent work [34] exploring this possibility, albeit in the Euclidean context. Such alternate formalisms are of interest since it is far from clear which ensemble would prove the most advantageous under quantisation. It is also possible that these different choices may lead to different quantum theories. For example, it is known in statistical mechanics that conjugate ensembles may not always be equivalent. Such issues are particularly acute in the case of long range forces like gravity. A classic example is the stability question of a black hole in equilibrium with thermal radiation in a box.

A notable feature of the boundary term Eqn (2.33) is that it is not gauge invariant, although its *variation* is, which means that the more *physical* equations of motion *are* gauge invariant. One must bear in mind that the boundary action is only determined up to a functional of the boundary data that is held fixed, in our case the pullback of the metric to the boundary. One may worry that the value of the action changes under change of gauge. However, there is no cause for concern. In a path integral formulation of quantum mechanics observable quantities are related to the absolute value squared of the Feynman amplitude in Eqn (2.1). This leads to expressions for physical probabilities having the form of a closed time double path integral of Schwinger-Keldysh form. The quantity that appears in the exponent in the double path integral is then a difference of two actions, $S(X_3, \Gamma) - S(X_3, \bar{\Gamma})$, where Γ and $\bar{\Gamma}$ are histories going between X_1 and X_3 . While the two histories share the same final geometry X_3 , they have different values of the connection at the final point. The two boundary terms at X_3 then combine to give a gauge invariant answer, since the *difference* of two connections transforms homogeneously. Another situation that arises is when one considers asymptotically flat spacetimes, takes the boundary to infinity, and interprets the boundary term in terms of the total mass.

In this case, as is well known, we need to make a background subtraction in order to get a finite answer. Once again, this subtraction results in a gauge invariant boundary term, since the difference of two connections is a gauge covariant object. The gauge non-invariance of the boundary term is precisely what we have exploited in order to identify the corner terms. This remark has a parallel in the GHY format of the boundary term too. The integrand in the boundary term Eqn (2.44) is not coordinate invariant since it depends on the parameter λ .

In the literature, it is suggested that the corner terms [28] or their close analogs [35] may pick up imaginary contributions (imaginary contributions figure heavily in the Lorentzian Gauss-Bonnet theorem as well.) Using our methods, such contributions would not be detected, as they have zero variation. However, the origin of such terms can be understood when the normal changes from timelike to spacelike. We have chosen different adapted frames depending on whether the normal to the boundary is null, spacelike or timelike. This is because no Lorentz transformation can connect these different normals. However, in connecting spacelike normals to timelike normals, it is possible to use complex Lorentz transformations, which may allow us to connect up the two results. In certain situations these imaginary contributions can be interpreted as black hole entropy, as was done by Neiman (see [28] for a fuller discussion). While such a term affects the *value* of the action, it does not affect the *variation*. In a double path integral for quantum gravity such imaginary contributions would also cancel out.

The case of null boundaries has not received much attention till the recent works of Neimann[28–31], Parattu et al [26, 27] and Lehner et al [33]. Neimann was mainly interested in imaginary contributions to the action at the join of null boundaries. He used affine parametrisations to describe the null generators, which is unnecessarily restrictive in the present context. The treatment of Parattu et al [26] allows for arbitrary parametrisation of the null generators and correctly identifies the form of the boundary action for null surfaces. However, these authors do not consider the corner terms, which are necessary for a more complete treatment of the boundary action. In a second paper [27], they attempt a unified description of both the null and non-null case. Their treatment is coordinate bound and makes assumptions about the behaviour of the normal away from the boundary. Lehner et al [33] provide a metric treatment of the null boundary terms and identify the corner terms. They also have a detailed discussion of reparameterisation invariance and suggest counterterms to be added to the boundary action. In this work we offer a perspective on reparameterisation invariance (RI) in the null case which differs slightly from [33]. Rather than try to restore RI, we note that the lack of RI in the

boundary action does not affect any physical quantity in the double path integral or the equations of motion.

Finally, it should be noted that this work is not a complete treatment of boundary terms for the action in General Relativity. We have not treated the case in which a timelike or spacelike boundary component tends to a null surface *just* as it meets another boundary component at a join. Our results would suggest that the join contribution from such a situation would be divergent, but more work should be done to confirm this. We have also not stated whether codimension-3 lines (meetings of joins), or codimension-4 points (meetings of codimension-3 lines) contribute to the action.

Chapter 3

Boundary Terms and Related Geometry in Causal Set Theory

3.1 Introduction

One approach to constructing a quantum dynamics for the causal set approach to quantum gravity [36] is to discover a discrete counterpart of the gravitational action, $S[\mathcal{C}]$ that can furnish the weight, $e^{iS[\mathcal{C}]}$, of each causal set, \mathcal{C} , in the gravitational sum over histories. A start in this direction has been made with a proposal for scalar curvature estimators for causal sets of dimension d [9–11]. Summing such a scalar curvature estimator over all elements of a causal set (*causet* for short) gives a natural proposal for a causet analogue of the Einstein-Hilbert action, a proposal that remains to be studied in depth. This chapter will be concerned with the boundary terms for the action of causets. This is likely to be important as, in the continuum, we have seen that the Einstein-Hilbert action, S_{EH} , is not the full story in the presence of spacetime boundaries. Indeed, the gravitational action must include a boundary term S_{GHY} , the Gibbons-Hawking-York (GHY) boundary term, in order to yield a well-defined variational principle when the pullback of the metric is fixed on the boundary of spacetime [37, 38]. If the classical limit of quantum gravity is to arise from the path integral in the expected way, such a term in the action will be essential when boundaries are present. Whilst we do not yet know how to fix boundary conditions for causal sets in general, it is likely to be useful to have an analogue of the GHY boundary term for any causal set which is well-approximated by a manifold with a boundary. In this chapter we will propose a causal set analogue of the continuum boundary term in the case of spacelike boundaries. We will also look at other causal set analogues of geometrical objects relating to spatial boundaries, as

well as investigating the above mentioned bulk causal set action for a causal interval with null boundaries. First we consider causal sets which are well approximated by (M, g) , a d -dimensional, causal, Lorentzian spacetime with finite volume which admits a compact spacelike submanifold, Σ , such that the causal past and future sets, $M^\pm := J^\pm(\Sigma)$, satisfy $M^+ \cap M^- = \Sigma$. Then Σ is a component of the future (past) spacelike boundary for M^- (M^+) and the GHY term for Σ , considered as a boundary of M^+ or M^- , is given by

$$S_{GHY}[\Sigma, M^\pm] = \mp \frac{1}{l_p^{d-2}} \int_\Sigma d^{d-1}x \sqrt{h} K, \quad (3.1)$$

where $x^\mu = (x^0, \dots, x^{d-1})$ are the spacetime coordinates, K is the trace of the extrinsic curvature tensor $K_{\mu\nu} = h_\mu^\rho h_\nu^\sigma \nabla_\rho n_\sigma$ of Σ , $h_{\mu\nu}$ is the transverse metric on Σ , $l_p = (8\pi G)^{\frac{1}{d-2}}$ is the rationalised Planck length, and we are working in units where $\hbar = 1$. Here we take n_μ to be the future-pointing timelike unit covector normal to Σ . We work with a mostly plus convention for the metric so n^μ is past-pointing¹.

We recall that the integral in (3.1) is equal to the normal derivative of the volume of Σ along the unit normal vector field, n^μ :

$$\int_\Sigma d^{d-1}x \sqrt{h} K = \frac{\partial}{\partial n} \int_\Sigma d^{d-1}x \sqrt{h}, \quad (3.2)$$

where this is the rate of change of the volume backwards in time, as n^μ is past-pointing. This observation suggests a natural candidate for an analogue of the GHY boundary term for Σ for a causet that can be faithfully embedded in M . Spacetime volume corresponds to cardinality in a causet. Hence the spatial volume gradient corresponds intuitively to the difference between the number of causet elements that are future nearest neighbours of Σ and the number of past nearest neighbours. This intuition turns out to be a good guide and we will identify a family of causal set boundary terms based on it. The family of causet boundary terms we find corresponds to the different ways to define a discrete derivative that tend to the same limit in the continuum. We will also find higher order discrete derivatives and relate them to geometrical objects in the continuum.

Before discussing the causal set expressions we will need to derive a particular continuum result in Section 3.2. In Sections 3.3 and 3.4 we will use this continuum result to construct our causal set expressions for geometric objects relating to the boundary, and show that they have the appropriate continuum limits. In Section 3.5 we investigate the proposed causal set bulk action for causal intervals in flat

¹This convention of an always past-pointing normal vector differs from the convention in the previous chapter. We have chosen it here for convenience.

spacetime and show that its mean takes the form, in the continuum limit, of a boundary contribution from the codimension-2 “joint” of the interval’s boundary.

There are many geometric quantities that already have causal set analogues, and in this chapter we will add to that list. The more quantities that are accumulated, the more evidence there is that any geometrical quantity can be “read off” from the causal set. This growing list of quantities also provides evidence for the *Hauptvermutung* — the conjecture that two very different Lorentzian manifolds cannot be good approximations of the same causal set [39].

3.2 Volume of a Small Causal Cone

One aspect of spacetime structure in which research has been fruitful recently is the geometry of certain small spacetime regions [2, 40–46]. Understanding the geometry of such regions has led to new ways of deriving Einstein’s equations from a different set of fundamental principles [41], and an understanding of the geometry of small spacetime intervals, in particular, has been beneficial for the causal set approach to quantum gravity [39, 47]. There is motivation, therefore, to study small spacetime regions in Lorentzian geometry, to further our understanding of spacetime and to provide tools in the search for quantum gravity.

In order to construct our causal set expressions we need to study a particular small region of spacetime — the *causal cone*, which will be defined shortly. In this section we will derive a universal formula for the volume of a small causal cone. This formula will be general in that it can be applied to a wide class of spacetimes.

3.2.1 The Setup

We will restrict our discussion to a d -dimensional, causal, Lorentzian spacetime, (M, g) , of finite volume that admits a compact spacelike submanifold, Σ . A *causal cone* is then constructed in the following way. Choose a *base point* $p \in \Sigma$ and let γ be the affinely parameterised timelike geodesic starting at p with tangent vector, V_p , normal to Σ and future pointing. Travel along this geodesic (in the positive time direction) a proper time T , to a point q . Past going null rays are sent out from q to form the past light-cone of q , denoted by $\partial J^-(q)$. We can then define the *causal cone* to be the region that is the intersection of the future of Σ and the past of q , i.e. the region $\mathcal{X}_q := J^+(\Sigma) \cap J^-(q)$. The *base* of the causal cone is the region $B_q := \Sigma \cap J^-(q)$ and the upper bounding null surface, the *hat*, is the region

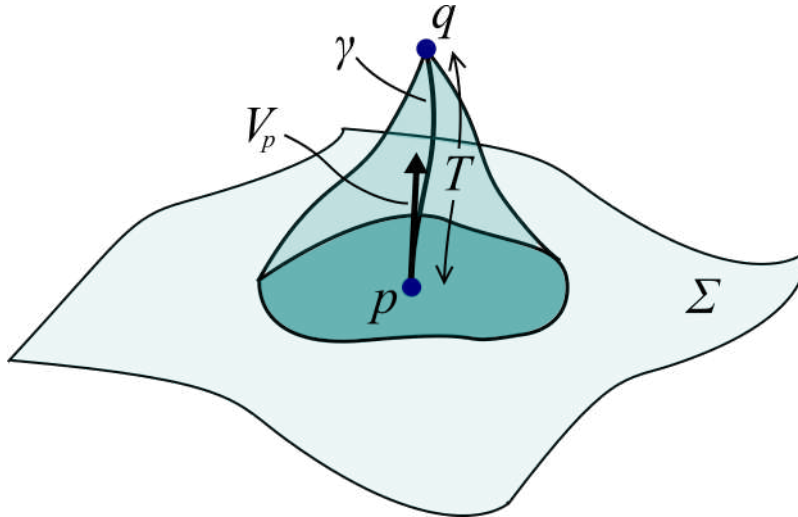


Figure 3.1: A illustration of a causal cone in 3 dimensions of spacetime.

$T_q := J^+(\Sigma) \cap \partial J^-(q)$. An illustration of this setup is shown in Figure 3.1.

We then ask, what is the spacetime volume of this causal cone as an expansion in small T (relative to the curvature scales of the chosen spacetime and hypersurface)? The terms in front of each power of T in the expansion will be universal, in that they will have the same form (in terms of known geometrical quantities) for any sufficiently well behaved spacetime. These terms can only depend upon the geometry of the spacetime local to the small causal cone (global topology does not enter the discussion, as we assume the causal cone is small enough to not see it). We can encode this local geometric dependence by having the terms depend upon geometrical quantities evaluated at p . If we chose the terms to depend upon geometrical quantities at another point, say q , then we could always represent these quantities at q as series expansions in T with coefficients depending upon the quantities evaluated at p . In this way one can see that any choice of where to evaluate the geometric quantities (local to the small causal cone) can be related to the choice we make here — to evaluate them at p . For small enough T this volume should tend to the volume of a flat cone in Minkowski spacetime with a flat base. In the next section we will discuss this in more detail, along with the leading order correction to the cone volume after this flat contribution.

3.2.2 Leading Order Correction to Small Volume

In this section we will use special coordinates in order to simplify the calculation of the cone volume correction.

Let $x^\mu = (t, \mathbf{x})$ be “synchronous” or Gaussian Normal Coordinates (GNCs)

adapted to Σ such that in a neighbourhood U_Σ of Σ the line element is

$$ds^2 = -dt^2 + h_{ij}(t, \mathbf{x})dx^i dx^j . \quad (3.3)$$

In these coordinates the surface Σ corresponds to $t = 0$, and the spatial coordinates on Σ are \mathbf{x} . Each point $x \in U_\Sigma$ lies on a unique timelike geodesic with a tangent vector whose components at Σ are $-n^\alpha$, where n^α is the past pointing normal to the surface as defined previously. The t coordinate of x is equal to the proper time from Σ to x along that geodesic. The restriction of the spacetime to this neighbourhood of Σ is globally hyperbolic with Cauchy surface Σ . These coordinates will also be useful later when deriving the causal set expressions.

Recall that p is the point on Σ where the unique timelike geodesic through q , whose tangent is normal to Σ , intersects Σ . Let the values of q 's GNCs be $x_q^\mu = (t_q, \mathbf{x}_q)$, then p has GNCs $x_p^\mu := x^\mu(p) = (0, \mathbf{x}_q)$. We choose T small enough such that there exists a Riemann normal neighbourhood centred on p containing the cone region \mathcal{X}_q . We choose Riemann Normal Coordinates (RNCs) centered at p , $y^{\bar{\mu}} = (y^{\bar{0}}, \mathbf{y}) = (\bar{t}, \mathbf{y})$, such that the GNC time coordinate of q equals the RNC time coordinate of q : $t_q = \bar{t}_q =: T$.

The relationship between RNCs $y^{\bar{\mu}}$ and GNCs x^ν is, to second order,

$$y^{\bar{\mu}} = A^{\bar{\mu}}_{\nu} (x^\nu - x_p^\nu) + \frac{1}{2} A^{\bar{\mu}}_{\mu} \Gamma^{\mu}_{\nu\rho}(p) (x^\nu - x_p^\nu) (x^\rho - x_p^\rho) + O((x - x_p)^3) . \quad (3.4)$$

The constant matrix $A^{\bar{\mu}}_{\mu}$ obeys

$$A^{\bar{\mu}}_{\mu} A^{\bar{\nu}}_{\nu} \eta_{\bar{\mu}\bar{\nu}} = g_{\mu\nu}(p) , \quad (3.5)$$

and the metric and Christoffel symbols in RNCs are flat at p :

$$\begin{aligned} g_{\bar{\mu}\bar{\nu}}(p) &= \eta_{\bar{\mu}\bar{\nu}} , \\ \Gamma^{\bar{\mu}}_{\bar{\nu}\bar{\rho}}(p) &= 0 . \end{aligned} \quad (3.6)$$

The inverse coordinate transformation is

$$x^\mu = x_p^\mu + A^{\mu}_{\bar{\mu}} y^{\bar{\mu}} + O(y^3) , \quad (3.7)$$

where $A^{\mu}_{\bar{\mu}}$ is the inverse matrix of $A^{\bar{\mu}}_{\mu}$, i.e. $A^{\bar{\mu}}_{\mu} A^{\mu}_{\bar{\nu}} = \delta^{\bar{\mu}}_{\bar{\nu}}$ and $A^{\mu}_{\bar{\mu}} A^{\bar{\nu}}_{\nu} = \delta^{\mu}_{\nu}$. There is no $O(y^2)$ term in (3.7) due to the fact that $\Gamma^{\bar{\mu}}_{\bar{\nu}\bar{\rho}}(p) = 0$. The components of $A^{\bar{\mu}}_{\mu}$ satisfy $A^{\bar{0}}_0 = 1$, $A^{\bar{0}}_i = 0$, $A^{\bar{i}}_i A^{\bar{j}}_j \delta_{\bar{i}\bar{j}} = h_{ij}(p)$ and $\delta_{\bar{i}\bar{j}} = A^i_{\bar{i}} A^j_{\bar{j}} h_{ij}(p)$.

In the $T \rightarrow 0$ limit we have that $q \rightarrow p$ along the geodesic normal to Σ . That

makes the region \mathcal{X}_q , whose volume we need, tend to a truncated solid, nearly flat cone with apex q and a base on Σ defined by a quadratic form in the three spatial RNCs around p . The leading contribution to the volume,

$$V_{\blacktriangle}(q) = \int_{\mathcal{X}_q} d^d y \sqrt{-g(y)}, \quad (3.8)$$

is therefore the volume, $\frac{\text{vol}(S_{d-2})}{d(d-1)} T^d$, of the flat cone of height T with a flat base on surface $\bar{t} = 0$, where $\text{vol}(S_{d-2})$ is the volume of a unit $(d-2)$ -sphere. Corrections to this are higher order in T and come from three sources: (i) $\sqrt{-g(y)} \neq 1$, (ii) the null geodesics down from q to Σ , making up the hat T_q , are not straight, and (iii) the base, B_q is not a flat disc. The first two corrections are due to the curvature of M and the third comes from the extrinsic curvature of Σ .

The correction from (iii) is found by taking the spacetime to be flat, so that RNCs are the usual Cartesian coordinates centred at p and T_q is the top boundary of the flat cone, satisfying $\sum_{i=1}^{d-1} (y^{\bar{i}})^2 = (T - \bar{t})^2$ and $\bar{t} \in [0, T]$. The base B_q in GNCs lies in the surface $t = 0$, so we can use (3.4) to find the equation for the surface in RNCs. This gives

$$\bar{t} = \frac{1}{2} \Gamma_{ij}^0(p) (x^i - x_p^i) (x^j - x_p^j) + O((x - x_p)^3). \quad (3.9)$$

The linear part on the right hand side of (3.4) vanishes, since $A_{\mu}^{\bar{0}}(x^{\mu} - x_p^{\mu}) = t$ (which follows from $A_{\bar{i}}^{\bar{0}} = 0$ and $A_{\bar{0}}^{\bar{0}} = 1$) and $t = 0$ on the bottom surface. Using the inverse RNC relation (3.7), the equation for B_q in RNCs is

$$\bar{t} = \frac{1}{2} \Gamma_{ij}^0(p) A_{\bar{i}}^i A_{\bar{j}}^j y^{\bar{i}} y^{\bar{j}} + O(y^3). \quad (3.10)$$

Let us rewrite this equation in spherical polar coordinates, i.e. define $r := \sqrt{\delta_{\bar{i}\bar{j}} y^{\bar{i}} y^{\bar{j}}}$ and the usual angular coordinates $\phi_1, \dots, \phi_{d-2}$ in terms of the spatial coordinates $y^{\bar{1}} = r \cos(\phi_1), \dots, y^{\bar{d-1}} = r \sin(\phi_1) \cdots \sin(\phi_{d-3}) \sin(\phi_{d-2})$. Then

$$\bar{t} = \frac{1}{2} \left(\Gamma_{ij}^0(p) A_{\bar{i}}^i A_{\bar{j}}^j \frac{y^{\bar{i}} y^{\bar{j}}}{r^2} \right) r^2 + O(y^3) = \frac{1}{2} f(\mathbf{x}_q, \boldsymbol{\phi}) r^2 + O(y^3), \quad (3.11)$$

where $\boldsymbol{\phi}$ stands collectively for all the angular coordinates $\phi_1, \dots, \phi_{d-2}$. The function $f(\mathbf{x}_q, \boldsymbol{\phi})$ depends on \mathbf{x}_q since Γ_{ij}^0 and $A_{\bar{i}}^i$ depend on the position p .

With the boundaries of the integration region in hand, we can now write down

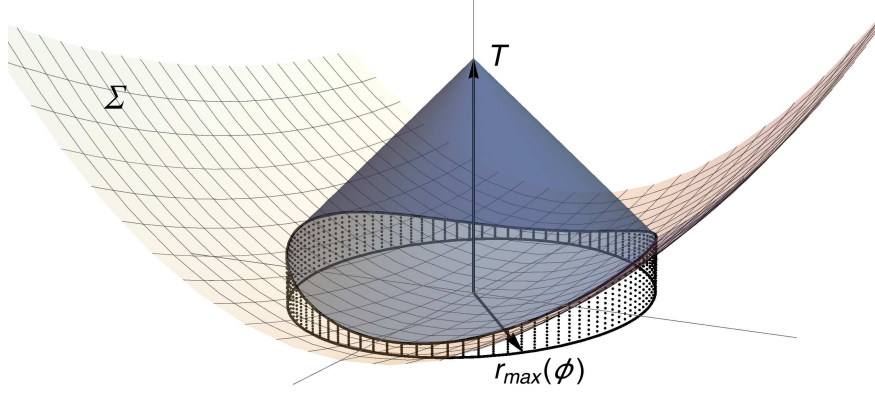


Figure 3.2: A 3-dimensional representation of the region \mathcal{X}_q in RNCs. The hat, T_q , of $\partial\mathcal{X}_q$ can be approximated as a flat cone, and the base, B_q , intersects T_q at a radial coordinate, $r_{max}(\phi)$, which will in general be a function of the angles ϕ (in 3 dimensions there is one angle ϕ). This function is found by projecting down from the intersection to the \bar{t} plane.

the integral explicitly in spherical coordinates:

$$\int_{\mathcal{X}_q \text{ in flat space}} d^d y = \int_{S^{d-2}} d\Omega_{d-2} \int_0^{r_{max}(\phi)} r^{d-2} dr \int_{\frac{1}{2}f(\mathbf{x}_q, \phi)r^2}^{-r+T} d\bar{t} + O(T^{d+2}), \quad (3.12)$$

where $r_{max}(\phi)$ is the value of the radial coordinate for which B_q intersects T_q at an angle ϕ , as shown in Figure 3.2. Equating the time coordinates of T_q and B_q gives

$$\frac{1}{2}f(\mathbf{x}_q, \phi)r_{max}^2(\phi) = -r_{max}(\phi) + T. \quad (3.13)$$

We solve this for $r_{max}(\phi)$ and take the positive solution. The solution can be expanded in T and is simply $r_{max} = T + O(T^2)$, with angular dependent terms contributing at $O(T^2)$. The $O(T^2)$ term will contribute at $O(T^{d+2})$ in the volume integral. Substituting $r_{max} = T$ into (3.12) allows us to evaluate the integral (3.12), which equals

$$\frac{\text{vol}(S_{d-2})}{d(d-1)} T^d \left(1 - \frac{d}{2(d+1)} \Gamma_{ij}^0(p) A_{\bar{i}}^i A_{\bar{j}}^j \delta^{\bar{i}\bar{j}} T \right) + O(T^{d+2}), \quad (3.14)$$

where the $\delta^{\bar{i}\bar{j}}$ comes from the fact that cross terms ($\bar{i} \neq \bar{j}$) vanish under the angular integration. The defining relations for $A_{\bar{i}}^i$ can be rearranged to give $A_{\bar{i}}^i A_{\bar{j}}^j \delta^{\bar{i}\bar{j}} = h^{ij}(p)$, and in GNCs the extrinsic curvature on the surface is given by

$$K = -\Gamma_{ij}^0 h^{ij} = -\frac{1}{2} \frac{\dot{h}}{h}. \quad (3.15)$$

Substituting this into (3.14) we obtain

$$\frac{\text{vol}(S_{d-2})}{d(d-1)} T^d \left(1 + \frac{d}{2(d+1)} K(0, \mathbf{x}_q) T \right) + O(T^{d+2}), \quad (3.16)$$

where the arguments of the extrinsic curvature K are the GNC's of p . We can now see that the first contribution is the volume of the flat cone with flat base as expected, and the first correction is of order T^{d+1} .

The corrections (i) and (ii) come from the non-flatness of the metric. The determinant $\sqrt{-g}$ can be expanded in RNCs and the deviation of T_q from straight lines considered. The curvature contribution to the volume of a small, approximately flat causal interval – or Alexandrov neighbourhood – of these effects has been calculated [40, 46, 48] and the same arguments show that the corrections (i) and (ii) in our case are of the same order, $O(T^{d+2})$, which means they are suppressed with respect to the correction derived above. This is to be expected on dimensional grounds as extrinsic curvature has dimensions of inverse length whereas Riemann curvature has dimensions of inverse length squared. We will see that $O(T^{d+2})$ corrections do not contribute to the causal set boundary term in the limit.

If (T, \mathbf{x}) are the GNCs of a point $q \in U_\Sigma \cap M^+$ then we have $T > 0$. If we allow ourselves to use the GNCs of q as the argument of the cone volume function, i.e $V_\blacktriangle(q) = V_\blacktriangle(T, \mathbf{x})$, we have

$$V_\blacktriangle(T, \mathbf{x}) = \frac{\text{vol}(S_{d-2})}{d(d-1)} T^d \left(1 + \frac{d}{2(d+1)} K(0, \mathbf{x}) T \right) + O(T^{d+2}). \quad (3.17)$$

If we take $(-T, \mathbf{x})$ to be the GNCs of a point $q \in U_\Sigma \cap M^-$, then $T > 0$ and T denotes the absolute value of the proper time along the geodesic from p to q . Following the same steps as above we can compute the volume of the ‘‘upside down’’ causal cone to the past of Σ . Such a cone is constructed by moving backwards in time along the geodesic from p to q , and by sending out forward going null rays from q till they intersect Σ . The upside down causal cone is the region $J^-(\Sigma) \cap J^+(q)$ and its volume, $V_\blacktriangledown(q) = V_\blacktriangledown(-T, \mathbf{x})$, is:

$$V_\blacktriangledown(-T, \mathbf{x}) = \frac{\text{vol}(S_{d-2})}{d(d-1)} T^d \left(1 - \frac{d}{2(d+1)} K(0, \mathbf{x}) T \right) + O(T^{d+2}), \quad (3.18)$$

where $T > 0$.

3.2.3 Definitions for Higher Order Terms

We now turn to the question of the higher order corrections to the cone volume. There may be more geometric objects, other than the extrinsic curvature, that can contribute at this order, and in the next section we derive exactly which geometric objects enter into the formula for the volume, up to the order we are considering. Some of these geometric quantities relate to the past pointing normal vector (one could equally use the future pointing normal) to Σ , which we denote by N_Σ , and the future pointing tangent vector along γ (the geodesic from p to q), V_γ . To simplify our search for the different geometric quantities we define a vector field that captures the information of both N_Σ and V_γ . Finding all of the quantities relating to N_Σ and V_γ then reduces to enumerating all the possible derivatives of this single vector field, up to the relevant order, and evaluating them at p . We now define such a vector field.

Let x^α be coordinates for (M, g) , where $\alpha = 0, \dots, d-1$. In Section 2.2 we used a function $S(x)$ to define the normal, and we will do something similar here. Choose a function $S(x)$ (where $x \in M$) that increases to the future, equals zero on Σ , and equals the proper time along γ from p to x for $x \in \gamma$ ². We then define the normalised covector $n_\alpha := (-g^{\mu\nu} \partial_\mu S \partial_\nu S)^{-\frac{1}{2}} \partial_\alpha S$, and the past pointing vector $n^\alpha := g^{\alpha\beta} n_\beta$. When evaluated on the surface, n^α are the components of N_Σ , and when evaluated along γ they are the components of $-V_\gamma$ (the factor of -1 comes from the fact that n^α is past pointing and the tangent vector to γ is future pointing). In this way the vector field n^α encodes the vectors N_Σ and V_γ at the same time.

The conditions that our chosen function must satisfy afford us a lot of freedom. Any function satisfying the above conditions will give the same vector n^α evaluated at $x \in \Sigma \cup \gamma$, but two such functions will in general give rise to vector fields that differ for $x \notin \Sigma \cup \gamma$. When we choose our function $S(x)$ we are effectively choosing the form of n^α away from $\Sigma \cup \gamma$. This choice is independent of our causal cone setup, and any geometric quantities relating to our setup cannot depend on this choice.

Recall the transverse metric on Σ is defined as $h_{\alpha\beta} := g_{\alpha\beta} + n_\alpha n_\beta$. If we raise an index with $g^{\alpha\beta}$ then we get the tensor h^α_β which projects vectors into the tangent space of Σ , and satisfies $h^\alpha_\beta n^\beta = 0$ and $h^\alpha_\beta h^\beta_\gamma = h^\alpha_\gamma$. The extrinsic curvature tensor is defined as $K_{\alpha\beta} := n_{\sigma;\rho} h^\rho_\alpha h^\sigma_\beta$, where the semi-colon denotes the covariant derivative. The extrinsic curvature scalar is then $K := K_{\alpha\beta} g^{\alpha\beta}$, and it can be shown

²The definition of $S(x)$ may be reminiscent of the construction of the time coordinate in Gaussian normal coordinates. The definition of the time coordinate in that case requires us to talk about *all* the geodesics with tangent vectors normal to Σ . Here we only care about the single geodesic γ .

that $K = n^\alpha{}_{;\alpha}$ and $K^{\alpha\beta}K_{\alpha\beta} = n^\alpha{}_{;\beta}n^\beta{}_{;\alpha}$ on Σ . The last two relations are both independent of our choice of n^α away from Σ . For more discussion on the geometric quantities mentioned here we refer the reader to [49].

3.2.4 All Possible Contributions

In this section we will work out the next-to-leading contributions to the general volume formula for a small causal cone. In section 3.2.2 we saw that

$$V_\blacktriangle(T) = V_{\text{flat}}(T) \left(1 + \frac{d}{2(d+1)}KT + \mathcal{O}(T^2) \right), \quad (3.19)$$

where K is evaluated at p , $V_{\text{flat}}(T) := \frac{\text{vol}(S_{d-2})}{d(d-1)}T^d$ is the volume of a flat cone in Minkowski spacetime with a flat base, and we have omitted the spatial coordinates of p from the arguments for brevity. Here, we are interested in the $\mathcal{O}(T^2)$ term in the brackets in (3.19), which is $\mathcal{O}(T^{d+2})$ if we include the prefactor. The expression multiplying T^2 in this term will be a sum of geometric scalars which, by dimensional analysis, must all have dimensions of length L^{-2} . The only scalars that contribute are K^2 , $K^{\alpha\beta}K_{\alpha\beta}$, R and $R_{\alpha\beta}n^\alpha n^\beta$ (where we have used the usual definitions of the Ricci tensor and Ricci scalar), which we will now show.

To systematically determine all the possible scalar quantities we start with the basic dimensionless objects, $g_{\alpha\beta}$ and n^α , from which any geometric expression relating to our setup can be constructed. In order to get the right dimensions of length we then form all the scalars involving these objects that contain two derivatives. Every scalar we form will either contain a second order derivative or a product of first order derivatives.

Let us start with the metric $g_{\alpha\beta}$. There are no covariant expressions that can be formed from first order derivatives of $g_{\alpha\beta}$ so we only need to consider its second order derivatives. At second order we have the Riemann tensor, $R_{\alpha\beta\gamma\delta}$, and in order to make a scalar we must contract it with $g^{\alpha\beta}$ and/or n^α . The only two resulting expressions that can be formed from such contractions are R and $R_{\alpha\beta}n^\alpha n^\beta$.

There are no terms related to the intrinsic curvature of Σ that can be included. For example, the intrinsic Ricci scalar ${}^{d-1}R$ cannot be included as it is not independent from the four quantities we have already, which can be seen from the Gauss-Codazzi equations [49]. The only other possibility is the Ricci tensor of Σ , but we cannot include this as there is nothing to contract it with to give a non-zero quantity other than ${}^{d-1}R$.

We now turn to the vector field n^α . It still remains to be checked that there

are no other scalars that should be included involving a second order derivative or a product of first order derivatives of n^α . To completely exhaust the latter possibility let us write down the most general (in the sense that we have not contracted any indices) product of two first order derivatives: $n^\alpha{}_{;\beta}n^\gamma{}_{;\delta}$. We can use the fact that $n^\alpha{}_{;\beta}n^\beta = 0$ at p , and that $n_{\alpha;\beta}n^\alpha = \frac{1}{2}(n^\alpha n_\alpha)_{;\beta} = 0$ to show that contracting any of the indices with n^μ will give 0. We, therefore, must contract with the metric to get something non-zero, and one can show that such contractions will give either K^2 or $K^{\alpha\beta}K_{\alpha\beta}$. For example, take the following contraction:

$$\begin{aligned}
n^\alpha{}_{;\beta}n^\gamma{}_{;\delta}g_{\alpha\gamma}g^{\beta\delta} &= n_{\alpha;\beta}n_{\gamma;\delta}g^{\alpha\gamma}g^{\beta\delta} \\
&= n_{\alpha;\beta}n_{\gamma;\delta}h^{\alpha\gamma}h^{\beta\delta} \\
&= n_{\alpha;\beta}n_{\gamma;\delta}h^\alpha{}_\rho h^\gamma{}_\sigma g^{\rho\sigma}h^\beta{}_\mu h^\delta{}_\nu g^{\mu\nu} \\
&= K_{\mu\rho}K_{\nu\sigma}g^{\rho\sigma}g^{\mu\nu} \\
&= K^{\nu\sigma}K_{\nu\sigma} .
\end{aligned} \tag{3.20}$$

In the first line we have used the fact that $g^{\alpha\beta} = h^{\alpha\beta} - n^\alpha n^\beta$, and that the resulting contractions with n^μ vanish. In the second line we have used the fact that $h^{\alpha\beta} = h^\alpha{}_\gamma h^\beta{}_\delta g^{\gamma\delta}$, and in the third line we have combined the relevant terms to form the two extrinsic curvature tensors. The other possible contractions of $n^\alpha{}_{;\beta}n^\gamma{}_{;\delta}$ with the metric trivially result in either K^2 or $K^{\alpha\beta}K_{\alpha\beta}$.

The most general second order derivative of n^α is $n^\alpha{}_{;\beta\gamma}$ (in the sense that no indices have been contracted). If we do not contract the bottom two indices with $n^\beta n^\gamma$ or $h^\beta{}_\delta h^\gamma{}_\sigma$ the resulting expression will depend on our choice of n^α away from $\Sigma \cup \gamma$, which cannot be the case for any quantity relating to our geometric setup. To see this let us do the following contraction: $n^\alpha{}_{;\beta\gamma}n^\beta h^\gamma{}_\sigma$. If we evaluate this at p then the contraction with n^β projects the first derivative along the geodesic γ , and the contraction with $h^\gamma{}_\sigma$ projects the second derivative tangent to the surface. Such a second order derivative will depend on the form of n^α away from $\Sigma \cup \gamma$. If we stick to contractions with $n^\beta n^\gamma$ or $h^\beta{}_\delta h^\gamma{}_\sigma$ then we only have to deal with second order derivatives along γ or within the surface respectively, which do not depend on n^α away from $\Sigma \cup \gamma$. If we contract $n^\alpha{}_{;\beta\gamma}$ with $n^\beta n^\gamma$ the resulting expression vanishes at p , using the fact that $n^\alpha{}_{;\beta}n^\beta = 0$ along γ and that $n^\alpha{}_{;\beta}n_\alpha = 0$. If we contract with $h^\beta{}_\delta h^\gamma{}_\sigma$ then the two indices δ and σ must be contracted with $g^{\delta\sigma}$, as a contraction with n^δ will give 0. We also need to contract the free α index, which we can only do with n_α . The resulting expression does not give anything new, as can be seen by

manipulating it as follows:

$$\begin{aligned}
n^\alpha{}_{;\beta\gamma} n_\alpha h^\beta{}_\delta h^\gamma{}_\sigma g^{\delta\sigma} &= n^\alpha{}_{;\beta\gamma} n_\alpha g^{\beta\gamma} \\
&= \left((n^\alpha{}_{;\beta} n_\alpha)_{;\gamma} - n^\alpha{}_{;\beta} n_{\alpha;\gamma} \right) g^{\beta\gamma} \\
&= -n^\alpha{}_{;\beta} n_{\alpha;\gamma} g^{\beta\gamma} \\
&= -n_{\alpha;\beta} n_{\rho;\gamma} g^{\alpha\rho} g^{\beta\gamma} \\
&= -K^{\alpha\beta} K_{\alpha\beta} .
\end{aligned} \tag{3.21}$$

The equality in the first line comes from the fact that $h^\beta{}_\delta h^\gamma{}_\sigma g^{\delta\sigma} = h^{\beta\gamma} = g^{\beta\gamma} + n^\beta n^\gamma$, and that the resulting contraction with $n^\beta n^\gamma$ vanishes, as explained above. The first term in brackets on the second line vanishes as $n^\alpha{}_{;\beta} n_\alpha = 0$, and in the fourth line we have used (3.20). We have now exhausted the list of possible scalars that can contribute to the volume formula.

The most general formula for the expansion of $V_\blacktriangle(T)$ up to $\mathcal{O}(T^{d+2})$ can be written down as

$$\begin{aligned}
V_\blacktriangle(T) = V_{\text{flat}}(T) &\left(1 + \frac{d}{2(d+1)} KT + (c_1 K^2 + c_2 K^{\alpha\beta} K_{\alpha\beta} \right. \\
&\left. + c_3 R + c_4 R_{\alpha\beta} n^\alpha n^\beta) T^2 + \mathcal{O}(T^3) \right),
\end{aligned} \tag{3.22}$$

where the geometric quantities are evaluated at p . The coefficients c_1, c_2, c_3 and c_4 cannot depend on any geometrical quantities related to the spacetime, since we have already incorporated this information in the four quantities $K^2, K^{\alpha\beta} K_{\alpha\beta}, R$ and $R_{\alpha\beta} n^\alpha n^\beta$. The only remaining quantity that we can encode in these coefficients, and that is local to the causal cone, is the dimension of the spacetime. Therefore, the coefficients c_1, c_2, c_3 and c_4 can only depend on the dimension, and their form in terms of the dimension will not depend on the geometry of the spacetime, i.e. they are universal for a given dimension.

We could proceed as in 3.2.2 and use RNC's to find these coefficients as was done in [44, 46], but this would be more complicated now that we are dealing with a higher order contribution to the volume. Instead, we can follow the approach of Gibbons and Solodukhin in [40]. Their approach only requires us to use different spacetime setups in which we know the volume expansions and the relevant geometric quantities. The different spacetime setups can then be used to pin down the dependence of these coefficients on the dimension.

It should be mentioned that our derivation of this volume formula has not presupposed a specific spacetime. This volume formula can be applied to any

sufficiently well behaved spacetime. Different spacetimes will give different causal cone volumes if the geometric quantities present in (3.22) differ for the given spacetimes, or if their dimensions differ.

Finally, the next order correction to this volume expansion is assumed to be of order T^{d+3} , since all of the volume expansions we have encountered in specific spacetimes have had this form.

3.2.5 Intrinsic Curvature Terms

In order to determine the coefficients in front of the terms involving R and $R_{\alpha\beta}n^\alpha n^\beta$ we can follow what was done in [40]. There, Gibbons and Solodukhin derive the volume formula for a small interval in a general spacetime by calculating the volume of specific intervals in the Einstein static universe and in de Sitter spacetime. In both spacetimes we can form causal cones from the intervals that Gibbons and Solodukhin considered by taking their “top-halves”. The construction of the top-half of the interval in the Einstein static universe or the de Sitter spacetime is as follows.

Take the geodesic going from the past-most point of the interval to the future-most point, and take p to be the point half way along that geodesic in proper time. The point q is the future-most point of the interval and the tangent vector of this geodesic at p is V_p . This tangent vector is orthogonal to a family of spacelike vectors which generate geodesics expanding out from p . We can take the union of these geodesics to be Σ . Given that we have p , q and Σ , we can construct our causal cone as above. In both spacetimes the base surface generated in this way will have zero extrinsic curvature, and hence we can write the volume expansion as

$$V_{\blacktriangle}(T) = V_{\text{flat}}(t) \left(1 + (c_3 R + c_4 R_{\alpha\beta} n^\alpha n^\beta) T^2 + \mathcal{O}(T^3) \right) . \quad (3.23)$$

In both spacetimes the volume of the causal cone is simply half the volume of interval from which it was constructed. Therefore, the values of the coefficients c_3 and c_4 can immediately be determined from the interval volume formula in [40]. We find that

$$\begin{aligned} c_3 &= -\frac{d}{6(d+1)(d+2)} \\ c_4 &= \frac{d}{6(d+1)} . \end{aligned} \quad (3.24)$$

3.2.6 Extrinsic Curvature Terms

We now move on to the extrinsic curvature terms in (3.22). For simplicity we can take the spacetime to be Minkowski so that the intrinsic curvature terms all vanish, and look at two curved surfaces within the spacetime. The two surfaces will be specific cases of a one parameter family of surfaces defined by

$$\Sigma_a := \{x \in M \mid S_a(x) = 0\} , \quad (3.25)$$

where a is the one (positive) parameter and

$$S_a(x) := t - r^2 (a \cos^2(\theta_1) + \sin^2(\theta_1)) . \quad (3.26)$$

We have used spherical polar coordinates for the spatial coordinates, such that the coordinates are $x^\mu = (t, r, \theta_1, \dots, \theta_{d-2})$ (where θ_{d-2} ranges over $[0, 2\pi)$ while the others range over $[0, \pi]$). Each surface in the family is not necessarily spacelike everywhere, so we choose the base point of the cone, p , to be at the origin of the coordinate system where the surfaces are spacelike. We also choose T small enough, with respect to a , such that the causal cone's base is a region of the surface that is entirely spacelike. We will first determine the volume of a causal cone for a general choice of the parameter a , and then specify at the end to determine the coefficients c_1 and c_2 .

Using the function $S_a(x)$ one can determine the geometric quantities of interest:

$$\begin{aligned} K &= -2(a + d - 2) , \\ K^{\alpha\beta} K_{\alpha\beta} &= 4(a^2 + d - 2) , \end{aligned} \quad (3.27)$$

evaluated at p . The volume of the causal cone is

$$\begin{aligned} V_\blacktriangle(T) &= \int d\Omega_{d-2} \int_0^{r_{int}(\theta_1)} dr r^{d-2} \int_{r^2(a \cos^2 \theta_1 + \sin^2 \theta_1)}^{-r+T} dt \\ &= \text{vol}(S_{d-3}) \int_0^\pi d\theta_1 \sin^{d-3}(\theta_1) \int_0^{r_{int}(\theta_1)} dr r^{d-2} \int_{r^2(a \cos^2 \theta_1 + \sin^2 \theta_1)}^{-r+T} dt \\ &= \frac{\text{vol}(S_{d-2})}{d(d-1)} T^d \left(1 - \frac{d(a+d-2)}{d+1} T \right. \\ &\quad \left. + \frac{d(3a^2 + 2a(d-2) + d(d-2))}{2(d+1)} T^2 + \mathcal{O}(T^3) \right) . \end{aligned} \quad (3.28)$$

In the first line we have evaluated the integrals for the angular coordinates that do not appear in the rest of the integral. In this case the radius of intersection of the

hat and base, $r_{int}(\theta_1)$, depends on θ_1 . Explicitly this radius is

$$r_{int}(\theta_1) = \frac{-1 + \sqrt{1 + 4aT \cos^2(\theta_1) + 4T \sin^2(\theta_1)}}{2(a \cos^2(\theta_1) + \sin^2(\theta_1))}. \quad (3.29)$$

Given that we only need the $\mathcal{O}(T^2)$ correction to the flat volume of the causal cone, we only require $r_{int}(\theta_1)$ up to $\mathcal{O}(T^2)$. We can, therefore, Taylor expand the RHS of (3.29) in small T and only keep up to $\mathcal{O}(T^2)$. Using this expansion in place of $r_{int}(\theta_1)$ in (3.28) makes it possible to evaluate the θ_1 integral and arrive at the final expression.

We equate the $\mathcal{O}(T^2)$ correction in the volume to $c_1 K^2 + c_2 K^{\alpha\beta} K_{\alpha\beta}$, and by using (3.27) we find the following equation for c_1 and c_2 :

$$(a + d - 2)^2 c_1 + (a^2 + d - 2) c_2 = \frac{d(3a^2 + 2a(d - 2) + d(d - 2))}{8(d + 1)}. \quad (3.30)$$

We now specialise to the two surfaces given by $a = 0$ and $a = 1$. Both choices of a can be substituted into (3.30) to give two simultaneous equations for c_1 and c_2 , the solution for which is

$$c_1 = \frac{d}{8(d + 1)}, \quad (3.31)$$

$$c_2 = \frac{d}{4(d + 1)}. \quad (3.32)$$

The final formula for the volume of a causal cone is then

$$V_{\blacktriangle}(T) = V_{\text{flat}}(T) \left(1 + \frac{d}{2(d + 1)} KT + \frac{d}{4(d + 1)} \left(\frac{1}{2} K^2 + K^{\alpha\beta} K_{\alpha\beta} - \frac{2}{3(d + 2)} R + \frac{2}{3} R_{\alpha\beta} n^\alpha n^\beta \right) T^2 + \mathcal{O}(T^3) \right). \quad (3.33)$$

Similar steps can be carried out to determine the formula for the volume of the ‘‘upside down’’ causal cone $V_{\blacktriangledown}(-T)$:

$$V_{\blacktriangledown}(-T) = V_{\text{flat}}(T) \left(1 - \frac{d}{2(d + 1)} KT + \frac{d}{4(d + 1)} \left(\frac{1}{2} K^2 + K^{\alpha\beta} K_{\alpha\beta} - \frac{2}{3(d + 2)} R + \frac{2}{3} R_{\alpha\beta} n^\alpha n^\beta \right) T^2 + \mathcal{O}(T^3) \right), \quad (3.34)$$

where we recall that $T > 0$.

3.3 Use In Causal Set Theory

In this section we will apply (3.33) and (3.34) to causal set theory. The general motivation for this work is to add to the list of geometric quantities that we can glean from the causal set. Each new quantity added to this list provides further evidence in favor of the Hauptvermutung, and strengthens the idea that the causal set can encode all of spacetime geometry.

3.3.1 The Mean of \mathbf{P}_k and \mathbf{F}_k

We say an element of a causal set, \mathcal{C} , is of \mathcal{P}_k (\mathcal{F}_k) type if it has k elements to its past (future), and we understand that this property can only be attributed to an element if \mathcal{C} is past (future) finite. We define the functions $P_k[\mathcal{C}]$ and $F_k[\mathcal{C}]$ on a causal set, \mathcal{C} , to be those that return the number of \mathcal{P}_k and \mathcal{F}_k elements in \mathcal{C} respectively.

We will restrict ourselves to sprinklings into the spacetime (M, g) described above with a spatial surface Σ and its future and past sets $M^\pm = J^\pm(\Sigma)$. A sprinkling into such a spacetime naturally generates a partition of the sprinkled causal set, that which has been sprinkled to the future of Σ , M^+ , which we call \mathcal{C}^+ , and that which has been sprinkled to the past of Σ , M^- , which we call \mathcal{C}^- . We define the random variable \mathbf{P}_k (\mathbf{F}_k) as that which takes the value of the function P_k (F_k) acting on the sprinkled causal set \mathcal{C}^+ (\mathcal{C}^-). It should be noted that strictly speaking the random variable is a function of the spacetime, the surface Σ and the sprinkling density ρ . In this section we aim to find the average over the sprinkling process of \mathbf{P}_k and \mathbf{F}_k as an expansion in large ρ . This will allow us to then craft causal set expressions that give continuum geometrical quantities on average in the $\rho \rightarrow \infty$ limit. An illustrative sketch of the idea is shown in Figure 3.3.

The probability that, in a given sprinkling, a point $x \in M^+$ is a \mathcal{P}_k element of \mathcal{C}^+ is given by the probability that k points of the sprinkling lie in the region $J^-(x) \cap J^+(\Sigma)$. For the Poisson process the probability of such an event is

$$\mathbb{P}(\mathbf{k} \text{ points in } J^-(x) \cap J^+(\Sigma)) = \frac{(\rho V_\blacktriangle(x))^k}{k!} e^{-\rho V_\blacktriangle(x)}, \quad (3.35)$$

We have written the causal cone volume as a function of the point x , as given a point x above Σ we can find the geodesic that intersects x with an initial tangent vector normal to Σ on the surface. From this geodesic we can get the proper time, T , between Σ and x , which we then insert into the causal cone volume formula in (3.33).

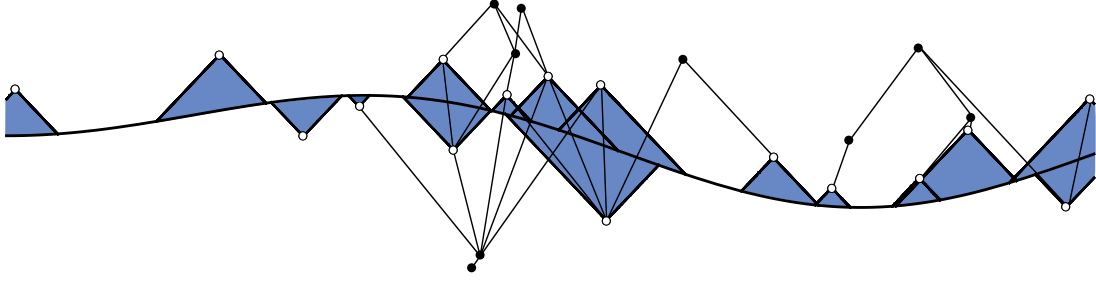


Figure 3.3: An illustration of a sprinkling into a spacetime partitioned by a spacelike hypersurface. Black points correspond to causal set elements and links (irreducible causal relations) between elements are shown as thin black lines. The maximal (\mathcal{F}_0) elements in \mathcal{C}^- and the minimal (\mathcal{P}_0) elements in \mathcal{C}^+ have been highlighted with white filling. The shaded areas illustrate the regions whose volumes are V_{\blacktriangle} and V_{\blacktriangledown} . In this sketch $P_0[\mathcal{C}^+] = 11$ and $F_0[\mathcal{C}^-] = 5$ (with time flowing upwards).

The probability of sprinkling an element into an infinitesimal d -volume, dV_x , at x is ρdV_x , and so the expected number of \mathcal{P}_k elements above Σ is an integral of the product of these probabilities, over all the spacetime points in M^+ . We, therefore, have the following expression for the expectation value of \mathbf{P}_k :

$$\langle \mathbf{P}_k \rangle = \rho \int_{J^+(\Sigma)} dV_x \frac{(\rho V_{\blacktriangle}(x))^k}{k!} e^{-\rho V_{\blacktriangle}(x)}. \quad (3.36)$$

Similarly the expected number of \mathcal{F}_k elements below Σ is

$$\langle \mathbf{F}_k \rangle = \rho \int_{J^-(\Sigma)} dV_x \frac{(\rho V_{\blacktriangledown}(x))^k}{k!} e^{-\rho V_{\blacktriangledown}(x)}, \quad (3.37)$$

where $V_{\blacktriangledown}(x) = \text{vol}(J^-(\Sigma) \cap J^+(x))$.

In order to evaluate (3.36) and (3.37) for large ρ we use ‘‘synchronous’’ or Gaussian Normal Coordinates (GNCs), $x^\mu = (t, \mathbf{x})$, adapted to Σ as was done in section 3.2.2. In a neighbourhood U_Σ of Σ the line element is

$$ds^2 = -dt^2 + h_{ij}(t, \mathbf{x}) dx^i dx^j, \quad (3.38)$$

the surface Σ corresponds to $t = 0$, and the spatial coordinates on Σ are \mathbf{x} . The t coordinate is the proper time along the geodesics from Σ that are generated by the normal vectors to Σ .

The integrals (3.36) and (3.37) seem intractable as they stand, since the integration is over the entire causal past/future of the surface. However, since Σ is compact and M^+ and M^- are of finite volume, we can always find a subneighbourhood of U_Σ such that the contribution to the integrals from the complement of that

subneighbourhood tends to zero exponentially quickly as $\rho \rightarrow \infty$. Let $\varepsilon > 0$ be small enough such that for all $p \in \Sigma$ and $|t| < \varepsilon$, $(t, \mathbf{x}(p))$ are the GNCs of a point in U_Σ . Define $U_\Sigma(\varepsilon) := \{q \in U_\Sigma : |t(q)| < \varepsilon\}$ and consider the integral in (3.37) restricted to $W := J^+(\Sigma) \setminus U_\Sigma(\varepsilon)$:

$$\left| \int_W dV_x \frac{(\rho V_\blacktriangle(x))^k}{k!} e^{-\rho V_\blacktriangle(x)} \right| \leq \|e^{-\rho V_\blacktriangle}\| \int_W dV_x \frac{(\rho V_\blacktriangle(x))^k}{k!}, \quad (3.39)$$

where $\|e^{-\rho V_\blacktriangle}\|$ is the uniform norm over the integration region W . Since $V_\blacktriangle(x)$ increases with t along the geodesics from Σ , and $\{q \in U_\Sigma : t(q) = \varepsilon\}$ is diffeomorphic to Σ and so is compact, $V_\blacktriangle(x)$ achieves its minimum value $V_{min} > 0$ in W at some point with $t = \varepsilon$. Then $\|e^{-\rho V_\blacktriangle}\| = e^{-\rho V_{min}}$ and so the integral (3.39) falls off exponentially fast as $\rho \rightarrow \infty$. Similarly for (3.36).

Thus, so long as ρ is large enough, we make only an exponentially small error by cutting off the integration ranges in (3.36) and (3.37) at $t = \pm\varepsilon$ with ε as small as we need in order to be able to expand in powers of t .

In GNC's we can expand the determinant of the metric around $t = 0$ to write the volume factor as

$$\begin{aligned} \sqrt{-g} &= h^{\frac{1}{2}} \left(1 + \frac{1}{2} \frac{\dot{h}}{h} t + \frac{1}{4} \left(\frac{\ddot{h}}{h} - \frac{1}{2} \left(\frac{\dot{h}}{h} \right)^2 \right) t^2 + \mathcal{O}(t^3) \right) \\ &= h^{\frac{1}{2}} \left(1 - Kt + \frac{1}{2} (K^2 - K^{\alpha\beta} K_{\alpha\beta} - R_{tt}) t^2 + \mathcal{O}(t^3) \right) \end{aligned} \quad (3.40)$$

where $h := \det(h_{ij})$, and we use a dot for a partial derivative with respect to t . All the geometric quantities have been evaluated at $t = 0$ and their spatial dependence has been omitted for brevity. To arrive at the second line we have used the fact that, in GNC's, we have that $K = -\dot{h}/2h$ and $\dot{K} = R_{tt} + K^{\alpha\beta} K_{\alpha\beta}$. Using the above expansion, the integrals in (3.36) and (3.37) become

$$\begin{aligned} \langle \mathbf{F}_k \rangle &= \rho \int_\Sigma d^{d-1}x \int_{-\varepsilon}^0 dt h^{\frac{1}{2}} \left(1 - Kt + \frac{1}{2} (K^2 - K^{\alpha\beta} K_{\alpha\beta} - R_{tt}) t^2 + \mathcal{O}(t^3) \right) \\ &\quad \times \frac{(\rho V_\blacktriangledown(t, \mathbf{x}))^k}{k!} e^{-\rho V_\blacktriangledown(t, \mathbf{x})} + \dots, \\ \langle \mathbf{P}_k \rangle &= \rho \int_\Sigma d^{d-1}x \int_0^\varepsilon dt h^{\frac{1}{2}} \left(1 - Kt + \frac{1}{2} (K^2 - K^{\alpha\beta} K_{\alpha\beta} - R_{tt}) t^2 + \mathcal{O}(t^3) \right) \\ &\quad \times \frac{(\rho V_\blacktriangle(t, \mathbf{x}))^k}{k!} e^{-\rho V_\blacktriangle(t, \mathbf{x})} + \dots, \end{aligned} \quad (3.41)$$

where we have used the GNC's as the arguments of the cone volume function, and $+\dots$ denotes “terms that vanish exponentially fast with ρ in the limit $\rho \rightarrow \infty$ ”. It should be noted that the spatial integrals above are over the entire hypersurface Σ . The spatial integrals involved in the causal cone volume calculations, however, are only over the base surface region of Σ .

3.3.2 Use of the Cone Volume Expansion

We will now use the expansions of the cone volumes (3.33) and (3.34) in (3.41), and evaluate the integrals in the large ρ limit. We will focus our attention on $\langle \mathbf{P}_k \rangle$ as the case of $\langle \mathbf{F}_k \rangle$ is very similar.

If we substitute in the formula for the volume expansion we get

$$\begin{aligned} \langle \mathbf{P}_k \rangle &= \rho \int_{\Sigma} d^{d-1}x h^{\frac{1}{2}} \int_0^{\varepsilon} dt (1 - Kt + Dt^2 + \mathcal{O}(t^3)) \\ &\quad \times \frac{(\rho At^d (1 + Bt + Ct^2 + \mathcal{O}(t^3)))^k}{k!} e^{-\rho At^d (1 + Bt + Ct^2 + \mathcal{O}(t^3))} + \dots, \end{aligned} \quad (3.42)$$

where we have defined

$$\begin{aligned} A &:= \frac{\text{vol}(S_{d-2})}{d(d-1)}, \quad B := \frac{d}{2(d+1)}K, \\ C &:= \frac{d}{4(d+1)} \left(\frac{1}{2}K^2 + K^{\alpha\beta}K_{\alpha\beta} - \frac{2}{3(d+2)}R + \frac{2}{3}R_{tt} \right), \\ D &:= \frac{1}{2} (K^2 - K^{\alpha\beta}K_{\alpha\beta} - R_{tt}). \end{aligned} \quad (3.43)$$

The definitions of C and D are consistent with previous formulae for the volume of the small causal cone as $R_{\alpha\beta}n^{\alpha}n^{\beta} = R_{tt}$ in our setup with the GNC's. We will now try and manipulate the integrand into the form of a Gamma function. To do this we split the exponential into a product of two exponentials

$$\begin{aligned} e^{-\rho At^d (1 + Bt + Ct^2 + \mathcal{O}(t^3))} &= e^{-\rho At^d} e^{-\rho At^d (Bt + Ct^2 + \mathcal{O}(t^3))} \\ &= e^{-\rho At^d} (1 - \rho At^d (Bt + Ct^2 + \mathcal{O}(t^3)) + \mathcal{O}(t^{2(d+1)})). \end{aligned} \quad (3.44)$$

To get to the second line we have expanded the second exponential on the RHS in the first line in small t . If we use (3.44) in (3.42), and do a small t expansion of the rest of the integrand, then each term in this expansion gives an integral of the following form

$$\rho^n \int_0^{\varepsilon} dt t^{\zeta} e^{-\rho At^d}, \quad (3.45)$$

where $\eta, \zeta \in \mathbb{R}$. If we make the substitution $z = \rho A t^d$ then this integral takes on the form of an incomplete gamma function.

$$\frac{A^{-\left(\frac{\zeta+1}{d}\right)}}{d} \rho^{\eta - \left(\frac{\zeta+1}{d}\right)} \int_0^{\rho A \varepsilon^d} dz z^{\left(\frac{\zeta+1}{d}\right)-1} e^{-z}. \quad (3.46)$$

We then take $\rho \rightarrow \infty$ to get

$$\lim_{\rho \rightarrow \infty} \int_0^{\rho A \varepsilon^d} dz z^{\left(\frac{\zeta+1}{d}\right)-1} e^{-z} = \Gamma\left(\frac{\zeta+1}{d}\right) + \dots, \quad (3.47)$$

where, as before, $+\dots$ denotes terms that tend to zero exponentially fast in ρ , and so are zero in the limit $\rho \rightarrow \infty$.

We can now evaluate any integral in (3.42). This gives us the limiting behaviour of $\langle \mathbf{P}_k \rangle$ as

$$\begin{aligned} \langle \mathbf{P}_k \rangle &= \rho^{1-\frac{1}{d}} \frac{A^{-\frac{1}{d}} \Gamma\left(\frac{1}{d} + k\right)}{d k!} I_0 - \rho^{1-\frac{2}{d}} \frac{(d+2) A^{-\frac{2}{d}} \Gamma\left(\frac{2}{d} + k\right)}{d(d+1) k!} I_1 \\ &\quad + \rho^{1-\frac{3}{d}} \frac{A^{-\frac{3}{d}} \Gamma\left(\frac{3}{d} + k\right)}{4d(d+1)^2 k!} I_2 + \mathcal{O}\left(\rho^{1-\frac{4}{d}}\right), \\ \langle \mathbf{F}_k \rangle &= \rho^{1-\frac{1}{d}} \frac{A^{-\frac{1}{d}} \Gamma\left(\frac{1}{d} + k\right)}{d k!} I_0 + \rho^{1-\frac{2}{d}} \frac{(d+2) A^{-\frac{2}{d}} \Gamma\left(\frac{2}{d} + k\right)}{d(d+1) k!} I_1 \\ &\quad + \rho^{1-\frac{3}{d}} \frac{A^{-\frac{3}{d}} \Gamma\left(\frac{3}{d} + k\right)}{4d(d+1)^2 k!} I_2 + \mathcal{O}\left(\rho^{1-\frac{4}{d}}\right). \end{aligned} \quad (3.48)$$

where we have included $\langle \mathbf{F}_k \rangle$ as well for completeness, and we have defined the integrals over the geometric quantities as

$$\begin{aligned} I_0 &:= \int_{\Sigma} d^{d-1} x \sqrt{h} \\ I_1 &:= \int_{\Sigma} d^{d-1} x \sqrt{h} K \\ I_2 &:= \int_{\Sigma} d^{d-1} x \sqrt{h} \left(\omega_1(d) K^2 + \omega_2(d) K^{\alpha\beta} K_{\alpha\beta} + \omega_3(d) R + \omega_4(d) R_{\alpha\beta} n^{\alpha} n^{\beta} \right), \end{aligned} \quad (3.49)$$

with

$$\begin{aligned} \omega_1(d) &:= 11 + 2d(d+5) \\ \omega_2(d) &:= -(d+1)(2d+5) \\ \omega_3(d) &:= \frac{2(d+1)}{(d+2)} \\ \omega_4(d) &:= -2(d+1)(d+2), \end{aligned} \quad (3.50)$$

and where we have substituted $R_{\alpha\beta}n^\alpha n^\beta$ back in for R_{tt} in (3.49).

The three integrals I_0 , I_1 and I_2 that appear in (3.49) are all integrals over geometric quantities that only depend upon the metric and the hypersurface. This means that the integrals do not depend upon our particular choice of GNCs, and hence neither does the result (3.48).

The Gauss-Codazzi equations relate the four geometric quantities in I_2 to the Ricci scalar for the surface, ${}^{d-1}R$. We can use this relation to swap out any of the four quantities in I_2 for ${}^{d-1}R$.

It is interesting to note that from the limiting behaviour of $\langle \mathbf{P}_k \rangle$ or $\langle \mathbf{F}_k \rangle$ we can find the dimension, d , by taking the ratio of either $\langle \mathbf{P}_0 \rangle$ and $\langle \mathbf{P}_1 \rangle$, or $\langle \mathbf{F}_0 \rangle$ and $\langle \mathbf{F}_1 \rangle$. The limiting behaviour of the latter ratio, expressed in terms of the discreteness length $l = \rho^{-1/d}$, is found to be

$$\frac{\langle \mathbf{F}_0 \rangle}{\langle \mathbf{F}_1 \rangle} = d - \frac{b_d \Gamma\left(\frac{2}{d}\right)}{a_d \Gamma\left(\frac{1}{d} + 1\right)} \frac{\int_{\Sigma} d^{d-1}x \sqrt{h} K}{\int_{\Sigma} d^{d-1}x \sqrt{h}} l + O(l^2). \quad (3.51)$$

In the limit of $l \rightarrow 0$ one gets the dimension exactly. The fraction involving the two integrals is simply the average value of the extrinsic curvature across Σ . The case for the ratio of $\langle \mathbf{P}_0 \rangle$ and $\langle \mathbf{P}_1 \rangle$ is the same as (3.51) but with a positive sign after d .

3.4 Causal Set Expressions

3.4.1 The Boundary Terms

Given a finite causet, (\mathcal{C}, \preceq) , with two subcausets, \mathcal{C}^+ and \mathcal{C}^- we introduce the following family of causal set ‘‘boundary terms’’ (CBT):

$$S_{CBT}^{(d)}[\mathcal{C}, \mathcal{C}^-, \mathcal{C}^+; \vec{p}, \vec{q}] := (l/l_p)^{d-2} a_d \left(\sum_m p_m F_m[\mathcal{C}^-] + \sum_n q_n F_n[\mathcal{C}^+] \right), \quad (3.52)$$

where the constant a_d is given by

$$a_d = \frac{d(d+1)}{(d+2)} \left(\frac{\text{vol}(S_{d-2})}{d(d-1)} \right)^{\frac{2}{d}}. \quad (3.53)$$

$\text{vol}(S_d) = (d+1)\pi^{\frac{d+1}{2}}/\Gamma\left(\frac{d+1}{2} + 1\right)$ is the volume of the unit d -sphere, l is the discreteness length and l_p the Planck length. \vec{p} and \vec{q} denote finite strings of real numbers (p_0, \dots, p_m, \dots) and (q_0, \dots, q_n, \dots) respectively. The sums, which are over

the non-negative integers, will terminate at some point since \vec{p} and \vec{q} are finite strings. We have also partitioned the causal set into \mathcal{C}^+ and \mathcal{C}^- , and restricted the functions F_m and P_n to act on \mathcal{C}^- and \mathcal{C}^+ respectively. We can think of this as a family of functions, with each member of the family specified by their particular strings \vec{p} and \vec{q} .

We will now prove that the strings must satisfy the following conditions in order for $S_{CBT}^{(d)}$ to be considered a boundary term:

$$\sum_m p_m \frac{\Gamma(\frac{1}{d} + m)}{m!} + \sum_n q_n \frac{\Gamma(\frac{1}{d} + n)}{n!} = 0, \quad (3.54)$$

$$\sum_m p_m \frac{\Gamma(\frac{2}{d} + m)}{m!} - \sum_n q_n \frac{\Gamma(\frac{2}{d} + n)}{n!} = 1. \quad (3.55)$$

We call (3.52) a boundary term but in general, when \mathcal{C}^+ and \mathcal{C}^- are arbitrary subcausets of \mathcal{C} , it will have no physical significance.

Let (M, g) be a d -dimensional spacetime with finite volume and spacelike, compact hypersurface Σ as described above. Given such a spacetime (M, g) and the regions $M^\pm = J^\pm(\Sigma)$, $S_{CBT}^{(d)}$ defines a family of random variables in the following way. The Poisson process of sprinkling points into M with density $\rho = l^{-d}$ generates a random causet (\mathcal{C}, \preceq) together with subcausets \mathcal{C}^\pm which consist of those elements sprinkled into M^\pm . The functions P_k and F_k acting on the random causets \mathcal{C}^+ and \mathcal{C}^- respectively are random variables \mathbf{P}_k and \mathbf{F}_k . These random variables can be substituted into (3.52) to give the family of random variables $\mathbf{S}_{CBT}^{(d)}$:

$$\mathbf{S}_{CBT}^{(d)} [M, \Sigma, \rho; \vec{p}, \vec{q}] := (l/l_p)^{d-2} a_d \left(\sum_m p_m \mathbf{F}_m + \sum_n q_n \mathbf{P}_n \right). \quad (3.56)$$

We claim that in the limit of infinite density the expectation value, in the sprinkling process, of $\mathbf{S}_{CBT}^{(d)}$ tends to the continuum GHY boundary term of the surface Σ :

$$\lim_{l \rightarrow 0} \langle \mathbf{S}_{CBT}^{(d)} [M, \Sigma, \rho; \vec{p}, \vec{q}] \rangle = \frac{1}{l_p^{d-2}} \int_\Sigma d^{d-1}x \sqrt{h} K = S_{GHY} [\Sigma, M^-], \quad (3.57)$$

where $\langle \cdot \rangle$ denotes the mean over sprinklings.

Given the limiting behaviour of $\langle \mathbf{P}_k \rangle$ and $\langle \mathbf{F}_k \rangle$ in the previous section this

follows almost immediately:

$$\begin{aligned}
\lim_{\rho \rightarrow \infty} \langle \mathbf{S}_{CBT}^{(d)} \rangle &= \lim_{\rho \rightarrow \infty} \frac{\rho^{\frac{2}{d}-1}}{l_p^{d-2}} a_d \left(\sum_m p_m \langle \mathbf{F}_m \rangle + \sum_n q_n \langle \mathbf{P}_n \rangle \right) \\
&= \lim_{\rho \rightarrow \infty} \left[\frac{\rho^{\frac{1}{d}}}{l_p^{d-1}} \frac{(d+1)}{(d+2)} A^{\frac{1}{d}} \left(\sum_m p_m \frac{\Gamma(\frac{1}{d}+m)}{m!} + \sum_n q_n \frac{\Gamma(\frac{1}{d}+n)}{n!} \right) \int_{\Sigma} d^{d-1}x \sqrt{h} \right. \\
&\quad \left. + \frac{1}{l_p^{d-2}} \left(\sum_m \frac{\Gamma(\frac{2}{d}+m)}{m!} - \sum_n q_n \frac{\Gamma(\frac{2}{d}+n)}{n!} \right) \int_{\Sigma} d^{d-1}x \sqrt{h} K + O(\rho^{-\frac{1}{d}}) \right] \\
&= \frac{1}{l_p^{d-2}} \int_{\Sigma} d^{d-1}x \sqrt{h} K,
\end{aligned} \tag{3.58}$$

using the conditions (3.54) and (3.55) for \vec{p} and \vec{q} .

One can see that at least two non-zero entries in \vec{p} and \vec{q} together are necessary in order to satisfy (3.54) and (3.55) and if exactly two entries are non-zero they will be uniquely fixed, but if more than two entries are non-zero this uniqueness is lost. This accords with the continuum boundary term being a first derivative. The freedom of choice in \vec{p} and \vec{q} is the freedom to discretise a derivative in many ways but the difference of two nearby values is sufficient.

We introduce special notation for the simplest member of the family:

$$S_0^{(d)}[\mathcal{C}, \mathcal{C}^-, \mathcal{C}^+] := (l/l_p)^{d-2} \frac{a_d}{2\Gamma(\frac{2}{d})} (F_0[\mathcal{C}^-] - P_0[\mathcal{C}^+]) . \tag{3.59}$$

This is proportional to the difference in the numbers of minimal elements of \mathcal{C}^+ and maximal elements of \mathcal{C}^- . An example of this on a causal set can be seen in Figure 3.3. This case is the easiest to investigate computationally, and we shall use its random variable counterpart, $\mathbf{S}_0^{(d)}[M, \Sigma, \rho]$, later when we study the fluctuations of the discrete boundary terms numerically.

There are two special subfamilies of boundary terms, one defined by $\vec{p} = 0$ and the other by $\vec{q} = 0$. In the former (latter) case, this corresponds to defining a boundary term for the past (future) boundary of \mathcal{C}^+ (\mathcal{C}^-) using only data from \mathcal{C}^+ (\mathcal{C}^-) itself. The simplest cases of these boundary terms are

$$S_-^{(d)}[\mathcal{C}^+] := (l/l_p)^{d-2} \frac{a_d}{\Gamma(\frac{2}{d})} (P_0[\mathcal{C}^+] - d P_1[\mathcal{C}^+]) , \tag{3.60}$$

$$S_+^{(d)}[\mathcal{C}^-] := (l/l_p)^{d-2} \frac{a_d}{\Gamma(\frac{2}{d})} (d F_1[\mathcal{C}^-] - F_0[\mathcal{C}^-]) . \tag{3.61}$$

These give rise to random variables $\mathbf{S}_-^{(d)}[M, \Sigma, \rho]$ and $\mathbf{S}_+^{(d)}[M, \Sigma, \rho]$ via sprinkling at

density $\rho = l^{-d}$ as before.

3.4.2 The Surface Volume Family

We also propose a family of causet functions that will give the volume of a spacelike hypersurface in the appropriate context:

$$A^{(d)}[\mathcal{C}, \mathcal{C}^-, \mathcal{C}^+; \vec{p}, \vec{q}] := (l/l_p)^{d-1} b_d \left(\sum_m p_m F_m [\mathcal{C}^-] + \sum_n q_n P_n [\mathcal{C}^+] \right), \quad (3.62)$$

where

$$b_d = d \left(\frac{\text{vol}(S_{d-2})}{d(d-1)} \right)^{\frac{1}{d}}, \quad (3.63)$$

and \vec{p} and \vec{q} now satisfy

$$\sum_m p_m \frac{\Gamma(\frac{1}{d} + m)}{m!} + \sum_n q_n \frac{\Gamma(\frac{1}{d} + n)}{n!} = 1. \quad (3.64)$$

We see that only one non-zero entry is necessary to give an expression for the discrete surface volume. Once again, for (M, g) , Σ and $\rho = l^{-d}$, we can define a family of random variables,

$$\mathbf{A}^{(d)}[M, \Sigma, \rho; \vec{p}, \vec{q}] := (l/l_p)^{d-2} b_d \left(\sum_m p_m \mathbf{F}_m + \sum_n q_n \mathbf{P}_n \right). \quad (3.65)$$

In the limit of infinite density, the expectation value of $\mathbf{A}^{(d)}$ in the sprinkling process tends to the spatial volume of the surface Σ :

$$\lim_{l \rightarrow 0} \langle \mathbf{A}^{(d)}[M, \Sigma, \rho; \vec{p}, \vec{q}] \rangle = \frac{1}{l_p^{d-1}} \int_{\Sigma} d^{d-1}x \sqrt{h}, \quad (3.66)$$

since

$$\begin{aligned} \lim_{\rho \rightarrow \infty} \langle \mathbf{A}^{(d)} \rangle &= \lim_{\rho \rightarrow \infty} \frac{\rho^{\frac{1}{d}-1}}{l_p^{d-1}} b_d \left(\sum_m p_m \langle \mathbf{F}_m \rangle + \sum_n q_n \langle \mathbf{P}_n \rangle \right) \\ &= \lim_{\rho \rightarrow \infty} \left[\frac{1}{l_p^{d-1}} \left(\sum_m p_m \frac{\Gamma(\frac{1}{d} + m)}{m!} + \sum_n q_n \frac{\Gamma(\frac{1}{d} + n)}{n!} \right) \int_{\Sigma} d^{d-1}x \sqrt{h} + O(\rho^{-\frac{1}{d}}) \right] \\ &= \frac{1}{l_p^{d-1}} \int_{\Sigma} d^{d-1}x \sqrt{h}, \end{aligned} \quad (3.67)$$

using (3.64).

One can define functions for the volumes of future and past boundaries respectively as the two simplest members of the family:

$$A_+^{(d)}[\mathcal{C}^-] := (l/l_p)^{d-1} \frac{b_d}{\Gamma\left(\frac{1}{d}\right)} F_0[\mathcal{C}^-], \quad (3.68)$$

$$A_-^{(d)}[\mathcal{C}^+] := (l/l_p)^{d-1} \frac{b_d}{\Gamma\left(\frac{1}{d}\right)} P_0[\mathcal{C}^+]. \quad (3.69)$$

3.4.3 Higher Order Causal Set Expressions

In the last section we constructed causal set expressions for the integrals I_0 and I_1 in (3.49). Here we will focus on an expression for I_2 .

Take the following causal set function

$$I[\mathcal{C}, \mathcal{C}^+, \mathcal{C}^-; \vec{p}, \vec{q}] := l^{d-3} A_d \left(\sum_m p_m F_m[\mathcal{C}^-] + \sum_n q_n P_n[\mathcal{C}^+] \right), \quad (3.70)$$

where $l = \rho^{-\frac{1}{d}}$ is the discreteness length and A_d is a real constant that depends only on dimension.

Just as before the strings are not totally arbitrary, and we will show that they must satisfy certain constraints if we are to recover I_2 .

We define the random variable \mathbf{I} as that which takes the value $I[\mathcal{C}, \mathcal{C}^+, \mathcal{C}^-; \vec{p}, \vec{q}]$ under sprinkling into M . This random variable depends on the spacetime M , surface Σ , density ρ , and the strings \vec{p} and \vec{q} .

\mathbf{I} can be written in terms of the random variables \mathbf{F}_m and \mathbf{P}_n , where we recall that these random variables realise the values of $F_m[\mathcal{C}^-]$ and $P_n[\mathcal{C}^+]$ under a sprinkling into M . Writing \mathbf{I} in this way gives

$$\mathbf{I} := \rho^{\frac{3}{d}-1} A_d \left(\sum_m p_m \mathbf{F}_m + \sum_n q_n \mathbf{P}_n \right), \quad (3.71)$$

where we have omitted the arguments of the random variables for brevity. We want to take the expectation value of this random variable over the sprinkling process and extract out the integral I_2 in the limit of $\rho \rightarrow \infty$. That is, we are aiming for

$$\lim_{\rho \rightarrow \infty} \langle \mathbf{I} \rangle = I_2. \quad (3.72)$$

Given we have (3.48) we can take the expectation value of (3.71) in the limit of

$\rho \rightarrow \infty$ to find

$$\begin{aligned}
\lim_{\rho \rightarrow \infty} \langle \mathbf{I} \rangle &= \lim_{\rho \rightarrow \infty} \rho^{\frac{3}{d}-1} A_d \left(\sum_m p_m \langle \mathbf{F}_m \rangle + \sum_n q_n \langle \mathbf{P}_n \rangle \right) \\
&= A_d \lim_{\rho \rightarrow \infty} \left[\rho^{\frac{2}{d}} \frac{A^{-\frac{1}{d}}}{d} \left(\sum_m p_m \frac{\Gamma(\frac{1}{d} + m)}{m!} + \sum_n q_n \frac{\Gamma(\frac{1}{d} + n)}{n!} \right) I_0 \right. \\
&\quad + \rho^{\frac{1}{d}} \frac{(d+2)A^{-\frac{2}{d}}}{d(d+1)} \left(\sum_m p_m \frac{\Gamma(\frac{2}{d} + m)}{m!} - \sum_n q_n \frac{\Gamma(\frac{2}{d} + n)}{n!} \right) I_1 \\
&\quad \left. + \frac{A^{-\frac{3}{d}}}{4d(d+1)^2} \left(\sum_m p_m \frac{\Gamma(\frac{3}{d} + m)}{m!} + \sum_n q_n \frac{\Gamma(\frac{3}{d} + n)}{n!} \right) I_2 \right]. \tag{3.73}
\end{aligned}$$

In order for (3.72) to be satisfied we get the following conditions on \vec{p} and \vec{q} :

$$\begin{aligned}
\sum_m p_m \frac{\Gamma(\frac{1}{d} + m)}{m!} + \sum_n q_n \frac{\Gamma(\frac{1}{d} + n)}{n!} &= 0, \\
\sum_m p_m \frac{\Gamma(\frac{2}{d} + m)}{m!} - \sum_n q_n \frac{\Gamma(\frac{2}{d} + n)}{n!} &= 0, \\
\sum_m p_m \frac{\Gamma(\frac{3}{d} + m)}{m!} + \sum_n q_n \frac{\Gamma(\frac{3}{d} + n)}{n!} &= 1. \tag{3.74}
\end{aligned}$$

We also find that the constant A_d must be

$$A_d = 4d(d+1)^2 A^{\frac{3}{d}}, \tag{3.75}$$

where A was defined in (3.43). There are many different \vec{p} and \vec{q} strings that satisfy (3.74). This freedom comes from the fact that we are effectively discretising a mix of second order derivatives. From (3.74) we see that at least three non-zero entries in \vec{p} and \vec{q} are needed, which is consistent with the idea that it is a discrete second order derivative.

The simplest causal set expressions that give I_2 (in the sense of (3.72)) are those formed by taking only the smallest k components of p_k and q_k to be non-zero. For example, if the only non-zero components are p_0 , q_0 and q_1 then solving (3.74) gives

$$p_0 = \frac{1}{4\Gamma(\frac{3}{d})}, \quad q_0 = -\frac{3}{4\Gamma(\frac{3}{d})}, \quad q_1 = \frac{d}{2\Gamma(\frac{3}{d})}, \tag{3.76}$$

with all other components equal to 0.

We denote the strings with these as the only non-zero components by \vec{p}_a and \vec{q}_a .

Inserting these strings into (3.70) simplifies the causal set function to

$$I[\mathcal{C}, \mathcal{C}^+, \mathcal{C}^-; \vec{p}_a, \vec{q}_a] = l^{d-3} \frac{A_d}{4\Gamma\left(\frac{3}{d}\right)} (F_0[\mathcal{C}^-] - 3P_0[\mathcal{C}^+] + 2dP_1[\mathcal{C}^+]) \quad (3.77)$$

We define $I_a[\mathcal{C}, \mathcal{C}^+, \mathcal{C}^-]$ as the function on the RHS in (3.77), and its random variable counterpart as \mathbf{I}_a , where the counterpart is formed in the usual way by promoting the functions F_m and P_n to random variables.

One can also take an entire string to be zero. For example, take \vec{p} to be the zero string $\vec{0}$ (every component $p_k = 0$). If we take the first 3 components of \vec{q} to be the only non-zero components then, by solving (3.74), we find

$$q_0 = \frac{1}{\Gamma\left(\frac{3}{d}\right)}, \quad q_1 = -\frac{d(d+3)}{2\Gamma\left(\frac{3}{d}\right)}, \quad q_2 = \frac{d^2}{\Gamma\left(\frac{3}{d}\right)}. \quad (3.78)$$

We denote the string with these as the only non-zero components as \vec{q}_- .

If these strings are inserted into the arguments of I we find

$$I[\mathcal{C}, \mathcal{C}^+, \mathcal{C}^-; \vec{0}, \vec{q}_-] = l^{d-3} \frac{A_d}{\Gamma\left(\frac{3}{d}\right)} \left(P_0[\mathcal{C}^+] - \frac{d(d+3)}{2} P_1[\mathcal{C}^+] + d^2 P_2[\mathcal{C}^+] \right). \quad (3.79)$$

The causal set \mathcal{C}^- does not enter on the RHS as there are no F_k functions to act on it, and hence we can view the RHS as being a function on a single causal set, \mathcal{C}^+ , without reference to it being part of some larger causal set. We define the function $I_-[\mathcal{C}^+]$ as the RHS of (3.79). I_- is really a function of a single causal set, as it does not depend on \mathcal{C}^- . The random variable counterpart, \mathbf{I}_- , can be formed in the usual way. This random variable does not depend on $J^-(\Sigma)$, and so can be viewed as being a function of the spacetime $J^+(\Sigma)$ and its past boundary Σ only (and the density ρ). Thus, given a single causal set, \mathcal{C} , we can think of $I_-[\mathcal{C}]$ as the causal set analogue of the geometrical quantity I_2 corresponding, in some sense, to the “past boundary” of \mathcal{C} . A similar expression can be formed for the “future boundary” of a causal set by taking $\vec{q} = \vec{0}$ and having only the first 3 components of \vec{p} be non-zero.

The continuum quantity, I_2 , for which we have constructed the family of causal set expressions, I , contains four different geometric quantities. This means that given some causal set, and the value of I acting on that causal set, we do not know what contribution to that number has come from the causal set analogue of one of the four geometric quantities in I_2 alone. We also do not know whether this value will be close to the continuum value of some manifold from which our causal set could arise as a typical sprinkling. This question will be addressed in the next section.

The family of causal set functions found here are not as immediately useful as

causal set functions that correspond to a single geometrical quantity, such as those found for the integrals I_0 and I_1 . We can attempt to extract a single quantity from the integral I_2 using other causal set expressions alongside I . We will now sketch out how one might attempt to extract $K^{\alpha\beta}K_{\alpha\beta}$. The number of causal set elements in an interval gives the spacetime volume of the interval, and using the formulae in [40, 46] one might be able to extract $c_3R + c_4R_{\alpha\beta}n^\alpha n^\beta$ from this number. One could also determine K from the causal set expressions for the integrals I_0 and I_1 ³. The remaining quantity in I_2 , $K^{\alpha\beta}K_{\alpha\beta}$, can then be extracted on its own.

3.4.4 Finite ρ and Fluctuations

To decide under what circumstances the causal set expressions above, evaluated on a single causal set sprinkled into M , are close to the continuum expressions for Σ , it is necessary to know both the size of the fluctuations about the mean and when that mean is close to its limiting value.

To take the second point first, the mean is close to its limiting value when the next order term in the expansions performed in the previous sections can be ignored. Firstly, ρ must be large enough that an $\varepsilon > 0$ exists such that the expansions in GNCs are valid in a neighbourhood $U_\Sigma(\varepsilon)$, and such that $\rho V_{min} \gg 1$ so $e^{-\rho V_{min}} \ll 1$, and the integral over the region outside $U_\Sigma(\varepsilon)$ is negligible. $V_{min} \sim \varepsilon^d$, and so $\varepsilon \gg l$. The expansions in equations (3.41), (3.33) and (3.34) are valid if the curvature scales of the surface and spacetime are much larger than ε , i.e. that $\mathcal{K}\varepsilon \ll 1$ and $\mathcal{R}\varepsilon^2 \ll \mathcal{K}\varepsilon$, where \mathcal{K} and \mathcal{R} stand for any component of the extrinsic curvature of Σ and spacetime curvature of M , respectively, evaluated on Σ . The resulting conditions are $\mathcal{R}l^2 \ll \mathcal{K}l \ll 1$. This simply tells us that the discreteness length must be much smaller than the curvature scales of the surface and spacetime, which is just what one would expect if the discrete causal set is to encode the geometry of Σ and M around Σ .

We now turn to the fluctuations or standard deviation, and we will start by looking at those of the boundary terms, i.e. $\sigma[\mathbf{S}_{CBT}^{(d)}] = \text{Var}[\mathbf{S}_{CBT}^{(d)}]^{1/2}$. A heuristic argument gives an estimate of the dependence of fluctuations on $\rho = l^{-d}$. In any spacetime region of fixed volume V the number of causal set elements in a sprinkling is a Poisson random variable, \mathbf{N} , with mean $\langle \mathbf{N} \rangle = \rho V$ and s.d. $\sqrt{\langle \mathbf{N} \rangle}$. Consider the

³The causal set expressions for I_0 and I_1 give the spatial volume of the hypersurface and the extrinsic curvature integrated over the hypersurface respectively. If we divide the latter by the former we get the average value of the extrinsic curvature over the hypersurface, K_{avg} . We can only use these expressions to determine K when the region of the hypersurface that we are interested in is such that $K_{avg} \approx K$ for any point in that region.

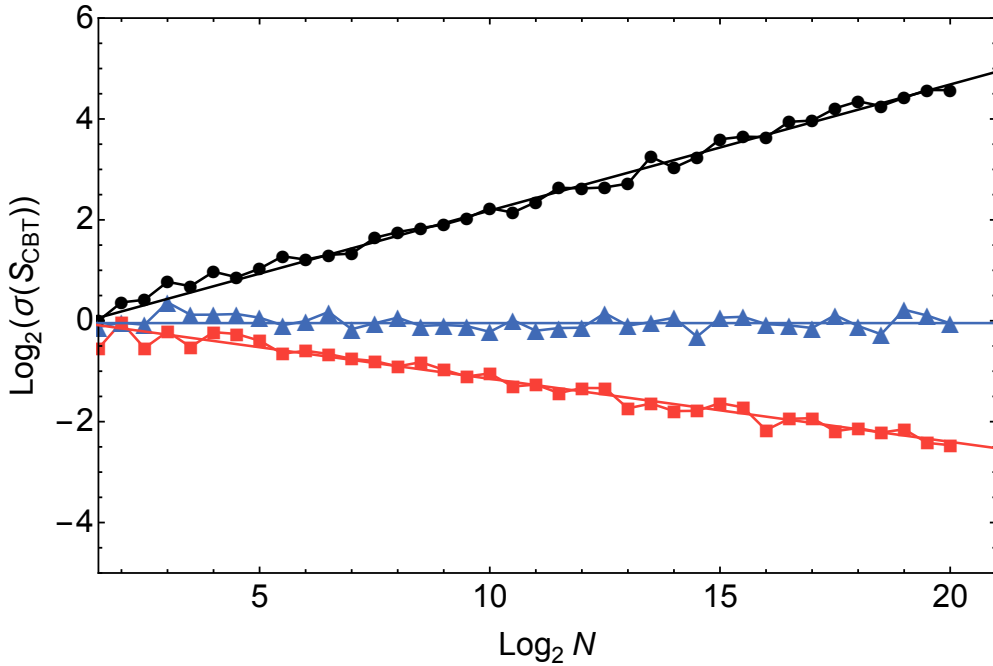


Figure 3.4: A plot of the standard deviation in samples of 100 of $\mathbf{S}_0^{(d)}$ for a flat ($K = 0$) surface bisecting a $d = 2, 3$ and 4-dimensional unit cube in Minkowski space for different values of $N = \rho$. Black dots, blue triangles and red squares correspond to the simulation results in $d = 2, 3$ and 4 dimensions, respectively. The corresponding black, blue and red lines have gradients $\frac{1}{4}$, 0 and $-\frac{1}{8}$ and best-fit intercepts of order 1.

simplest boundary term $\mathbf{S}_0^{(d)}$. The volume of a region corresponding to a thickening of the hypersurface Σ by one unit of the discreteness scale l (e.g. by Lie dragging the surface along its normal by an amount l) is approximately $\text{vol}(\Sigma)l = \text{vol}(\Sigma)\rho^{-\frac{1}{d}}$. Since \mathbf{F}_0 and \mathbf{P}_0 are random variables that count nearest neighbours of Σ we may therefore expect their mean values to scale like $\rho \text{vol}(\Sigma)l = \text{vol}(\Sigma)\rho^{\frac{d-1}{d}} \propto \langle \mathbf{N} \rangle^{\frac{d-1}{d}}$, and indeed this agrees with the leading order behaviour of (3.48). This suggests that \mathbf{P}_0 and \mathbf{F}_0 will be subject to fluctuations of order $\langle \mathbf{N} \rangle^{\frac{d-1}{2d}} = (\rho V)^{\frac{d-1}{2d}}$ in the limit of large ρ , and we should see similar fluctuations for \mathbf{P}_k and \mathbf{F}_k . Moreover \mathbf{F}_0 and \mathbf{P}_0 are independent and so $\sigma[\mathbf{S}_{CBT}^{(d)}]$ should behave like $\rho^{\frac{2-d}{d}} \rho^{\frac{d-1}{2d}} = \rho^{\frac{3-d}{2d}}$. Hence for $d = 2$ these fluctuations should grow like $\rho^{\frac{1}{4}}$ as $\rho \rightarrow \infty$, for $d = 3$ they should be constant, and for $d > 3$ they should be damped.

We tested this with simulations in the simplest case of flat spacetime and flat surface Σ . For each different sprinkling density, $\rho = l^{-d}$, we took a sample of 100 sprinklings of a d -cube $[0, 1]^d$ in d -dimensional Minkowski space with hypersurface $\Sigma : t = 1/2$, and evaluated the sample mean and (corrected) sample standard deviation of $\mathbf{S}_0^{(d)}$. The expectation value of $\mathbf{S}_0^{(d)}$ is exactly zero due to the symmetry of the situation.

Figure 3.4 shows the results for $d = 2, 3, 4$ spacetime dimensions, with $\langle \mathbf{N} \rangle = \rho$ ranging up to 2^{20} . Each data point represents the sample standard deviation for a sample of 100. The solid lines have been obtained by fitting an arbitrary constant multiplier in the scaling law predicted by the argument above, $\gamma(d) \times \langle \mathbf{N} \rangle^{\frac{3-d}{2d}}$, to the data. The best fit values are all of order 1: $\gamma(2) = 0.80$, $\gamma(3) = 0.97$, and $\gamma(4) = 1.07$. The data are evidence for the scaling predicted by the heuristic argument. The sample means (not shown) for different ρ are consistent with zero within the standard error. Simulations for the boundary term $\mathbf{S}_+^{(d)}$ (which is proportional to $d\mathbf{F}_1 - \mathbf{F}_0$) show the same dimension dependent scaling behaviour for the standard deviation, though in this case the heuristic argument is complicated by the fact that the random variables of which the boundary term is a sum are not independent.⁴

This complication of the heuristic argument also arises when estimating the fluctuations of \mathbf{I} , since every member of the family has at least two \mathbf{F}_k 's or two \mathbf{P}_k 's (examples of this can be seen above in (3.77) and (3.79)). Since the heuristic argument gave the correct scaling behaviour of $\mathbf{S}_+^{(d)}$, even though the random variables involved were not independent, we shall use the same argument here for the fluctuations, $\sigma[\mathbf{I}] = \text{Var}[\mathbf{I}]^{\frac{1}{2}}$, in the hope that it will be supported by numerical evidence. The argument then says that the deviation of \mathbf{I} will go like that of \mathbf{F}_k or \mathbf{P}_k (as $\rho^{\frac{d-1}{2d}}$) but multiplied by the dependence on ρ from the factor of l^{d-3} (or $\rho^{\frac{3-d}{d}}$ in terms of the density) at the front of the RHS in (3.71). That is, $\sigma[\mathbf{I}]$ should scale like $\rho^{\frac{3-d}{d}} \rho^{\frac{d-1}{2d}} = \rho^{\frac{5-d}{2d}}$, or as $\langle \mathbf{N} \rangle^{\frac{5-d}{2d}}$ in terms of the mean number of elements sprinkled.

This scaling law was tested numerically by sprinkling into a d -dimensional cube as we did for the boundary terms. In this case the mean number of sprinkled elements, $\langle \mathbf{N} \rangle$, ranged from 2^7 to 2^{12} , and for each mean number of elements we did 400 sprinklings. The mean and standard deviation of \mathbf{I}_a was then calculated for the sample of 400 sprinklings at each $\langle \mathbf{N} \rangle$. In this setup the mean of \mathbf{I}_a is zero as the surface and spacetime are flat. This was done for dimensions $d = 3, 4, 5, 6$ and the results of $\log_2(\sigma[\mathbf{I}_a])$ against $\log_2(\langle \mathbf{N} \rangle)$ can be seen in Figure 3.5. The fitted lines have the form $\frac{5-d}{2d} \log_2(\langle \mathbf{N} \rangle) + \xi$, where the constants ξ for each dimension are of order 1. The results for $\sigma[\mathbf{I}_-]$ also show a similar scaling.

These results suggest that the heuristic argument is correct as it has predicted the right scaling. Unfortunately, this means that in 4 dimensions the causal set random variable \mathbf{I} has fluctuations that grow with $\langle \mathbf{N} \rangle$, much like the Benincasa-

⁴While the heuristic argument predicts a scaling of the mean and standard deviations consistent with the data, a closer look at the samples we generated for \mathbf{F}_k and \mathbf{P}_k for $k = 0, 1$ suggests that their distributions deviate from a Poisson distribution: they are ‘‘underdispersed’’, i.e. their s.d. grows like the square root of the mean but is related to it by a constant of proportionality less than 1. We have begun to investigate this further and hope to return to a more careful study of the distributions of these random variables in a future note.

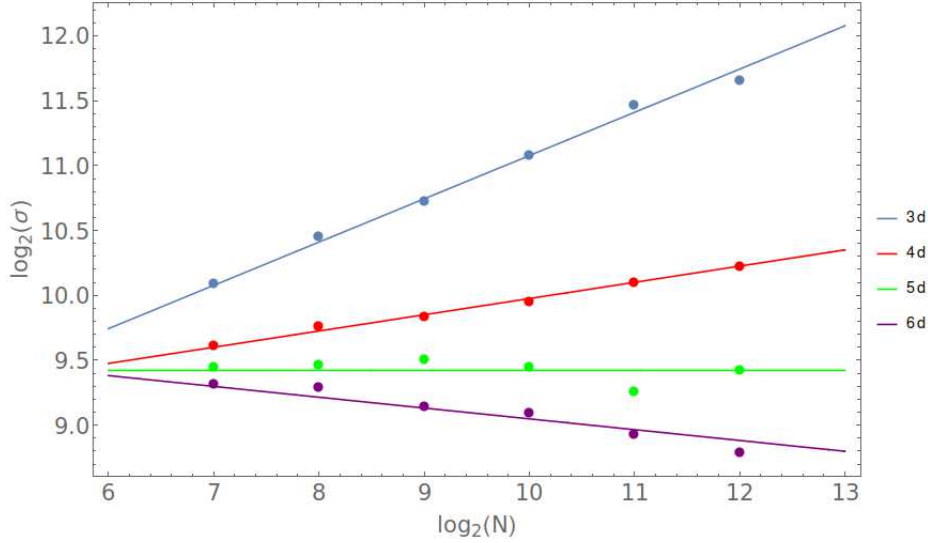


Figure 3.5: Base-2 log-log plot of the standard deviation of \mathbf{I}_a against $\langle \mathbf{N} \rangle$. In the graph these quantities have been denoted by σ and N respectively. From top to bottom the data and the corresponding best fit lines are for dimensions $d = 3, 4, 5$ and 6 respectively.

Dowker-Glaser action [42, 43, 50, 51]. In the case of the action one can modify it with an intermediate length scale to dampen the fluctuations. Perhaps this can be done here too. Without this damping the fluctuations about the mean will only be small for large ρ if $d > 5$. Further work should be done to determine if the scaling of the fluctuations persists in cases where the spacetime and/or the hypersurface are not flat.

3.4.5 Normal Derivatives of a Scalar Field

The techniques we have seen in the previous sections can be used to find causal set expressions relating to the normal derivatives of a scalar field. A scalar field on a causal set is a function from the causal set to the real numbers (or complex numbers for a complex scalar field). These real numbers can be denoted by ϕ_i where the index i runs over the causal set elements.

The functions F_k and P_k sum up the number of \mathcal{F}_k and \mathcal{P}_k elements respectively. We will now define functions that sum up the values of ϕ_i on those particular elements. Explicitly, we define these new functions as

$$F_k^\phi[\mathcal{C}] = \sum_{i \in \{\mathcal{F}_k\}} \phi_i, \quad (3.80)$$

$$P_k^\phi[\mathcal{C}] := \sum_{i \in \{\mathcal{P}_k\}} \phi_i, \quad (3.81)$$

where we take $\{\mathcal{F}_k\}$ and $\{\mathcal{P}_k\}$ to denote lists of the indices of the \mathcal{F}_k and \mathcal{P}_k elements respectively, so that the sums run over these elements. These functions depend on the causal set and the scalar field values, ϕ_i , defined on that causal set.

Under the sprinkling process the scalar field on the causal set defines random variables for the functions in (3.80) and (3.81) in the following way. We start with the usual notion of a scalar field, $\phi(x)$, defined on the manifold, M , we wish to sprinkle in to. The sprinkling generates a random causal set, \mathcal{C} , and we take x_i to be the spacetime point of the i th element. The scalar field value on the i th element of the causal set is then simply the value of the scalar field $\phi(x)$ evaluated at x_i , ie. $\phi_i = \phi(x_i)$. We then define the random variables \mathbf{F}_k^ϕ and \mathbf{P}_k^ϕ as those that return the values of the functions $F_k^\phi[\mathcal{C}^-]$ and $P_k^\phi[\mathcal{C}^+]$ respectively, where we have the same spacetime setup as before. These random variables, for a given k , are functions of the manifold, sprinkling density, surface Σ , and the scalar field $\phi(x)$.

We wish to find the expectation values of these random variables in the hope that we can use them to construct causal set expressions for continuum quantities. To get the expectation value of \mathbf{P}_k^ϕ , say, we need to take the product of the probability for an element to have been sprinkled in an infinitesimal volume element at x , times the probability that it is a \mathcal{P}_k element, times the value of the scalar field at x , $\phi(x)$, and then integrated over all x in the region to the future of Σ . The expectation value is then

$$\langle \mathbf{P}_k^\phi \rangle = \rho \int_{J^+(\Sigma)} dV_x \phi(x) \frac{(\rho V_\blacktriangle(x))^k}{k!} e^{-\rho V_\blacktriangle(x)}. \quad (3.82)$$

Likewise, for \mathbf{F}_k^ϕ we have

$$\langle \mathbf{F}_k^\phi \rangle = \rho \int_{J^-(\Sigma)} dV_x \phi(x) \frac{(\rho V_\blacktriangledown(x))^k}{k!} e^{-\rho V_\blacktriangledown(x)}. \quad (3.83)$$

We can, once again use GNCs, $x^\mu = (t, \mathbf{x})$, adapted to Σ such that in a neighbourhood U_Σ of Σ the line element is given by (3.3), and Σ is the surface defined by $t = 0$. The integrals can be simplified as before, so that we only integrate to ε in the time coordinate, and only make an exponentially small error in doing so. The addition of $\phi(x)$ in the integrand will not change this fact as it does not depend on ρ and so will not alter how the integrand changes with ρ . We take ε small enough such that we can expand the determinant of the metric about Σ as before. We will

also expand the scalar field about Σ as

$$\phi(t, \mathbf{x}) = \phi + \dot{\phi}t + \frac{1}{2}\ddot{\phi}t^2 + \mathcal{O}(t^3), \quad (3.84)$$

where the dots above ϕ denote time derivatives and the terms ϕ , $\dot{\phi}$ and $\ddot{\phi}$ are evaluated at $t = 0$ and depend on the surface coordinate \mathbf{x} .

We can now write the expectation values as

$$\begin{aligned} \langle \mathbf{F}_k^\phi \rangle &= \rho \int_{\Sigma} d^{d-1}x \int_{-\varepsilon}^0 dt h^{\frac{1}{2}} \left(1 - Kt + \frac{1}{2} (K^2 - K^{\alpha\beta} K_{\alpha\beta} - R_{tt}) t^2 + \mathcal{O}(t^3) \right) \\ &\quad \times \left(\phi + \dot{\phi}t + \frac{1}{2}\ddot{\phi}t^2 + \mathcal{O}(t^3) \right) \frac{(\rho V_{\mathbf{V}}(t, \mathbf{x}))^k}{k!} e^{-\rho V_{\mathbf{V}}(t, \mathbf{x})} + \dots, \\ \langle \mathbf{P}_k^\phi \rangle &= \rho \int_{\Sigma} d^{d-1}x \int_0^{\varepsilon} dt h^{\frac{1}{2}} \left(1 - Kt + \frac{1}{2} (K^2 - K^{\alpha\beta} K_{\alpha\beta} - R_{tt}) t^2 + \mathcal{O}(t^3) \right) \\ &\quad \times \left(\phi + \dot{\phi}t + \frac{1}{2}\ddot{\phi}t^2 + \mathcal{O}(t^3) \right) \frac{(\rho V_{\mathbf{A}}(t, \mathbf{x}))^k}{k!} e^{-\rho V_{\mathbf{A}}(t, \mathbf{x})} + \dots, \end{aligned} \quad (3.85)$$

where all of the geometric quantities are defined similarly to (3.40). Again, we use $+\dots$ to stand for “terms that vanish exponentially fast in the limit $\rho \rightarrow \infty$ ”.

As before we expand the cone volumes in t and evaluate the integrals by transforming them into the form of Gamma functions. The only difference here is that one must take into account of one more expansion, that of the scalar field. Because of the similarities we will just state the final expansion in large ρ for both of the required expectation values:

$$\begin{aligned} \langle \mathbf{P}_k^\phi \rangle &= \rho^{1-\frac{1}{d}} \frac{A^{-\frac{1}{d}} \Gamma(\frac{1}{d} + k)}{d k!} I_0^\phi - \rho^{1-\frac{2}{d}} \frac{A^{-\frac{2}{d}} \Gamma(\frac{2}{d} + k)}{d k!} \left(\frac{(d+2)}{(d+1)} I_1^\phi - I_0^\phi \right) \\ &\quad + \rho^{1-\frac{3}{d}} \frac{A^{-\frac{3}{d}} \Gamma(\frac{3}{d} + k)}{d k!} \left(\frac{1}{4(d+1)^2} I_2^\phi - \frac{(2d+5)}{2(d+1)} I_1^\phi + \frac{1}{2} I_0^\phi \right) + \mathcal{O}(\rho^{1-\frac{4}{d}}), \\ \langle \mathbf{F}_k^\phi \rangle &= \rho^{1-\frac{1}{d}} \frac{A^{-\frac{1}{d}} \Gamma(\frac{1}{d} + k)}{d k!} I_0^\phi + \rho^{1-\frac{2}{d}} \frac{A^{-\frac{2}{d}} \Gamma(\frac{2}{d} + k)}{d k!} \left(\frac{(d+2)}{(d+1)} I_1^\phi - I_0^\phi \right) \\ &\quad + \rho^{1-\frac{3}{d}} \frac{A^{-\frac{3}{d}} \Gamma(\frac{3}{d} + k)}{d k!} \left(\frac{1}{4(d+1)^2} I_2^\phi - \frac{(2d+5)}{2(d+1)} I_1^\phi + \frac{1}{2} I_0^\phi \right) + \mathcal{O}(\rho^{1-\frac{4}{d}}), \end{aligned} \quad (3.86)$$

where we have added superscripts to the integrals $I_{0,1,2}$ given in (3.49) to mean that one must include whatever is in the superscript in the integrand. For example,

$$I_1^\phi = \int_{\Sigma} d^{d-1}x \sqrt{h} K \dot{\phi}, \quad (3.87)$$

which is the integral I_1 with the integrand multiplied by $\dot{\phi}$.

We can now define causal set expressions utilising (3.86) that give the different integrals in the expansion. First, we will construct an expression for I_0^ϕ . We define

$$J_0^\phi [\mathcal{C}, \mathcal{C}^+, \mathcal{C}^-; \vec{p}, \vec{q}] := l^{d-1} dA^{\frac{1}{d}} \left(\sum_m p_m F_m^\phi [\mathcal{C}^-] + \sum_n q_n P_n^\phi [\mathcal{C}^+] \right), \quad (3.88)$$

where p_m and q_n are strings of real numbers that satisfy

$$\sum_m p_m \frac{\Gamma(\frac{1}{d} + m)}{m!} + \sum_n q_n \frac{\Gamma(\frac{1}{d} + n)}{n!} = 1. \quad (3.89)$$

Only one of the components needs to be non-zero to satisfy (3.89).

We can also define the random variable counterpart, \mathbf{J}_0^ϕ , in the usual way, by promoting F_k^ϕ and P_k^ϕ to random variables. Given that the coefficients satisfy (3.89) one can follow the same steps as in (3.58) to show that

$$\lim_{\rho \rightarrow \infty} \langle \mathbf{J}_0^\phi \rangle = I_0^\phi, \quad (3.90)$$

where we have omitted the arguments of \mathbf{J}_0^ϕ , which are the spacetime M , the surface Σ , the density ρ , the field $\phi(x)$, and the strings \vec{p} and \vec{q} .

The simplest choices of p_m and q_n are those in which there is only one non-zero component. If we take the first element of \vec{p} to be the only non-zero one, so that $\vec{q} = \vec{0}$, then $p_0 = \Gamma(\frac{1}{d})^{-1}$ solves (3.89). Using these strings the RHS of (3.88) becomes

$$l^{d-1} \frac{dA^{\frac{1}{d}}}{\Gamma(\frac{1}{d})} F_0^\phi [\mathcal{C}^-]. \quad (3.91)$$

For the opposite case where $\vec{p} = \vec{0}$ and q_0 is the only non-zero component we get a causal set function which is proportional to $P_0^\phi [\mathcal{C}^+]$. These two causal set functions have corresponding random variables whose expectation values give $\int_\Sigma d^{d-1}x \sqrt{h} \phi$ in the $\rho \rightarrow \infty$ limit. This seems intuitively correct, as one would expect that summing the values of the scalar field at the causal set elements close to the surface will give something like $\int_\Sigma d^{d-1}x \sqrt{h} \phi$ in the continuum limit.

Next, we would like to construct a causal set expression for the part in brackets in the second term on the RHS in (3.86). We define the causal set function

$$J_1^\phi [\mathcal{C}, \mathcal{C}^+, \mathcal{C}^-; \vec{p}, \vec{q}] := l^{d-2} dA^{\frac{2}{d}} \left(\sum_m p_m F_m^\phi [\mathcal{C}^-] + \sum_n q_n P_n^\phi [\mathcal{C}^+] \right) \quad (3.92)$$

where the strings p_m and q_n now satisfy

$$\begin{aligned} \sum_m p_m \frac{\Gamma(\frac{1}{d} + m)}{m!} + \sum_n q_n \frac{\Gamma(\frac{1}{d} + n)}{n!} &= 0, \\ \sum_m p_m \frac{\Gamma(\frac{2}{d} + m)}{m!} - \sum_n q_n \frac{\Gamma(\frac{2}{d} + n)}{n!} &= 1. \end{aligned} \quad (3.93)$$

With this, one can verify that the random variable counterpart, \mathbf{J}_1^ϕ , for (3.92) satisfies

$$\lim_{\rho \rightarrow \infty} \langle \mathbf{J}_1^\phi \rangle = \frac{(d+2)}{(d+1)} I_1^\phi - I_0^\phi. \quad (3.94)$$

In order to form the simplest causal set expressions we can pick the strings \vec{p} and \vec{q} , where only the lowest k components are non-zero. Such strings are given in section 3.4.1 so we will not repeat them here. If we sprinkle into a flat spacetime with a flat surface then $I_1^\phi = 0$. In this case \mathbf{J}_1^ϕ is the causal set analogue of the normal derivative of $\phi(x)$ integrated across Σ .

Finally, we construct a causal set expression for the part in brackets in the third term on the RHS of (3.86). We define

$$J_2^\phi [\mathcal{C}, \mathcal{C}^+, \mathcal{C}^-; \vec{p}, \vec{q}] := l^{d-3} dA^{\frac{3}{d}} \left(\sum_m p_m F_m^\phi [\mathcal{C}^-] + \sum_n q_n P_n^\phi [\mathcal{C}^+] \right), \quad (3.95)$$

where p_m and q_n satisfy (3.74). The corresponding random variable, \mathbf{J}_2^ϕ , can be shown to satisfy

$$\lim_{\rho \rightarrow \infty} \langle \mathbf{J}_2^\phi \rangle = \frac{1}{4(d+1)^2} I_2^\phi - \frac{(2d+5)}{2(d+1)} I_1^\phi + \frac{1}{2} I_0^\phi. \quad (3.96)$$

The same simple strings that were chosen towards the end of section 3.4.3 can be chosen here to get simple causal set expressions that give the RHS of (3.96) as $\rho \rightarrow \infty$. Again, if we sprinkle into a flat spacetime with a flat surface, this expression will give something analogous to the second order normal derivative of $\phi(x)$ integrated across Σ .

The causal set expressions that we have derived involve normal derivatives of a scalar field. Such expressions may be of use when constructing the causal set analogue of the scalar field stress energy tensor contracted with a timelike vector.

3.5 The Causal Set Action for a Flat Alexandrov Interval

Section 3.4.1 provides us with a family of analogue GHY boundary terms for causal sets. We can now consider if such terms need to be included in any putative action for causal sets. In particular we can ask whether boundary terms need to be added to the recently proposed Benincasa-Dowker-Glaser (BDG) causal set actions [9–11]. Before that question can be answered, it is necessary to determine whether the BDG actions already contain any boundary contributions.

The BDG action $S_{BDG}^{(d)}[\mathcal{C}]$ of a finite causal set \mathcal{C} is

$$\frac{1}{\hbar} S_{BDG}^{(d)}[\mathcal{C}] = -\alpha_d (l/l_p)^{d-2} \left(N[\mathcal{C}] + \frac{\beta_d}{\alpha_d} \sum_{i=1}^{n_d-1} C_i^{(d)} N_i[\mathcal{C}] \right), \quad (3.97)$$

where $N_i[\mathcal{C}]$ is the number of $(i+1)$ -element inclusive order intervals in \mathcal{C} , $N[\mathcal{C}]$ is the cardinality of the causal set, and l/l_p is the ratio of a fundamental length to the Planck length⁵. The constants are

$$\alpha_d = \begin{cases} -\frac{1}{\Gamma(1 + \frac{2}{d})} c_d^{2/d} & d \text{ odd} \\ -\frac{2}{\Gamma(1 + \frac{2}{d})} c_d^{2/d} & d \text{ even}, \end{cases} \quad (3.98)$$

$$\beta_d = \begin{cases} \frac{d+1}{2^{d-1} \Gamma(1 + \frac{2}{d})} c_d^{2/d} & d \text{ odd} \\ \frac{\Gamma(\frac{d}{2} + 2) \Gamma(\frac{d}{2} + 1)}{\Gamma(\frac{2}{d}) \Gamma(d)} c_d^{2/d} & d \text{ even}, \end{cases} \quad (3.99)$$

and

$$n_d = \begin{cases} \frac{d}{2} + \frac{3}{2} & d \text{ odd} \\ \frac{d}{2} + 2 & d \text{ even}, \end{cases} \quad (3.100)$$

where $c_d = 2^{1-\frac{d}{2}} \text{vol}(S_{d-2}) / (d(d-1))$ (recall that $\text{vol}(S_d)$ is the volume of the unit d -sphere). The coefficients $C_i^{(d)}$ of the terms $N_i[\mathcal{C}]$ in the sum are

$$C_i^{(d)} = \begin{cases} \sum_{k=0}^{i-1} (-1)^k \binom{i-1}{k} \frac{\Gamma(\frac{d}{2}(k+1) + \frac{3}{2})}{\Gamma(\frac{d}{2} + \frac{3}{2}) \Gamma(\frac{d}{2}k + 1)} & d \text{ odd} \\ \sum_{k=0}^{i-1} (-1)^k \binom{i-1}{k} \frac{\Gamma(\frac{d}{2}(k+1) + 2)}{\Gamma(\frac{d}{2} + 2) \Gamma(\frac{d}{2}k + 1)} & d \text{ even}. \end{cases} \quad (3.101)$$

⁵We reintroduce \hbar in this section.

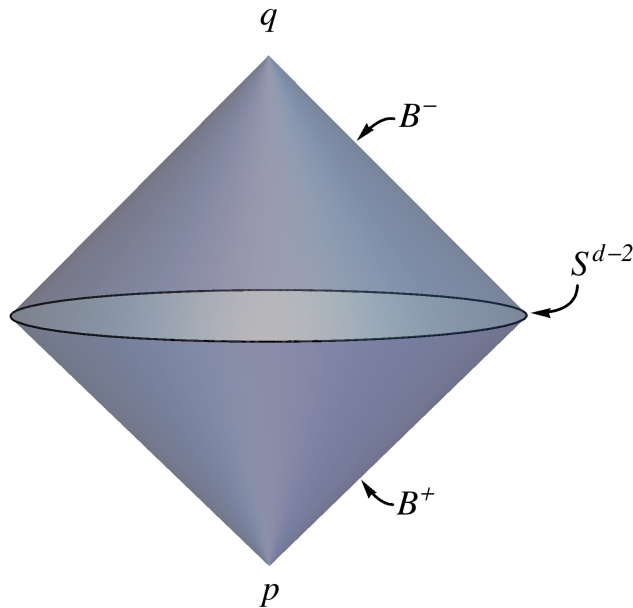


Figure 3.6: The Alexandrov interval $I(p, q)$. The boundary consists of the null sections B^\pm and the spatial sphere S^{d-2} at their joint.

We note here that these coefficients can be expressed more compactly as generalised hypergeometric functions of type $\{q + 1, q\}$:

$$C_i^{(d)} = {}_{q+1}F_q(\{a_1, \dots, a_q, i - 1\}, \{b_1, \dots, b_q\} | 1) , \quad (3.102)$$

with $q = \frac{d+1}{2}$, $a_i = \frac{d+2i}{d}$ and $b_i = \frac{2i}{d}$ for d odd, and $q = \frac{d}{2}$, $a_i = \frac{d+2i+2}{d}$ and $b_i = \frac{2i}{d}$ for d even.

As in Section 3.4, given a causal Lorentzian spacetime (M, g) , the sprinkling process at density $\rho = l^{-d}$ turns this function of causal sets into a random variable $\mathbf{S}_{BDG}^{(d)}[M, \rho]$, the “random discrete action” of (M, g) . A requirement for the causal set action to be physically interesting is that its mean should tend to the continuum action of (M, g) as $\rho \rightarrow \infty$. The question at hand is whether in this limit it includes boundary contributions in addition to the Einstein-Hilbert term.

We will explore this question by calculating the mean of the d -dimensional BDG action for causal sets sprinkled into causal intervals or “Alexandrov intervals” in d -dimensional flat spacetime. Since the Einstein-Hilbert contribution is expected to be zero, this will teach us something about what boundary contributions, if any, are included in the BDG action. The boundary of an Alexandrov interval consists of a past and a future null cone which intersect at a codimension-2 *joint* of topology S^{d-2} (see Figure 3.6). From Chapter 2 we know that the boundary terms for the

interval will depend on the parameterisation of the null generators of the boundary.

As was shown in [52], when $d = 2$ the continuum limit of the expectation value of the discrete random action of an Alexandrov interval of arbitrary size is equal to 2. While this might suggest topological invariance, we will now show that it is a part of a more general result for $d > 2$ and has a geometrical origin. Namely, it corresponds to the volume of the joint of the Alexandrov interval, which in flat spacetime is a $(d - 2)$ -sphere and independent of the interval size *only* in $d = 2$.

Consider an Alexandrov interval, $I(p, q)$, of proper height τ between two points p and q in d -dimensional Minkowski spacetime. Its boundary consists of the two null cones from p and q which intersect at the joint, $\mathcal{J}^{(d-2)} := \partial J^+(p) \cap \partial J^-(q)$, a codimension-2 sphere of radius $\tau/2$. The joint has volume $\text{vol}(\mathcal{J}^{(d-2)}) = (\tau/2)^{d-2} \text{vol}(S_{d-2})$. The interval itself has volume $\text{vol}(I(p, q)) = 2(\text{vol}(S_{d-2})/(d(d-1)))(\tau/2)^d$. For the sprinkling process at density $\rho = l^{-d}$, the mean, $N := \langle \mathbf{N} \rangle$, of the number of causal set elements sprinkled into $I(p, q)$ is $N = \rho \text{vol}(I(p, q))$. In what follows we take the continuum limit $\rho \rightarrow \infty$ while keeping τ fixed. The mean of the random discrete action of this flat region should give, in the limit of large ρ , contributions from the boundary only.

In [53] a closed form expression was obtained for the mean value of the number of $(i+1)$ -element inclusive intervals contained in an Alexandrov interval in d -dimensional flat spacetime:

$$\langle \mathbf{N}_i^{(d)} \rangle = \frac{\Gamma(d)^2 N^{i+2}}{\Gamma(i)} \sum_{k=0}^{\infty} \frac{(-N)^k \Gamma(k+i+1) \Gamma\left(\frac{d(k+i)}{2} + 1\right) \Gamma\left(\frac{d(k+i+1)}{2} + 1\right)}{\Gamma(k+i+3) \Gamma(k+1) \Gamma\left(\frac{d(k+i)}{2} + d\right) \Gamma\left(\frac{d(k+i+1)}{2} + d\right)}, \quad (3.103)$$

where $i \geq 1$. Importantly, this power series can be expressed more compactly in terms of a generalised hypergeometric function of type $\{d, d\}$ as shown in [53], and is therefore convergent for all N . All the power series in N that appear subsequently in this section are therefore also convergent. We now use this to evaluate $\langle \mathbf{S}_{BDG}^{(d)} \rangle$ in an Alexandrov interval in flat spacetimes of different dimensions.

We begin with the simplest case of $d = 2$, where

$$\frac{1}{\hbar} \langle \mathbf{S}_{BDG}^{(2)} \rangle = 2 \left(N - 2 \langle \mathbf{N}_1^{(2)} \rangle + 4 \langle \mathbf{N}_2^{(2)} \rangle - 2 \langle \mathbf{N}_3^{(2)} \rangle \right). \quad (3.104)$$

Using (3.103) gives a power series expansion in N with coefficients $\frac{(-1)^{i-1}}{i!}$, $i \in \mathbb{N}$, so that

$$\frac{1}{\hbar} \langle \mathbf{S}_{BDG}^{(2)} \rangle = 2 (1 - e^{-N}), \quad (3.105)$$

which agrees with the result in [52]. In anticipation of the results for higher d we

note that the volume of the zero sphere at the joint, $\text{vol}(\mathcal{J}^{(0)}) = \text{vol}(S_0) = 2$, so that

$$\lim_{N \rightarrow \infty} \frac{1}{\hbar} \langle \mathbf{S}_{BDG}^{(2)} \rangle = \text{vol}(\mathcal{J}^{(0)}) . \quad (3.106)$$

This is in agreement with the result obtained for a 2-dimensional flat causal interval [52].

Next, substituting (3.103) into the $d = 3$ averaged BDG action,

$$\frac{1}{\hbar} \langle \mathbf{S}_{BDG}^{(3)} \rangle = -\alpha_3 \left(\frac{l}{l_p} \right) \left(N - \langle \mathbf{N}_1^{(3)} \rangle + \frac{27}{8} \langle \mathbf{N}_2^{(3)} \rangle - \frac{9}{4} \langle \mathbf{N}_3^{(3)} \rangle \right) , \quad (3.107)$$

gives a power series expansion in N with coefficients

$$-\alpha_3 \left(\frac{l}{l_p} \right) \times \frac{(-1)^{i+1}}{i!} \frac{8}{(3i+1)(3i-1)} , \quad (3.108)$$

where $i \in \mathbb{N}$. Rearranging indices we find a closed form for the action:

$$\frac{1}{\hbar} \langle \mathbf{S}_{BDG}^{(3)} \rangle = -8\alpha_3 \left(\frac{l}{l_p} \right) \times \left(-1 + {}_2F_2 \left(\left\{ \frac{1}{3}, -\frac{1}{3} \right\}, \left\{ \frac{4}{3}, \frac{2}{3} \right\} \middle| -N \right) \right) , \quad (3.109)$$

where ${}_2F_2$ is a generalised hypergeometric function of type $\{2, 2\}$. This can be re-expressed more simply as

$$\frac{1}{\hbar} \langle \mathbf{S}_{BDG}^{(3)} \rangle = -8\alpha_3 \left(\frac{l}{l_p} \right) \left(-1 + \frac{1}{6N^{\frac{1}{3}}} \gamma \left(\frac{1}{3}, N \right) - \frac{N^{\frac{1}{3}}}{6} \gamma \left(-\frac{1}{3}, N \right) \right) , \quad (3.110)$$

where $\gamma(s, x) \equiv \int_0^x t^{s-1} e^{-t} dt$ is a lower incomplete Gamma function. The large N behaviour is thus dominated by the last term in the above expression. Using $\gamma(s, x) = \Gamma(s) - \Gamma(s, x)$, where the upper incomplete Gamma function $\Gamma(s, x) \sim x^{s-1} e^{-x}$ in the asymptotic limit, the dominant term in (3.110) simplifies to $-4\alpha_3 l N^{1/3} \Gamma(2/3) / l_p = \text{vol}(\mathcal{J}^{(1)}) / l_p$. Hence

$$\lim_{N \rightarrow \infty} \frac{1}{\hbar} \langle \mathbf{S}_{BDG}^{(3)} \rangle = \frac{1}{l_p} \text{vol}(\mathcal{J}^{(1)}) . \quad (3.111)$$

For $d = 4$

$$\frac{1}{\hbar} \langle \mathbf{S}_{BDG}^{(4)} \rangle = -\alpha_4 \left(\frac{l}{l_p} \right)^2 \left(N - \langle \mathbf{N}_1^{(4)} \rangle + 9 \langle \mathbf{N}_2^{(4)} \rangle - 16 \langle \mathbf{N}_3^{(4)} \rangle + 8 \langle \mathbf{N}_4^{(4)} \rangle \right) . \quad (3.112)$$

Excluding the first term, this is a power series in N with coefficients

$$-\alpha_4 \left(\frac{l}{l_p} \right)^2 \times \frac{(3!)^2 (-1)^{i+1} (i-1)(2i-3)!}{3 i! (2i+1)!} , \quad (3.113)$$

where now $i \in \mathbb{N}$. Using this, *Mathematica* yields the closed form expression

$$\frac{1}{\hbar} \langle \mathbf{S}_{BDG}^{(4)} \rangle = -\alpha_4 \left(\frac{l}{l_p} \right)^2 \left(\frac{3(2N-1)}{2\sqrt{N}} \sqrt{\pi} \text{Erf}(\sqrt{N}) - 3(\gamma - e^{-N} + \Gamma(0, N) + \ln(N)) \right), \quad (3.114)$$

where γ is the Euler-Mascheroni constant, and Erf is the error function. Since $\text{Erf}(\sqrt{N})$ goes to 1 in the asymptotic limit, the dominant contribution to the above expression comes from the second term, $-3\alpha_4 l^2 \sqrt{\pi N}/l_p^2$, which simplifies to $2\sqrt{6\pi N} l^2/l_p^2 = \text{vol}(\mathcal{J}^2)/l_p^2$. Thus, again

$$\lim_{N \rightarrow \infty} \frac{1}{\hbar} \langle \mathbf{S}_{BDG}^{(4)} \rangle = \frac{1}{l_p^2} \text{vol}(\mathcal{J}^{(2)}). \quad (3.115)$$

We now turn to the case of general d . We begin by writing the (averaged) sum in (3.97) as a power series in N :

$$\sum_{i=1}^{n_d} C_i^{(d)} \langle \mathbf{N}_i \rangle = \sum_{j=1}^{\infty} A_j^{(d)} N^{j+1}. \quad (3.116)$$

After a rearrangement and redefinition of indices we find that

$$A_j^{(d)} = \Gamma(d)^2 \frac{(-1)^j \Gamma(\frac{d}{2}(j-1)+1) \Gamma(\frac{d}{2}j+1)}{(j+1)! \Gamma(\frac{d}{2}(j-1)+d) \Gamma(\frac{d}{2}j+d)} \sum_{i=1}^{D+2} (-1)^i \binom{j-1}{i-1} C_i^{(d)}, \quad (3.117)$$

where $d = 2D$ for d even and $d = 2D + 1$ for d odd. While (3.116) can be directly evaluated by *Mathematica* for small values of $d = 2, \dots, 5$, it is greatly assisted by the following simplifications to the $A_j^{(d)}$ for higher d .

We begin by evaluating the sum in (3.117). We first use *Mathematica* to evaluate it for $d = 2, \dots, 20$ which then suggests the general form

$$\sum_{i=1}^{D+2} (-1)^i \binom{j-1}{i-1} C_i^{(d)} = \begin{cases} \frac{(-1)^D ((2D+1)^2 j^2 - 1) (3 - (2D+1)j/2)_{D-1}}{4\Gamma(2+D)} & d \text{ odd} \\ \frac{(-1)^D D j (2+2D) (1-Dj)_{D-1}}{2\Gamma(2+D)} & d \text{ even}, \end{cases} \quad (3.118)$$

where $(a)_k$ is the Pochhammer symbol. Inserting this into (3.117) we use *Mathematica* to evaluate it for $d = 2, \dots, 20$. After some manipulations this suggests the general expression

$$A_j^{(d)} = \frac{\Gamma(d)^2 (-1)^{j+1}}{\Gamma(\frac{d}{2}(j+1)) \Gamma(\frac{d}{2}(2+j)) \Gamma(2+j)} \gamma_j^{(d)}, \quad (3.119)$$

where

$$\gamma_j^{(d)} = \begin{cases} \frac{\sqrt{\pi} \Gamma(2 + dj)}{2^{1+dj} \Gamma\left(\frac{d-1}{2}\right)} & d \text{ odd} \\ \frac{\Gamma\left(1 + \frac{d}{2}j\right) \Gamma\left(2 + \frac{d}{2}j\right)}{\Gamma\left(\frac{d}{2}\right)} & d \text{ even} . \end{cases} \quad (3.120)$$

Taking a hint from the behaviour of $\langle \mathbf{S}_{BDG}^{(d)} \rangle$ for $d = 2, 3, 4$ in the $N \rightarrow \infty$ limit, we will consider the ratio

$$\frac{l_p^{d-2} \langle \mathbf{S}_{BDG}^{(d)} \rangle}{\hbar \text{vol}(\mathcal{J}^{(d-2)})} = \frac{\varepsilon_d}{d(d-1)\Gamma\left(1 + \frac{2}{d}\right) N^{\frac{d-2}{d}}} \left(N + \frac{\beta_d}{\alpha_d} \sum_{i=1}^{n_d} C_i^{(d)} \langle \mathbf{N}_i \rangle \right) , \quad (3.121)$$

where $\varepsilon_d = 1$ for d odd and 2 for d even. Finally inserting (3.119) into (3.121) *Mathematica* gives for $d = 2, \dots, 16$

$$\lim_{N \rightarrow \infty} \frac{1}{\hbar} \langle \mathbf{S}_{BDG}^{(d)} \rangle = \frac{1}{l_p^{d-2}} \text{vol}(\mathcal{J}^{(d-2)}) . \quad (3.122)$$

This is the main result of this section and can be interpreted as saying that, in the continuum limit, the mean of the random discrete action of a causal diamond is a pure boundary term coming only from the volume of the codimension-2 joint. Interestingly, this may coincide with the joint contribution to the action given in Chapter 2, with the causal set possibly ‘‘picking-out’’ a particular parameterisation of the null generators. The result we have obtained is for flat spacetime and it would be interesting to see how the presence of curvature affects it by repeating this calculation in RNCs to the lowest order corrections.

Finally, while efforts have been made to find a closed form expression of $\frac{1}{\hbar} \langle \mathbf{S}_{BDG}^{(d)} \rangle$ for arbitrary d this has proved difficult, even in the asymptotic limit. As we now show, the most obvious approach of using the asymptotic form of the $\langle \mathbf{N}_i^{(d)} \rangle$'s is insufficient for this purpose. In the large N limit [53]

$$\langle \mathbf{N}_i^{(d)} \rangle = \frac{\Gamma\left(\frac{2}{d} + i\right) \Gamma(d)}{i! \left(\frac{d}{2} - 1\right) \left(\frac{d}{2} + 1\right)_{d-2}} N^{2-\frac{2}{d}} + O(N^\alpha f(N)) , \quad (3.123)$$

where $\alpha = 1$ for $d = 3, 4$ and $2 - \frac{4}{d}$ for $d > 4$, and $f(N) = \ln N$ for $d = 4$ and 1 otherwise. For $d = 2$

$$\langle \mathbf{N}_i^{(2)} \rangle = N \ln N + O(N) . \quad (3.124)$$

Since this dominates the leading order contribution of $N^{\frac{d-2}{d}}$ to $\frac{1}{\hbar} \langle \mathbf{S}_{BDG}^{(d)} \rangle$ for all d , it is clear that this contribution must vanish. Inserting (3.123) and (3.124) into the BDG action confirms that this is indeed the case for $d = 2, \dots, 16$. In fact, the next

to leading order terms in (3.123) and (3.124) also do not have the requisite $N^{\frac{d-2}{d}}$ dependence, and are dominant in comparison. Hence their contribution too should vanish, but we do not have an explicit expression for their coefficients to check this. Suffice to say that the asymptotic behaviour of $\langle \mathbf{N}_i^{(d)} \rangle$ is indeed not enough to find the leading order dependence of the BDG action in the flat spacetime interval.

3.6 Summary

We have derived a family of causal set boundary terms that agree in the mean with the Gibbons-Hawking-York boundary term for a spacelike hypersurface. We have also found causal set expressions for the surface area and other geometric objects relating to the surface. We presented a heuristic argument for how the fluctuations of these expressions go with ρ , and provided numerical evidence in different dimensions to support that reasoning. In 4 dimensions the fluctuations of the boundary terms decrease with ρ , and increase for the causal set expressions in 3.4.3. The use of an intermediate length scale in the BDG action seems like a promising approach that may dampen these fluctuations. More work should be done to determine how the fluctuations scale in more complicated spacetimes, and in the case where a scalar field is included. It would also be interesting to also find causal set analogues of the GHY boundary term for timelike boundaries. The situation is more complicated in that case because the identification of “nearest neighbours” to a timelike hypersurface in terms of causal structure is less straight-forward than in the spacelike case.

The other major result of this chapter is that the average over sprinklings of the BDG action for an interval in Minkowski spacetime is proportional to the volume of the “joint” of that interval, which may indicate that the BDG action contains the joint contribution to the continuum action with a particular choice of null parameter. There is still more work to be done to determine what sort of boundary contributions are already contained in the BDG action, and we do not know if the joint contribution is contained in the BDG action for a general spacetime.

Other interesting results obtained along the way were causal set expressions for the normal derivatives of a scalar field and the dimension of the manifold the causet has been sprinkled into.

In order to obtain these results we derived a universal formula for the expansion of the volume of a small causal cone, up to $\mathcal{O}(T^{d+2})$. As the geometrical setup of the causal cone involves a hypersurface one might hope that the small volume formula can be used to derive the Hamiltonian formulation of General Relativity in

the continuum, in a similar way to how Jacobson derives the Einstein equations using the volume of a small spacetime region in [41]. The geometric quantities that are encoded in the causal set expressions in 3.4.3 appear in the Hamiltonian formulation of General Relativity. Perhaps these causal set expressions can be used to formulate the dynamics of causal sets from a Hamiltonian perspective.

Chapter 4

Topology Change in Quantum Gravity

4.1 Introduction

Thusfar we have seen how causal structure can be used to recover spacetime geometry in causal set theory. In this chapter we utilise causal structure to enlarge the set of spacetimes in which we can study quantum field theory to those that include topology change. There are good reasons to believe that topology change will play a role in quantum gravity. From the point of view of a gravitational sum-over-histories, dimensional analysis of the path integral suggests that structures on Planckian scales will have a gravitational action of order \hbar , which would lead to very little suppression in the path-integral [54]. Such considerations suggest that Planck scale topology-change, at least, should be taken into account in a quantum theory of gravity. Going further, Sorkin has argued that without topology change quantum gravity would be inconsistent, with the strongest evidence coming from the theory of topological geons [55], particles built on non-trivial spatial topology. Geons suffer from violations of the spin-statistics correlation and other problems in a framework with frozen spatial topology. Allowing topology change might solve these problems and, conversely, considering how to make the physics of geons consistent might give clues about the rules that govern topology change in quantum gravity [56–58].

At a formal level, it is easy enough to conceive of including topology changing manifolds in the gravitational path integral. However, a theorem of Geroch [59] tells us that a Lorentzian metric on a manifold in which the spatial topology changes must contain closed timelike curves. If one wants to avoid the pathologies that go along with closed timelike curves [54, 60], one can consider the alternatives of metrics

that are Lorentzian *almost everywhere* (degenerating at a finite set of isolated points) and which retain a well-defined causal order [57], or, going further, metrics with signature change [61] or Euclidean signature [62]. One can then investigate the action of a topology changing spacetime in a background field approximation by studying linear-order quantum fluctuations, or as a first step by investigating a free massless scalar quantum field in the background spacetime, a study within the framework of quantum field theory in curved spacetime.

Choosing the histories in the path integral to be Lorentzian spacetimes with well-defined causal order and isolated singularities, one is then faced with the challenge that such topology changing spacetimes are not globally hyperbolic in the usual sense. Since global hyperbolicity is a basic assumption in textbook quantum field theory, this means that one is necessarily charting new territory in investigating quantum field theory in such spacetimes. New rules must be created and analysed to see if they are self-consistent and physically plausible.

Work along these lines was carried out by Anderson and DeWitt [63], who studied the quantum theory of a free massless scalar field on the topology-changing two-dimensional “trousers” spacetime, in which a circle splits into two (or vice-versa), see Figure 4.1. This spacetime admits an almost everywhere Lorentzian metric, which is flat everywhere except at an isolated singular point, the “crotch singularity”. Expanding the scalar field in terms of modes on a spacelike hypersurface in the “in”-region and specifying a particular “shadow rule” to propagate the modes past the topology-changing hypersurface into the “out”-region, Anderson and DeWitt concluded that the expectation value of the stress-energy tensor evaluated in the in-vacuum has incurable (squared Dirac-delta) divergences on the light-cone of the singularity. They argued that this means that the trousers-type topology-change is dynamically forbidden. Manogue et al. [64] revisited the problem with a more careful analysis. They argued that the propagation rule of Anderson and DeWitt is unphysical because the Klein-Gordon product is not conserved when using the shadow rule to propagate solutions past the topology-changing hypersurface. Deriving a one-parameter family of propagation laws that conserve the inner product they arrived, nevertheless, at the same conclusion: an infinite burst of energy emanating from the singularity.

Recently a new approach to QFT has been proposed by Sorkin [65, 66] based on work by Johnston on QFT on a causal set [67]. In this chapter we apply the Sorkin-Johnston (SJ) formalism to the trousers, not only to see what light it might shed on previous results, but also as an exercise in the new approach. The starting point of the SJ approach for a free scalar field is the retarded Green function, rather than

the field operator as a solution of the equations of motion. The Green function leads to a distinguished quantum state — a candidate “ground state” — for a spacetime region without further input. In a globally hyperbolic spacetime the retarded Green function is unique but in a topology changing spacetime we expect that there will be a choice of Green functions. This turns out to be the case and we will see that there is a separate QFT for each choice.

4.2 Background and Setup

4.2.1 The SJ Formalism

Here we give a brief review of the SJ formalism [65, 66] for a free scalar field, ϕ , in a globally hyperbolic spacetime, $(M, g_{\mu\nu})$, of finite volume. Given the retarded Green function, $G(x, y)$, the Pauli-Jordan function is defined as $\Delta(x, y) = G(x, y) - G(y, x)$ (x and y are spacetime points). Note that $\Delta(x, y)$ is antisymmetric. In a globally hyperbolic spacetime, the transpose of the retarded Green function is the advanced Green function and so $\Delta(x, y)$ is a solution of the equations of motion in both its arguments. We will see that this condition will need to be imposed by hand in the trousers spacetime, as the connection between retarded and advanced Green functions is not automatic.

The Hilbert space $L^2(M)$ of equivalence classes of complex functions on $(M, g_{\mu\nu})$ has inner product

$$\langle [f], [g] \rangle := \int_M dV_x f(x)^* g(x) \quad (4.1)$$

where $[f], [g] \in L^2(M)$ (square brackets denote equivalence classes and $*$ denotes complex conjugation), and dV_x denotes the spacetime volume element at x . In what follows we will abuse notation and refer to an element of the Hilbert space by one of its representative functions.

We define the *Pauli-Jordan operator* as an operator on the Hilbert space which is given by the integral operator on representative functions whose kernel is the Pauli-Jordan function $\Delta(x, y)$:

$$(\Delta f)(x) = \int_M dV_y \Delta(x, y) f(y). \quad (4.2)$$

Assuming that $\Delta(x, y)$ is a square integrable kernel, i.e. that $\Delta(x, y) \in L^2(M \times M)$, then the operator $i\Delta$ is a self-adjoint Hilbert-Schmidt operator [68, Thm. VI.23] and

the spectral theorem for such operators says that $i\Delta$ has a set of real eigenvalues $\lambda_{\mathbf{a}}$ and a complete orthonormal set of eigenfunctions $\mathbf{u}_{\mathbf{a}}$ which satisfy

$$i\Delta\mathbf{u}_{\mathbf{a}} = \lambda_{\mathbf{a}}\mathbf{u}_{\mathbf{a}}, \quad \lambda_{\mathbf{a}} \in \mathbb{R}. \quad (4.3)$$

Since $\Delta(x, y)$ is a real function, it follows that

$$i\Delta\mathbf{u}_{\mathbf{a}} = \lambda_{\mathbf{a}}\mathbf{u}_{\mathbf{a}} \implies i\Delta\mathbf{u}_{\mathbf{a}}^* = -\lambda_{\mathbf{a}}\mathbf{u}_{\mathbf{a}}^*, \quad (4.4)$$

which means that for the non-zero eigenvalues, the eigenfunctions of $i\Delta$ come in pairs:

$$i\Delta\mathbf{u}_{\mathbf{a}}^{\pm} = \pm\lambda_{\mathbf{a}}\mathbf{u}_{\mathbf{a}}^{\pm}, \quad (4.5)$$

where $\lambda_{\mathbf{a}} > 0$ and $\mathbf{u}_{\mathbf{a}}^- = \mathbf{u}_{\mathbf{a}}^{+*}$. Moreover, these eigenfunctions (appropriately normalised) are orthonormal in the $L^2(M)$ inner product:

$$\begin{aligned} \langle \mathbf{u}_{\mathbf{a}}^{\pm}, \mathbf{u}_{\mathbf{b}}^{\pm} \rangle &= \delta_{\mathbf{ab}} \\ \langle \mathbf{u}_{\mathbf{a}}^+, \mathbf{u}_{\mathbf{b}}^- \rangle &= 0. \end{aligned} \quad (4.6)$$

$i\Delta(x, y)$ is the sum of its positive and negative parts:

$$i\Delta(x, y) = Q(x, y) - Q(x, y)^*, \quad (4.7)$$

where

$$Q(x, y) = \sum_{\mathbf{a}} \lambda_{\mathbf{a}} \mathbf{u}_{\mathbf{a}}^+(x) \mathbf{u}_{\mathbf{a}}^-(y). \quad (4.8)$$

The SJ state is the pure Gaussian state defined by its Wightman function,

$$W_{SJ}(x, y) := Q(x, y) = \sum_{\mathbf{a}} \lambda_{\mathbf{a}} \mathbf{u}_{\mathbf{a}}^+(x) \mathbf{u}_{\mathbf{a}}^-(y). \quad (4.9)$$

Although the topology changing spacetime we will look at is not globally hyperbolic in the usual sense, it does have a well-defined causal structure so that the notion of retardedness of a Green function makes sense, and it has finite volume so the SJ formalism can be extended to our case if an appropriate Green function can be found.

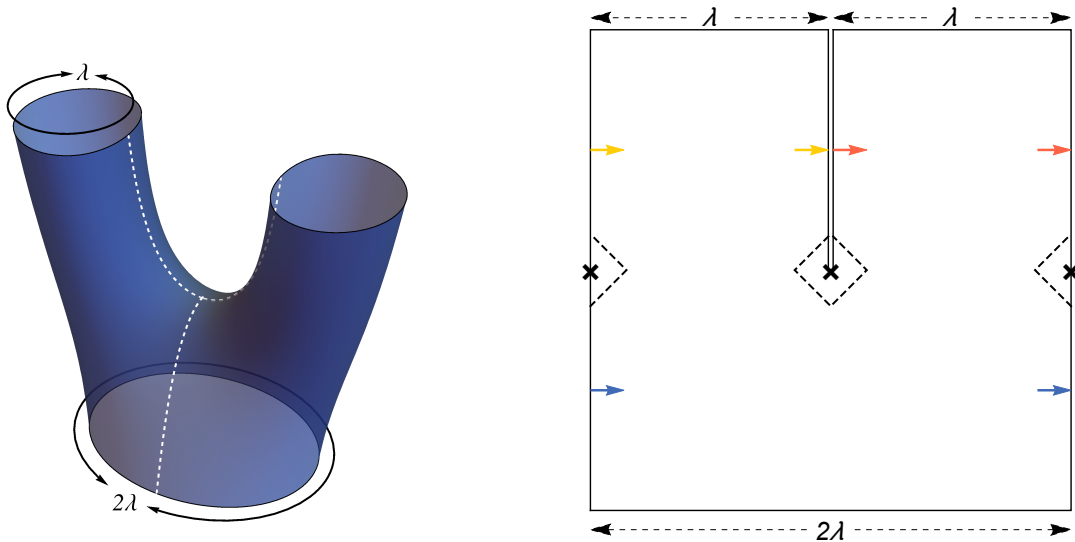


Figure 4.1: The trousers spacetime is shown on the left. The flat two-dimensional representation of the trousers on the right is obtained by cutting along the dotted lines and unwrapping the trousers on the left. The arrows indicate the respective identifications in the trunk and in the left and right legs. The crosses are identified and mark the location of x_c , the singularity. The dashed lines on the right form the boundary of a neighbourhood of x_c which we call the pair of diamonds.

4.2.2 The Trousers Spacetime

Keeping with tradition, let us hang the trousers upside down as in Figure 4.1 and use Cartesian coordinates (T, X) in which $T = 0$ separates the “legs” and the “trunk”. The spatial coordinate X lies in the range $[-\lambda, \lambda]$ and the singularity, x_c lies at the origin: $x_c = (0, 0)$. The coordinates in the trunk extend to coordinates in the left and right legs, i.e. we identify points $(0+, X)$ in the legs with points $(0-, X)$ in the trunk for $X \neq 0$. In the trunk, i.e. for $T < 0$, we identify $X = -\lambda$ with $X = \lambda$. In the legs $T > 0$. In the left leg we identify $X = -\lambda$ with $X = 0-$ and in the right leg, we identify $X = \lambda$ with $X = 0+$. The metric on the trousers is locally flat everywhere except at x_c where it is degenerate.

To build the SJ state in the trousers we need to identify the positive eigenvalue eigenfunctions of $i\Delta$ as in the analysis of the flat causal diamond [69]. For this, we need the Pauli-Jordan function $\Delta(x, y) = G(x, y) - G(y, x)$, and thus the retarded Green function in the trousers.

One way in which Green functions in the trousers differ from those in Minkowski space is due to the cylindrical topology of the trunk and legs. Consider the quantum field theory on a flat cylinder $S^1 \times \mathbb{R}$ (no topology-change). The future and past

light-cones of any point, x , will wrap around the cylinder and intersect at a set of conjugate points. This means that the retarded Green function on the cylinder is not equal to the retarded Green function $G_{\text{Mink}}(x, y)$ of two-dimensional Minkowski space. At the first conjugate point to the past of x , call it x' , there is a contribution $-\delta^{(2)}(x - x')$ to $\square_x G_{\text{Mink}}(x, y)$. The Green function on the cylinder is obtained by adding to $G_{\text{Mink}}(x, y)$ appropriate multiples of $G_{\text{Mink}}(x', y)$ for every conjugate point x' : the usual method of images.

In order to isolate the features of the trousers spacetime that are most pertinent to the physics of topology-change, we could restrict ourselves to a thin enough slab of the trousers containing the singularity such that no wrapping around occurs, e.g. $|T| \leq T_{max}$ for some $T_{max} < \frac{\lambda}{4}$. However, it will be most convenient to restrict further to a smaller neighbourhood of the singularity. Consider, therefore, two points, one in the left and one in the right leg, each lying directly above the singularity: $x_{leg}^{\pm} = (T_0, 0\pm)$. Consider the intersection of the union of their causal pasts with the causal future of two points in the trunk, $x_{trunk}^+ = (-T_0, 0)$ and $x_{trunk}^- = (T_0, \lambda)$, each of which lies directly below the singularity. This region consists of the two diamonds outlined with dashed lines in Figure 4.1. We refer to this spacetime as the *pair of diamonds*. Figure 4.2 shows the pair of diamonds, with the topological identifications inherited from the trousers. When the two diamonds are depicted next to each other as in Figure 4.2, the left diamond (A) corresponds to the diamond seen in the centre of the cut open trousers (the right diagram in Figure 4.1) and the right diamond (B) is made up of the two halves at the sides of the cut open trousers. Figure 4.3 shows how the pair of diamonds embeds in the original picture of the trousers. The pair of diamonds spacetime captures the essential causal structure of the trousers topology change.

4.2.3 The Pair of Diamonds

In order to discuss the pair of diamonds, denoted by \mathcal{M} , and functions on it, it will be useful to have a coordinate system that respects the symmetry between the two diamonds, A and B . We will use both Cartesian, (T_i, X_i) , and light-cone coordinates, (u_i, v_i) (where $u_i = \frac{1}{\sqrt{2}}(T_i - X_i)$ and $v_i = \frac{1}{\sqrt{2}}(T_i + X_i)$), and subscripts $i = A, B$, refer to the corresponding diamond. The trousers coordinates (without subscript) defined previously and the coordinates on the two diamonds are related as follows. The coordinate system on diamond A agrees with the trousers coordinate system since they have the same origin: $T_A = T$, $X_A = X$, $u_A = u$, $v_A = v$. On diamond B , the left side comes from the right edge of the trousers and the right side

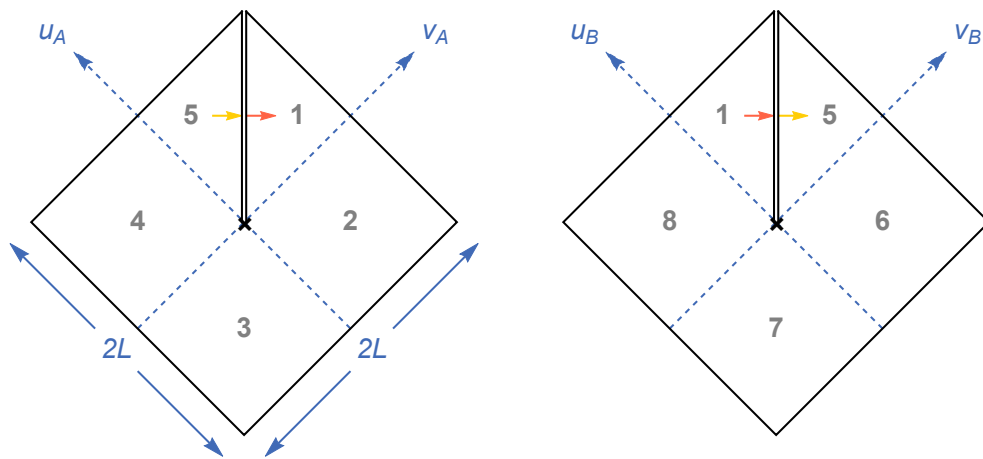


Figure 4.2: The pair of diamonds in more detail. Diamond A is on the left and diamond B is on the right. The arrows in regions 1 and 5 indicate the topological identifications inherited from the trousers. The dashed lines are the past and future lightcones from the singularity.

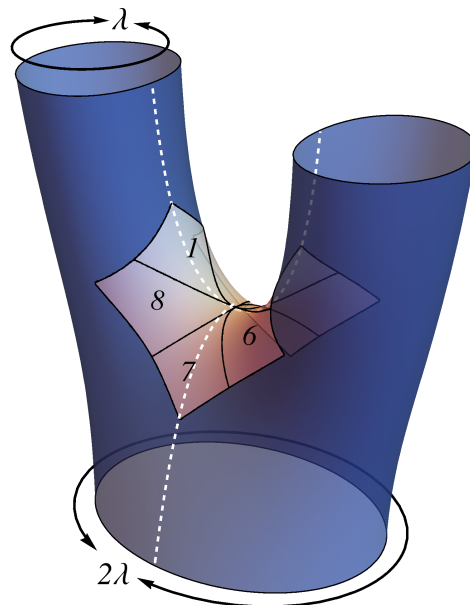


Figure 4.3: The pair of diamonds on the trousers. The numbers illustrate the different regions of the pair of diamonds.

comes from the left edge of the trousers, so the relations between the coordinate

systems are

$$\begin{array}{l}
 T_B = T \\
 X_B = X - \lambda \quad \text{for } X > 0 \\
 X_B = X + \lambda \quad \text{for } X < 0
 \end{array}
 \iff
 \begin{array}{l}
 \left. \begin{array}{l}
 u_B = u + \lambda/\sqrt{2} \\
 v_B = v - \lambda/\sqrt{2}
 \end{array} \right\} \text{ for } X > 0 \\
 \left. \begin{array}{l}
 u_B = u - \lambda/\sqrt{2} \\
 v_B = v + \lambda/\sqrt{2}
 \end{array} \right\} \text{ for } X < 0.
 \end{array}
 \quad (4.10)$$

The coordinate range for the light-cone coordinates on each diamond is $[-L, L]$ where $\sqrt{2}L < \lambda/2$. In both the A and B coordinate systems the singularity, x_c , is at the origin of coordinates. For $0 < T_A, T_B < \sqrt{2}L$, we identify $X_A = 0^-$ with $X_B = 0^+$ and vice versa. The two coordinate systems do not correspond to a split into left and right legs in the trousers manifold: for example, both the top left part of diamond A (i.e. $u_A > v_A > 0$) and the top right part of diamond 2 (i.e. $v_B > u_B > 0$) belong to the left leg of the trousers.

We will use notation x, y without subscripts to denote general points in the manifold and use indicator functions to restrict support of functions onto subregions. We define $\chi_R(x)$ to be the function that is 1 when $x \in R$ and zero otherwise. We define eight regions, R_i , where $i = 1, \dots, 8$, whose boundaries are the past and future null lines from the singularity, as shown in Figure 4.2. For definiteness we choose the regions to include their boundaries so that their union is the whole manifold minus the singularity x_c , but we could choose them to be open or assign the boundary points to exactly one of the regions. This does not make a difference, as we are working in $L^2(\mathcal{M})$.

For convenience we write the corresponding indicator functions as $\chi_i(x) := \chi_{R_i}(x)$. We will also use notation $\chi_{1,2}(x) := \chi_1(x) + \chi_2(x)$ and $\chi_{2,3,5}(x) := \chi_2(x) + \chi_3(x) + \chi_5(x)$ *etc.* to denote the indicator functions for unions of these regions.

We consider the singularity as a point of spacetime. The metric degenerates at the singularity but the pair of diamonds spacetime including the singularity nevertheless possesses a natural, well defined causal order. For example the singularity x_c is to the causal past (future) of all points in and on the boundaries of regions 1 and 5 (3 and 7) in Figure 4.2. We denote the causal order by \preceq where $y \preceq x$ (equivalently, $x \succeq y$) means that y is in the causal past of x . We denote by $[x, y]$ the causal interval, $[x, y] = \{z \in \mathcal{M} \mid x \succeq z \succeq y\}$.

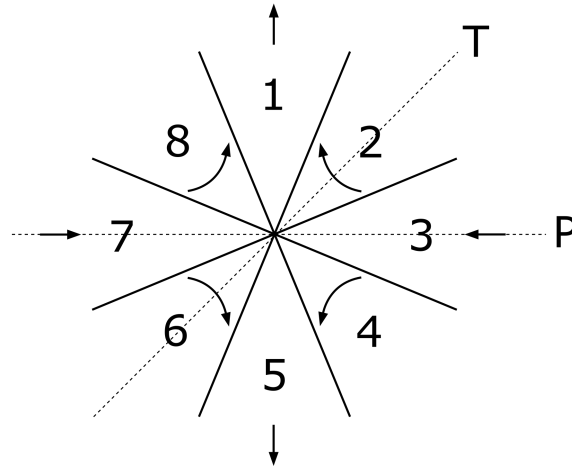


Figure 4.4: The pair of diamonds on the trousers, as “viewed from above”. The numbers correspond to the same 8 regions as before. The arrows represent the direction of time in each region. Isometry \mathfrak{P} is reflection in the dotted horizontal line, labelled P. Isometry \mathfrak{T} is reflection about the dotted line at 45° to the horizontal, labelled T.

4.2.4 Isometries of the Pair of Diamonds

The isometry group for the pair of diamonds is generated by two transformations, one of which can be thought of as a “parity” transformation and the other as a “time reversal”. The parity transformation, $\mathfrak{P} : \mathcal{M} \rightarrow \mathcal{M}$, is the isometry that reflects both diamonds, A and B , each in its own vertical axis of symmetry. To define the time reversal map, $\mathfrak{T} : \mathcal{M} \rightarrow \mathcal{M}$, we need only specify its action on a single region R_i and that fixes its action on the other regions by continuity. We choose to specify the action of \mathfrak{T} on R_1 to be a reflection of R_1 in its own horizontal axis of symmetry followed by a translation (in the obvious sense) of R_1 onto R_3 . Then the action of \mathfrak{T} on the other regions is: reflect R_2 in its horizontal axis; reflect R_3 in its horizontal axis and translate onto R_1 ; reflect R_4 in its horizontal axis and translate onto R_8 ; reflect R_5 in its horizontal axis and translate onto R_7 ; reflect R_6 in its horizontal axis; reflect R_7 in its horizontal axis translate onto R_5 ; reflect R_8 in its horizontal axis and translate onto R_4 .

There are actually two isometries that have an equal claim to being called “time reversal” on \mathcal{M} and we chose one of them above to be \mathfrak{T} . The isometry that time-reverses R_1 and then translates it onto R_7 — instead of R_3 — is equal to $\mathfrak{P} \circ \mathfrak{T} \circ \mathfrak{P}$. \mathfrak{P} and \mathfrak{T} generate the isometry group. For example, the “swap” isometry that interchanges the two diamonds, $A \leftrightarrow B$, is equal to $(\mathfrak{P} \circ \mathfrak{T})^2$.

The isometry group is the dihedral group, D_4 , the symmetry group of the square which can be seen by viewing the trousers in Figure 4.1 from above. From this point

of view, the regions R_1 to R_8 are arranged as in Figure 4.4. Representing topology change in this way is useful in studying the causality properties of topology change [70]. One can determine how the parity and time reversal operations act on this representation of the spacetime, Figure 4.4. \mathfrak{P} is reflection in the horizontal dotted line marked P and \mathfrak{T} is reflection in the dotted line marked T at 45° to the horizontal. The group D_4 is the symmetry group of a square and is generated by a reflection in the horizontal axis and a reflection in a diagonal. Thus, the isometry group of the pair of diamond is D_4 .

4.3 Green Functions

4.3.1 1 + 1 dimensional Minkowski

To construct the SJ theory of a massless scalar field, ϕ , on the pair of diamonds, \mathcal{M} , we must decide what it means to be a solution of the wave equation at the singularity, as the differential equation is not defined there. So let us first look at different ways to express the wave equation in 1+1 dimensional Minkowski space.

The wave equation is

$$\square f = 0 \quad (4.11)$$

so that

$$\int_A dV \square f = 0 \quad (4.12)$$

for every measurable region A . By Stokes' theorem we have

$$\int_A dV \square f = \oint_{\partial A} d\Sigma^\mu \frac{\partial}{\partial x^\mu} f, \quad (4.13)$$

where the boundary ∂A is traversed anti-clockwise and $d\Sigma_x^\mu$ is the normal surface element. We have implicitly assumed here that A is such that its boundary is nice enough — say, connected, non-self intersecting and piecewise smooth, for definiteness — for this to be meaningful. If we define

$$\mathfrak{B}^A f := \oint_{\partial A} d\Sigma^\mu \frac{\partial}{\partial x^\mu} f \quad (4.14)$$

then a solution satisfies $\mathfrak{B}^A f = 0$ for all nice enough A .

When the region is a causal interval, or *causal diamond*, D , this boundary integral only picks up the values of the function at the corners of the diamond, because the

normal derivatives in the integrand become tangential when the boundary is null. The full boundary integral is a sum of the integrals along the four null segments, and each one of the integrands is a total derivative with respect to the null coordinate u or v , so that

$$\int_D dV \square f = \oint_{\partial D} d\Sigma_x^\mu \frac{\partial}{\partial x^\mu} f = -2 [f(x_1) - f(x_2) + f(x_3) - f(x_4)], \quad (4.15)$$

where x_1 is the future tip of the diamond and the other corners are labelled in clockwise order. The boundary integral condition can therefore be written

$$\mathfrak{E}^D f = 0, \quad (4.16)$$

for each causal diamond, D , where we have defined

$$\mathfrak{E}^D f := f(x_1) - f(x_2) + f(x_3) - f(x_4). \quad (4.17)$$

If f is differentiable then the condition (4.16) for all causal diamonds implies $\square f = 0$ since

$$\begin{aligned} \square f(u, v) &= -2 \frac{\partial}{\partial u} \frac{\partial}{\partial v} f(u, v) \\ &= -2 \lim_{\delta u, \delta v \rightarrow 0} \frac{f(u + \delta u, v + \delta v) - f(u, v + \delta v) + f(u, v) - f(u + \delta u, v)}{\delta u \delta v} \\ &= 0. \end{aligned}$$

Green's equation is

$$\square_x G(x, y) = \delta(x, y) \quad (4.18)$$

for all x, y , where \square_x denotes the d'Alembertian with respect to argument x . This means that

$$\int_A dV_x \square_x G(x, y) = \chi_A(y) \quad (4.19)$$

for any measurable region A .

Again, Stokes' theorem gives the boundary integral form of the condition,

$$\mathfrak{B}_x^A G(x, y) = \chi_A(y) \quad (4.20)$$

for each point y and each nice enough region A , where

$$\mathfrak{B}_x^A G(x, y) := \oint_{\partial A} d\Sigma_x^\mu \frac{\partial}{\partial x^\mu} G(x, y). \quad (4.21)$$

And, when the region is a causal diamond, D , with corners x_1, \dots, x_4 as before we have

$$\mathfrak{E}_x^D G(x, y) = -\frac{1}{2}\chi_D(y), \quad (4.22)$$

where

$$\mathfrak{E}_x^D G(x, y) := G(x_1, y) - G(x_2, y) + G(x_3, y) - G(x_4, y), \quad (4.23)$$

and the subscript x denotes that \mathfrak{E}_x^D acts on the argument x of $G(x, y)$.

Similarly to the solution, the condition (4.23) for all causal diamonds and all points y is equivalent to Green's equation.

Finally, we note that the explicit form of the 1+1 dimensional Minkowski space retarded Green function is

$$G_{\text{Mink}}(x, y) = -\frac{1}{2}\chi_{\succ}(x, y), \quad (4.24)$$

where $\chi_{\succ}(x, y) = 1$ when $x \succ y$ and is 0 otherwise.

4.3.2 The Pair of Diamonds

Consider now the massless scalar field theory on the pair of diamonds, \mathcal{M} . We say that function f is a solution of the wave equation if it satisfies

$$\mathfrak{E}^D f = 0, \quad (4.25)$$

for every causal diamond D that does not contain x_c , as illustrated in Figure 4.5, and

$$\mathfrak{E}^{DD} f = 0, \quad (4.26)$$

for each “double diamond”, DD , whose interior contains x_c — like the example shown in Figure 4.6 — and where the definition of \mathfrak{E}^{DD} is the obvious generalisation of (4.23), the alternating sum of the values of f at the vertices of DD :

$$\mathfrak{E}^{DD} f := f(x_1) - f(x_2) + f(x_3) - f(x_4) + f(x_5) - f(x_6) + f(x_7) - f(x_8). \quad (4.27)$$

The order of the labels of the vertices is clockwise starting from the futuremost vertex in region R_1 as in Figure 4.6. Note that for every double diamond, exactly one of its corners lies in the interior of each of the regions R_i of \mathcal{M} . In the labelling we have chosen, $x_i \in R_i$.

It is straightforward to extend this concept of solution to define a Green function

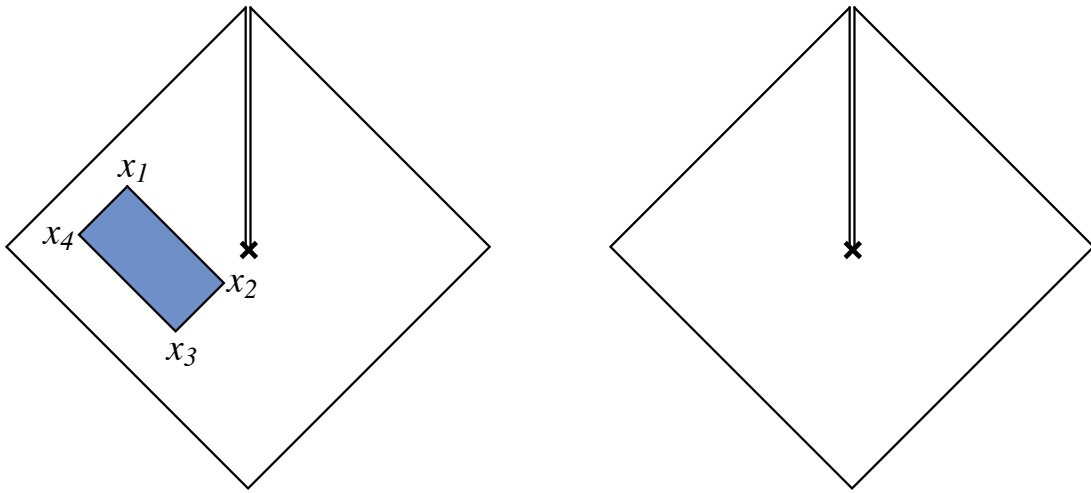


Figure 4.5: A causal interval or causal diamond not containing the singularity.

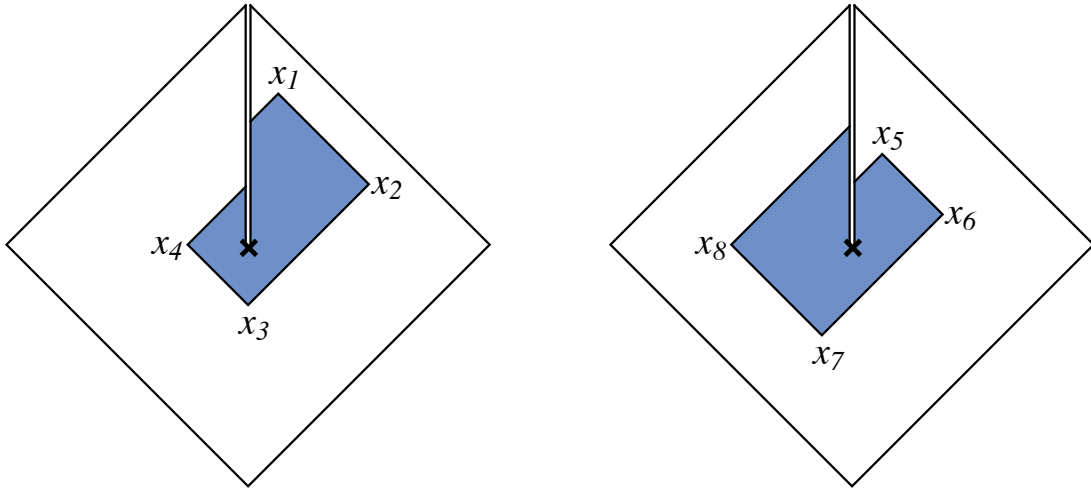


Figure 4.6: Example of a double diamond containing the singularity.

in \mathcal{M} . A Green function $G(x, y)$ satisfies

$$\mathfrak{C}_x^D G(x, y) = -\frac{1}{2}\chi_D(y), \quad (4.28)$$

for every causal diamond, D , that does not contain x_c , and, in addition,

$$\mathfrak{C}_x^{DD} G(x, y) = -\frac{1}{2}\chi_{DD}(y), \quad (4.29)$$

for every double diamond, DD , surrounding x_c . The subscript x on the operator \mathfrak{C}_x^{DD} indicates that it acts on the argument x of $G(x, y)$.

The Hilbert space we are working in is $L^2(\mathcal{M})$, in which members of the same

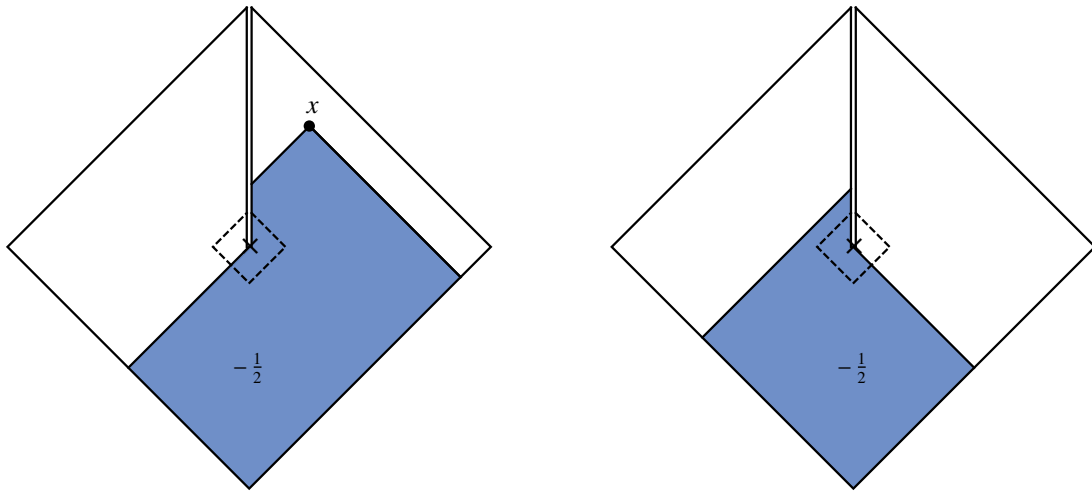


Figure 4.7: The Minkowski retarded Green function $G_{\text{Mink}}(x, y) = -\frac{1}{2}\chi_{>}(x, y)$ in the pair of diamonds, drawn as a function of y for fixed x where x is in the causal future of the singularity. The dashed contour corresponds to the boundary of a double diamond, DD , centred on the singularity.

equivalence class differ only on a set of measure zero. We say that an element of $L^2(\mathcal{M})$ is a solution if it contains a member, $f(x)$, that satisfies the above requirements, (4.25) and (4.26). Other members of the equivalence class can fail the above conditions but only on a set of diamonds and double diamonds of measure zero in the space of all diamonds.

4.3.3 A One-Parameter Family of Green Functions

In the SJ construction of the quantum theory the role of the retarded Green function $G(x, y)$ is its appearance in the Pauli-Jordan function $\Delta(x, y) = G(x, y) - G(y, x)$. The causal structure of the spacetime is imposed on the quantum field theory through the commutation relations $[\phi(x), \phi(y)] = i\Delta(x, y)$, the covariant form of the equal-time canonical commutation relation. For the field operators to be solutions of the field equations we also have that Δ must be a solution to the field equations in both its arguments. We satisfy this condition by requiring that $G(x, y)$ be a Green function in *both* its arguments.

If a causal interval $[x, y]$ does *not* contain the singularity then $[x, y]$ is contained in an open, globally hyperbolic subregion of Minkowski space, and so the retarded Green function $G(x, y)$ will take its usual Minkowski form, $G(x, y) = G_{\text{Mink}}(x, y)$.

Consider, firstly, $G_{\text{Mink}}(x, y) = -\frac{1}{2}\chi_{>}(x, y)$ on the whole of the pair of diamonds as illustrated in Figure 4.7.

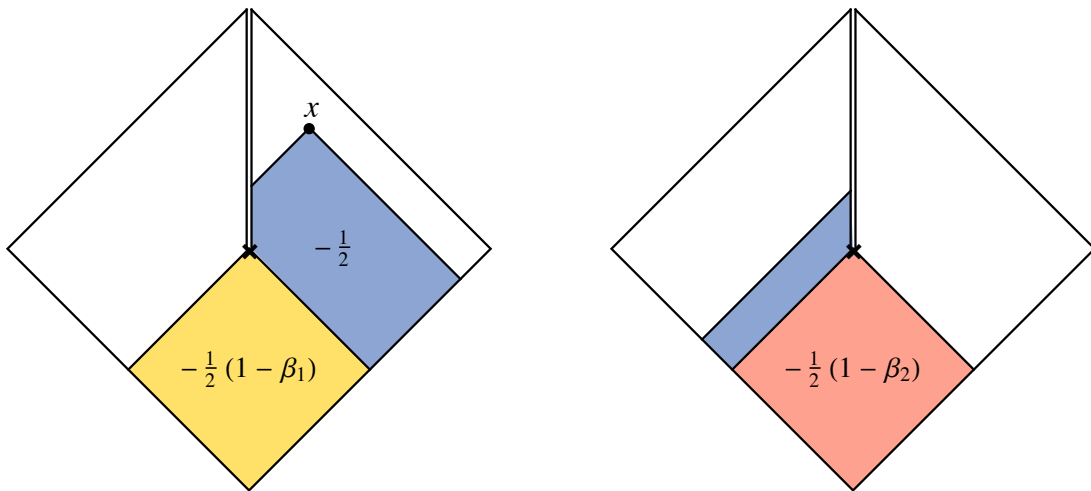


Figure 4.8: An ansatz for the retarded Green function $G(x, y)$ for fixed $x \in R_1$. If $\beta_1 + \beta_2 = 1$, then $\mathfrak{C}_y^{DD} G(x, y) = 0$ for any double diamond, DD , around the singularity.

Choose x to the future of x_c and let DD be a double diamond around x_c small enough that it does not contain x as shown in Figure 4.7. In order for $G(x, y)$ to be a Green function in both arguments we need it to satisfy, for example, $\mathfrak{C}_y^{DD} G(x, y) = 0$, since $\chi_{DD}(x) = 0$. However, $\mathfrak{C}_y^{DD} G_{\text{Mink}}(x, y) = -1/2$. This is reminiscent of the cylinder, in which $G_{\text{Mink}}(x, y)$ does not satisfy Green's equation due to the conjugate points on the cylinder, and this motivates an analogous method of images to find a Green function on the pair of diamonds.

If $x \notin R_1 \cup R_5$ and $y \prec x$ then the interval $[x, y]$ does not contain x_c and $G(x, y) = G_{\text{Mink}}(x, y)$. So the only cases we need to consider are $x \in R_5$ or $x \in R_1$, and $y \in R_3$ or $y \in R_7$.

For $x \in R_1$ let us add to the Minkowski Green function two contributions from an image point at x_c , one on diamond A and the other on diamond B :

$$G(x, y)|_{x \in R_1} = -\frac{1}{2} [\chi_{\succ}(x, y) - \beta_1 \chi_3(y) - \beta_2 \chi_7(y)]. \quad (4.30)$$

See Figure 4.8 for an illustration. Considering a double diamond, DD , around x_c we find that $\mathfrak{C}_y^{DD} G(x, y) = 0$ if $\beta_1 + \beta_2 = 1$.

Similarly, for $x \in R_5$, consider the ansatz,

$$G(x, y)|_{x \in R_5} = -\frac{1}{2} [\chi_{\succ}(x, y) - \alpha_1 \chi_3(y) - \alpha_2 \chi_7(y)]. \quad (4.31)$$

Then, $\mathfrak{C}_y^{DD} G(x, y) = 0$ implies $\alpha_1 + \alpha_2 = 1$.

This leaves us with a two-parameter family of retarded functions on \mathcal{M} , with

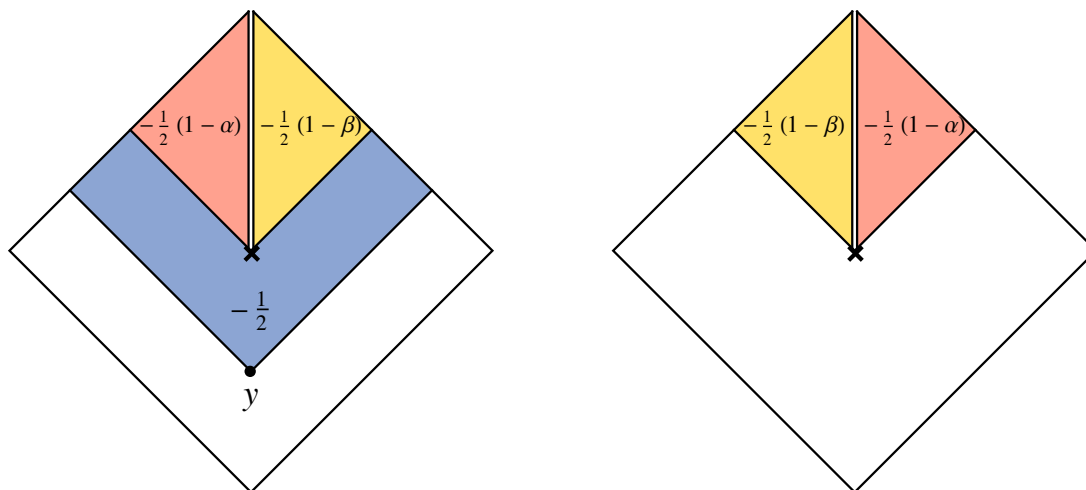


Figure 4.9: The retarded Green function $G_p(x, y)$ for fixed y in R_3 as a function of x .

parameters $\alpha := \alpha_1 = 1 - \alpha_2$ and $\beta := \beta_1 = 1 - \beta_2$. However, there is a further condition because G is a Green function in its first argument and from $\mathfrak{C}_x^{DD}G(x, y) = 0$ for $y \notin DD$ we obtain an additional constraint, $\alpha + \beta = 1$. To see this, fix $y \in R_3$ as in Figure 4.9, where we have plotted $G(x, y)$ as a function of x . If we take a double diamond, DD , such that $y \notin DD$, then $\mathfrak{C}_x^{DD}G(x, y) = -\frac{1}{2}(1 - \alpha - \beta)$, and since this must equal 0 we obtain the constraint $\alpha + \beta = 1$.

We are thus left with a one-parameter family of retarded Green functions $G_p(x, y)$ parametrised by $p := \alpha = 1 - \beta$. The case $p = \frac{1}{2}$ corresponds to the symmetric case in which the source at x_c is of equal strength in each of the two disconnected pieces of spacetime that come together or come apart at x_c (see Figures 4.8 and 4.9). These additional sources in $G_p(x, y)$ do not by themselves constitute an “infinite burst in energy”; at this stage they are merely a presage of trouble ahead. In order to reach such conclusions, one first has to obtain the quantum state and try to compute physical quantities.

4.4 Eigenfunctions of the Pauli-Jordan Operator

The one-parameter family of retarded Green functions derived in the previous section provides us with a one-parameter family of Pauli-Jordan functions $\Delta_p = G_p - G_p^T$. For an example illustrating its form see Figure 4.10. In order to calculate the SJ state our task is now to find the positive part of $i\Delta_p$ and to do that we will

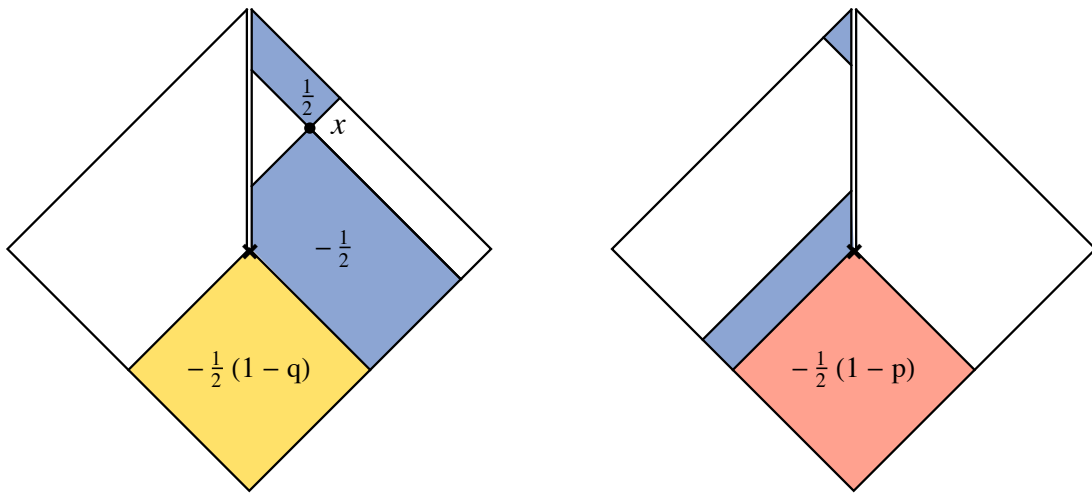


Figure 4.10: The Pauli-Jordan function $\Delta_p(x, y)$ in the pair of diamonds as a function of y , with the first argument x fixed in the causal future of the singularity. Here $q = 1 - p$.

solve for the eigenfunctions of $i\Delta_p$,

$$\int_{\mathcal{M}} dy i\Delta_p(x, y)f(y) = \lambda f(x), \quad (4.32)$$

for $\lambda > 0$. As mentioned before, the eigenfunctions of $i\Delta_p$ with non-zero eigenvalues come in pairs: the function f with eigenvalue $\lambda > 0$, and its complex conjugate, f^* , with eigenvalue $-\lambda$.

Since $i\Delta_p(x, y)$ is a solution in its argument x , (4.32) shows that every eigenfunction with non-zero eigenvalue will also be a solution. Indeed, the eigenfunctions with nonzero eigenvalues form a basis for the space of solutions of the equations of motion on the pair of diamonds. In Appendix A.1 we show that the eigenfunctions with zero eigenvalue — elements of the kernel of $i\Delta$ — are not solutions.

4.4.1 The Norm of the Pauli-Jordan Function

$i\Delta_p(x, y)$ is a Hilbert-Schmidt integral kernel and its L^2 -norm squared is equal to the sum of the squares of its eigenvalues λ_k :

$$\int_{\mathcal{M}} dV_x \int_{\mathcal{M}} dV_y |i\Delta_p(x, y)|^2 = \sum_k \lambda_k^2. \quad (4.33)$$

The eigenvalues come in pairs with opposite signs, so this sum is twice the sum of the squares of the positive eigenvalues. The integral on the LHS gives

$$\begin{aligned} \int_{\mathcal{M}} dV_x \int_{\mathcal{M}} dV_y |i\Delta_p(x, y)|^2 &= \sum_{i,j=1}^8 \int_{R_i} dV_x \int_{R_j} dV_y |i\Delta_p(x, y)|^2 \\ &= 2L^4 [2 - p(1 - p)] . \end{aligned} \quad (4.34)$$

Compare this to the single flat diamond, on which the norm squared of $i\Delta$ equals $2L^4$ [71]. The relation (4.34) is useful because one can check if a given set of eigenfunctions of $i\Delta_p$ is complete: if the eigenvalues sum to less than $2L^4 [2 - p(1 - p)]$ then there are missing eigenfunctions. Note that the value depends on p so the eigenvalues will be functions of p .

4.4.2 Isometries and the Pauli-Jordan Function

The isometries \mathfrak{P} and \mathfrak{T} that generate the isometry group can be represented as operators, $\hat{\mathfrak{P}}$ and $\hat{\mathfrak{T}}$, on the Hilbert space $L^2(\mathcal{M})$. The action of $\hat{\mathfrak{P}}$ on a function $f(x)$ is given by $\hat{\mathfrak{P}}(f)(x) := f(\mathfrak{P}^{-1}x)$. The action of $\hat{\mathfrak{T}}$ is given by $\hat{\mathfrak{T}}(f)(x) := f^*(\mathfrak{T}^{-1}x)$. We can ask if the operators $\hat{\mathfrak{P}}$ and $\hat{\mathfrak{T}}$ commute with $i\Delta_p$. We find that

$$\begin{aligned} \hat{\mathfrak{P}} \circ i\Delta_p &= i\Delta_{1-p} \circ \hat{\mathfrak{P}} \\ \hat{\mathfrak{T}} \circ i\Delta_p &= i\Delta_p \circ \hat{\mathfrak{T}} , \end{aligned} \quad (4.35)$$

so that for $p = \frac{1}{2}$ both $\hat{\mathfrak{P}}$ and $\hat{\mathfrak{T}}$ commute with $i\Delta_{\frac{1}{2}}$. This means that $i\Delta_{\frac{1}{2}}$ commutes with the full isometry group.

4.4.3 “Copy” Eigenfunctions

Since we know the SJ modes for the single causal diamond from [71], we can use them as a guide to finding eigenfunctions on the pair of diamonds. In [71] it was shown that on the single diamond of area $4L^2$, the eigenfunctions of $i\Delta_{\text{Mink}}(x, y) = -\frac{i}{2} [\chi_{\succ}(x, y) - \chi_{\succ}(y, x)]$ are linear combinations of positive frequency plane waves and a constant:

$$\begin{aligned} f_k(u, v) &:= e^{-iku} - e^{-ikv}, & \text{with } k &= \frac{n\pi}{L}, \quad n = 1, 2, \dots \\ g_k(u, v) &:= e^{-iku} + e^{-ikv} - 2\cos(kL), & \text{with } k &\in \mathcal{K} \end{aligned} \quad (4.36)$$

where $\mathcal{K} = \{k \in \mathbb{R} \mid \tan(kL) = 2kL \text{ and } k > 0\}$ and the eigenvalues are L/k . The eigenfunctions with eigenvalues $-L/k$ are the complex conjugates of these. Consider now each of these — f_k and g_k — modes in turn, extended to the pair of diamonds by duplicating the mode onto both diamonds in Figure 4.2, as if each were a disconnected single diamond. It can be shown that each of these “copy modes” on the pair of diamonds is an eigenfunction of $i\Delta_p$, for *any* p . The norm squared of the f_k copy mode on the pair of diamonds is

$$\|f_k\|^2 := \int_{-L}^L du_A \int_{-L}^L dv_A f_k^* f_k + \int_{-L}^L du_B \int_{-L}^L dv_B f_k^* f_k = 16L^2. \quad (4.37)$$

We define the normalised mode as $\hat{f}_k := \|f_k\|^{-1} f_k$. Similarly, we define the normalised mode $\hat{g}_k := \|g_k\|^{-1} g_k$, where $\|g_k\|^2 = 16L^2(1 - 2\cos(kL))$.

The (positive and negative) eigenvalues of the copy modes sum to $2L^4$, as was shown in [71]. Since this is less than the total in (4.34), the copy modes cannot be a complete set.

4.4.4 The Other Eigenfunctions

The form of the remaining eigenfunctions was investigated by solving for them in a discrete, finite version of the problem. The pair of diamonds was discretised in two different ways, with a regular lattice in the coordinates X and T , and with causal set sprinklings [36]. In each case, $i\Delta_p$ is a finite matrix whose indices run over the elements of the lattice or causal set. We solved for the eigenvectors of this matrix numerically and looked for those that did not resemble the \hat{f}_k or \hat{g}_k modes. This led to an ansatz for the extra modes as piecewise continuous functions with the following form:

$$f(x) = \sum_{i=1}^8 (a_i e^{-iku} + b_i e^{-ikv} + c_i) \chi_i(x), \quad (4.38)$$

where i denotes the region, as shown in Figure 4.2, and the coefficients a_i , b_i and c_i are complex. When x , the argument of f , is in diamond A (B) the coordinates (u, v) in (4.38) are equal to (u_A, v_A) ((u_B, v_B)).

The calculations provided evidence that each of the new modes is odd under interchange of the diamonds, $A \leftrightarrow B$. This implies that $a_i = -a_{i+4}$, $b_i = -b_{i+4}$ and $c_i = -c_{i+4}$ for $i = 1, \dots, 4$. The calculations also showed that the modes are discontinuous across the past and future directed null lines from the origin on both diamonds.

All the non-zero eigenvalue eigenfunctions of $i\Delta_p$ are solutions of the wave

equation. Using (4.25) for a diamond straddling the boundary between two regions, gives conditions on the constants:

$$a_1 = -a_4, \quad a_2 = a_3, \quad b_1 = b_2, \quad b_3 = b_4. \quad (4.39)$$

The above conditions leave us with 8 complex parameters $\{a_1, a_2, b_1, b_3, c_1, c_2, c_3, c_4\}$. These, and the allowed values of k , are fixed by the eigenvalue equation for $i\Delta_p$. In the following sections we will only discuss the eigenfunctions with positive eigenvalues unless otherwise stated. The eigenvalues are given in terms of k by $\lambda_k = L/k$.

4.4.5 $p = \frac{1}{2}$

In this case $k > 0$ satisfies

$$(2 + (kL)^2) \cos(kL) + 2kL \sin(kL) - 2 = 0. \quad (4.40)$$

The eigenvalue corresponding to each solution of this equation is degenerate and there are two modes with that eigenvalue, one for which $a_1 = b_1$ and one for which $a_1 = -b_1$.

$$a_1 = b_1$$

The coefficients are

$$\begin{aligned} a_1 = b_1 &= kL + 2i \\ a_2 = -b_3 &= ikL \cot\left(\frac{kL}{2}\right) e^{-ikL} \\ c_1 &= -2i(1 + e^{-ikL}) \\ c_2 = -c_4 &= -\frac{2}{kL}(1 - ikL - e^{-ikL}) \\ c_3 &= 0. \end{aligned} \quad (4.41)$$

We denote the mode with these coefficients as $f_k^{(\frac{1}{2})}$. The norm-squared of this mode is

$$\|f_k^{(\frac{1}{2})}\|^2 = 8\frac{L}{k} \left(8kL + 4kL \cos(kL) + (kL)^3 \csc^2\left(\frac{kL}{2}\right) - 8 \sin(kL) \right). \quad (4.42)$$

The mode that is normalised under the L^2 inner product is then $\hat{f}_k^{(\frac{1}{2})} := \|f_k^{(\frac{1}{2})}\|^{-1} f_k^{(\frac{1}{2})}$. The lowest k mode is plotted in Figure 4.11.

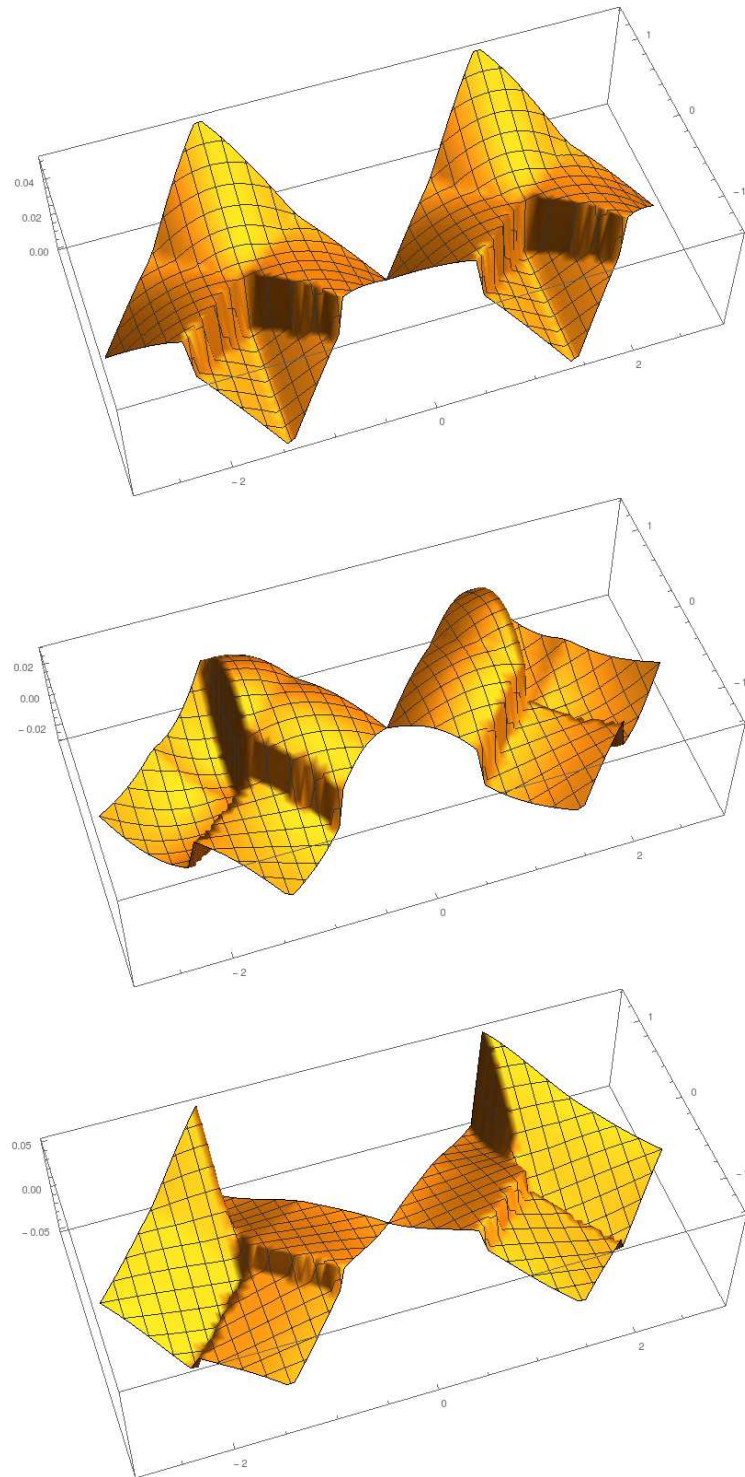


Figure 4.11: The $\hat{f}_k^{(\frac{1}{2})}$ mode for the lowest k satisfying (4.40). On the top we have plotted the absolute value of the mode across the pair of diamonds. In the middle we have plotted its real part, and at the bottom its imaginary part. The discontinuity across the line of $X = 0$ for $T > 0$ is not a discontinuity in the mode. It is simply a consequence of how we have set up the identifications on the pair of diamonds.

$$a_1 = -b_1$$

The coefficients are

$$\begin{aligned} a_1 = -b_1 &= ikL \cot\left(\frac{kL}{2}\right) e^{ikL} \\ a_2 = b_3 &= k - 2i \\ c_1 &= 0 \\ c_2 = c_4 &= -\frac{2}{kL} (1 + ikL - e^{ikL}) \\ c_3 &= 2i(1 + e^{ikL}). \end{aligned} \tag{4.43}$$

A mode with these coefficients will be denoted as $g_k^{(\frac{1}{2})}$. The norm-squared is $\|g_k^{(\frac{1}{2})}\| = \|f_k^{(\frac{1}{2})}\|$ and the normalised mode is $\hat{g}_k^{(\frac{1}{2})} := \|g_k^{(\frac{1}{2})}\|^{-1} g_k^{(\frac{1}{2})}$. The $\hat{f}_k^{(\frac{1}{2})}$ modes and the $\hat{g}_k^{(\frac{1}{2})}$ are orthogonal. The phase of $\hat{g}_k^{(\frac{1}{2})}$ was chosen such that $\hat{\mathfrak{T}}(\hat{f}_k^{(\frac{1}{2})}) = \hat{g}_k^{(\frac{1}{2})}$.

$i\Delta_{\frac{1}{2}}$ commutes with the isometry group D_4 and for each k the 2-dimensional eigensubspace of $i\Delta_{\frac{1}{2}}$, spanned by $\{g_k^{(\frac{1}{2})}, f_k^{(\frac{1}{2})}\}$, carries the 2-dimensional irreducible representation of D_4 .

In Appendix A.2 we verify that these, and the $\hat{f}_k^{(\frac{1}{2})}$ modes, are indeed all the extra modes. That is, we show that the sum of the squares of the eigenvalues (both the positive and negative values) for the modes $\hat{f}_k, \hat{g}_k, \hat{f}_k^{(\frac{1}{2})}$ and $\hat{g}_k^{(\frac{1}{2})}$ is

$$\sum_{\text{all modes}} \lambda_k^2 = \frac{7L^4}{2}. \tag{4.44}$$

The right side of (4.44) agrees with (4.34) when $p = \frac{1}{2}$.

4.4.6 $p \neq \frac{1}{2}$

We start with the ansatz for a mode (4.38) with $a_{i+4} = -a_i$, $b_{i+4} = -b_i$, $c_{i+4} = -c_i$ for $i = 1, \dots, 4$, $a_1 = -a_4$, $a_2 = a_3$, $b_1 = b_2$ and $b_3 = b_4$, as before. For $p \neq \frac{1}{2}$ we expect to see a dependence on p in the coefficients. With this ansatz one can show that each eigenvalue, λ_k , satisfies one of two possible equations:

$$((kL)^2 + 2) \cos(kL) + kL(2 \pm kL(1 - 2p)) \sin(kL) - 2 = 0, \tag{4.45}$$

where $k = \frac{L}{\lambda_k}$. This is consistent with the $p = \frac{1}{2}$ case as the above two equations become (4.40) when $p = \frac{1}{2}$. By using the ansatz (4.38), and by using (4.45) to

simplify the resulting equations we find that the coefficients are

$$\begin{aligned}
a_1 &= e^{ikL} kL \{ i(1 + kL(kLp + i)) + e^{ikL} [kL(2 - kL(kL + i)(p - 1)) - 3i] \\
&\quad + ie^{2ikL} [3 - kL(kL(p - 1) - i)] + e^{3ikL} [(kL)^2(kLp + i(p - 2)) - i] \} \\
a_2 &= kL \{ i - kL(2 + kL(kL + i)p) + e^{ikL} [kL(3 + ikL(p - 1)) - 3i] \\
&\quad + e^{2ikL} [(kL)^2(i(p + 1) + kL(p - 1)) + 3i] - ie^{3ikL} [1 + kL(kLp - i)] \} \\
b_1 &= e^{ikL} kL \{ i - (kL + ikL(p - 1)) - e^{ikL} [3i - kL(2 + kL(kL + i)p)] \\
&\quad + e^{2ikL} [(kL)(ikLp - 1) + 3i] - e^{3ikL} [(kL)^2(p + 1 + kL(p - 1)) + i] \} \\
b_3 &= kL \{ kL(2 - kL(kL + i)(p - 1)) - i + ie^{ikL} [3 + kL(kLp + 3i)] \\
&\quad + e^{2ikL} [i(kL)^2((p - 2) + kLp) - 3i] + e^{3ikL} [kL(1 - ikL(p - 1)) + i] \} \\
c_1 &= 2e^{ikL} (e^{ikL} + 1 - ikL) (e^{ikL} - 1) ((kL)^2 + 2) \cos(kL) + 2kL \sin(kL) - 2 \\
c_2 &= 2e^{2ikL} kL \sin(kL) [kL(ikL(1 - 2p) + 2) \sin(kL) - ((kL)^2 + 2) \cos(kL) + 2] \\
c_3 &= (kL)^2(2p - 1) (1 - e^{ikL})^2 (1 + e^{ikL}) (e^{ikL}(1 - ikL) - 1) \\
c_4 &= 2e^{2ikL} kL \sin(kL) [kL(ikL(1 - 2p) - 2) \sin(kL) + ((kL)^2 + 2) \cos(kL) - 2] .
\end{aligned} \tag{4.46}$$

A mode with these coefficients and k satisfying (4.45) with the “+” sign will be denoted as $f_k^{(p)}$. Likewise, for the “-” sign we call the mode $g_k^{(p)}$. The $p \neq \frac{1}{2}$ case differs from the $p = \frac{1}{2}$ case in that the coefficients have the same form in terms of k for both the $f_k^{(p)}$ and $g_k^{(p)}$ modes. The $f_k^{(p)}$ and $g_k^{(p)}$ modes still have different coefficients, though, because the allowed values of k are different as they come from (4.45) with either the “+” or “-” sign.

In Appendix A.2 we verify that these two sets of modes, together with the f_k and g_k copy modes, are all the eigenfunctions of $i\Delta_p$ with positive eigenvalues. There we show that the sum of the squares of the eigenvalues for all the modes agrees with the right hand side of (4.34). That is,

$$\sum_{\text{all modes}} \lambda_k^2 = 2L^4 (2 - p(1 - p)) . \tag{4.47}$$

The norm-squared for either mode has the same form in terms of k , and is

$$\begin{aligned}
\|f_k^{(p)}\|^2 &= \|g_k^{(p)}\|^2 = 32k^5 L^7 (1 - 2p)^2 \sin^2(kL) \\
&\quad \times [kL(3 + (kL)^2 - 2 \cos(kL) - \cos(2kL)) + 4(\cos(kL) - 1) \sin(kL)] .
\end{aligned} \tag{4.48}$$

We define the normalised modes $\hat{f}_k^{(p)} := \|f_k^{(p)}\|^{-1} f_k^{(p)}$ and $\hat{g}_k^{(p)} := \|g_k^{(p)}\|^{-1} g_k^{(p)}$.

Both these modes tend to the $\hat{f}_k^{(\frac{1}{2})}$ mode in the $p \rightarrow \frac{1}{2}$ limit. That is,

$$\lim_{p \rightarrow \frac{1}{2}} \hat{f}_k^{(p)} = \lim_{p \rightarrow \frac{1}{2}} \hat{g}_k^{(p)} = \hat{f}_k^{(\frac{1}{2})}. \quad (4.49)$$

The $\hat{g}_k^{(\frac{1}{2})}$ mode appears as an entirely new eigenfunction (in the sense that the coefficients for this mode have a different form in terms of k) only when $p = \frac{1}{2}$.

4.5 Energy momentum in the SJ State

Knowing the complete set of positive eigenvalue eigenfunctions of $i\Delta$ means that one knows the SJ state since its Wightman function can be expressed as the sum (4.9) over these eigenfunctions. For each p , we have found this complete set and so we have the SJ state. We can now turn to studying what physical properties this SJ state has. Sorokin argues that, ultimately, quantum field theory should be based on the path integral and will not be able to be fully self-consistent except within a theory of quantum gravity in which the effect of quantum matter on spacetime itself is taken into account [65]. Quantum gravity and the interpretation of path integral quantum theory are works in progress, so we will proceed here by seeing what can be gleaned by investigating the expectation value of the energy momentum tensor, $T_{\mu\nu}$. In order to calculate this expectation value one can regulate the divergence of the Wightman function and its derivatives in the coincidence limit using point splitting and subtraction of the corresponding quantity in the “same” theory in Minkowski spacetime, if the state has the Hadamard property. Fewster and Verch [72] showed that the SJ state in a finite slab of a cosmological spacetime with closed spatial sections generically is not Hadamard. It seems likely that the SJ state in the pair of diamonds is also not Hadamard since it seems like the SJ state for the single diamond is not [73]. It is possible that the SJ states in the single diamond and pair of diamonds can be rendered Hadamard by a smoothing of the boundary of the diamond [74] and it is an open question whether the Hadamard property should be considered to be physically significant when quantum gravity suggests that the differentiable manifold structure of spacetime breaks down at the Planck scale. Here we will simply ignore this question and provide heuristic evidence that an infinite burst of energy along the lightcones from the singularity will be present in the SJ state. It should be noted that this heuristic argument will not involve any regularisation, and we will only attempt such an endeavour in section 4.6.

A creation and annihilation operator can be assigned to each mode and the

field operator can be written as a sum over modes [65–67]

$$\phi(x) = \sum_{\mathbf{a}} \sqrt{\lambda_{\mathbf{a}}} (\mathbf{u}_{\mathbf{a}}(x)a_{\mathbf{a}} + \mathbf{u}_{\mathbf{a}}^*(x)a_{\mathbf{a}}^{\dagger}) , \quad (4.50)$$

where $\{\mathbf{u}_{\mathbf{a}}\}$ are the orthonormal eigenfunctions of $i\Delta_p$ with positive eigenvalues $\lambda_{\mathbf{a}}$ and $[a_{\mathbf{a}}, a_{\mathbf{b}}^{\dagger}] = \delta_{\mathbf{ab}}$ and $[a_{\mathbf{a}}, a_{\mathbf{b}}] = [a_{\mathbf{a}}^{\dagger}, a_{\mathbf{b}}^{\dagger}] = 0$. The SJ state, $|0_{(p)}\rangle$, is then the state that is annihilated by $a_{\mathbf{a}}$ for all \mathbf{a} . For each p there is an inequivalent quantum theory.

The operator for the stress energy of the massless field is

$$T_{\alpha\beta} = \phi_{,\alpha}\phi_{,\beta} - \frac{1}{2}\eta_{\alpha\beta}\eta^{\lambda\sigma}\phi_{,\lambda}\phi_{,\sigma} , \quad (4.51)$$

in Cartesian (T, X) coordinates in which the metric locally is the Minkowski metric, $\eta_{\alpha\beta}$. We can construct the operator for the energy on the future (or past) null boundary of the pair of diamonds by integrating $T_{\alpha\beta}\xi^{\beta}$ across the surface, where ξ^{α} is the Killing vector $\partial/\partial T$. Let N_+ be the future null boundary of \mathcal{M} . The energy operator for this boundary is

$$E_+ := \int_{N_+} d\Sigma^{\alpha} T_{\alpha\beta} \xi^{\beta} . \quad (4.52)$$

Using (4.51) and converting to light-cone coordinates, this becomes

$$E_+ = \frac{1}{\sqrt{2}} \left(\int_{-L}^L du_A (\phi_{,u_A})^2 \Big|_{v_A=L} + \int_{-L}^L dv_A (\phi_{,v_A})^2 \Big|_{u_A=L} \right. \\ \left. \int_{-L}^L du_B (\phi_{,u_B})^2 \Big|_{v_B=L} + \int_{-L}^L dv_B (\phi_{,v_B})^2 \Big|_{u_B=L} \right) , \quad (4.53)$$

where the first (second) line comes from integrating over the part of the surface on diamond A (B). We can similarly define the energy operator E_- for the past null boundary N_- .

4.5.1 $p = \frac{1}{2}$

Using the expansion for the field operator in the SJ modes gives the formal expression

$$\begin{aligned} \langle 0_{(\frac{1}{2})} | E_+ | 0_{(\frac{1}{2})} \rangle = & \sqrt{2}L \int_{-L}^L du \left(\sum_k k^{-1} \partial_u \hat{f}_k \partial_u \hat{f}_k^* + \sum_{k \in \mathcal{K}} k^{-1} \partial_u \hat{g}_k \partial_u \hat{g}_k^* \right. \\ & \left. + \sum_k k^{-1} \left(\partial_u \hat{f}_k^{(\frac{1}{2})} \partial_u \hat{f}_k^{(\frac{1}{2})*} + \partial_u \hat{g}_k^{(\frac{1}{2})} \partial_u \hat{g}_k^{(\frac{1}{2})*} \right) \right) \Big|_{v=L} \\ & + (u \leftrightarrow v) , \end{aligned} \quad (4.54)$$

where the (u, v) coordinates refer to the light-cone coordinates on either diamond, as both diamonds give the same result. In the first sum in (4.54) $k = \frac{n\pi}{L}$, where $n \in \mathbb{N}$, and the third sum runs over the positive roots of (4.40).

This expression (4.54) involves products of derivatives of the discontinuous SJ modes so it is not rigorously defined. However, we see that as the discontinuities are along the past and future directed light rays from x_c , the integrals along the $v = L$ and $u = L$ lines in (4.54) have integrands that contain squared Dirac-delta functions located at $u = 0$ and $v = 0$ respectively. The same situation also arises in the expectation value of E_- . This squared Dirac-delta divergence was found in previous works on the trousers, although here the divergence is along both the past and the future lightcones of the singularity, while in previous work the divergence only appears in the future. We now check that the delta-function squared terms have positive coefficients.

Restricting attention to the integral over the $v = L$ line, a mode has the following form:

$$(\Theta(u)a_1 + \Theta(-u)a_2) e^{-iku} + b_1 e^{-ikL} + (\Theta(u)c_1 + \Theta(-u)c_2) , \quad (4.55)$$

up to some normalisation constant, and the coefficients are given by (4.41) or (4.43).

Taking a u derivative of the mode in (4.55) and ignoring the parts with no δ -function dependence we get

$$\delta(u) \left((a_1 - a_2) e^{-iku} + c_1 - c_2 \right) . \quad (4.56)$$

Each of the terms $\partial_u \hat{f}_k^{(\frac{1}{2})} \partial_u \hat{f}_k^{(\frac{1}{2})*}$ and $\partial_u \hat{g}_k^{(\frac{1}{2})} \partial_u \hat{g}_k^{(\frac{1}{2})*}$ in the sum in (4.54) gives a contribution to the energy equal to $\delta(0)$ times a positive coefficient if the complex number $(a_1 - a_2 + c_1 - c_2)$ is non-zero. Using (4.41), and the eigenvalue equation (4.40),

we find that this complex number is zero for the $\hat{f}_k^{(\frac{1}{2})}$ mode and is non-zero for $\hat{g}_k^{(\frac{1}{2})}$.

A similar conclusion can be drawn for the integral over the $u = L$ line. There, the $\hat{f}_k^{(\frac{1}{2})}$ mode doesn't contribute whilst the $\hat{g}_k^{(\frac{1}{2})}$ mode does. For the expectation value of E_- the situation is reversed — the $\hat{g}_k^{(\frac{1}{2})}$ mode doesn't contribute while the $\hat{f}_k^{(\frac{1}{2})}$ mode does. Therefore, on both the past and future null boundaries of \mathcal{M} there appears to be a divergence in the energy. This divergence implies that the QFT in curved spacetime approximation in which back reaction on the spacetime is ignored must break down. It could be a signal that the trousers topology change cannot occur at all but at the very least it means that the spacetime cannot be approximated by the flat geometry we have been working with.

4.5.2 $p \neq \frac{1}{2}$

The expectation value of E_+ in the SJ state is

$$\begin{aligned} \langle 0_{(p)} | E_+ | 0_{(p)} \rangle = & \sqrt{2}L \int_{-L}^L du \left(\sum_k k^{-1} \partial_u \hat{f}_k \partial_u \hat{f}_k^* + \sum_{k \in \mathcal{K}} k^{-1} \partial_u \hat{g}_k \partial_u \hat{g}_k^* \right. \\ & \left. + \sum_k k^{-1} \partial_u \hat{f}_k^{(p)} \partial_u \hat{f}_k^{(p)*} + \sum_k k^{-1} \partial_u \hat{g}_k^{(p)} \partial_u \hat{g}_k^{(p)*} \right) \Big|_{v=L} \\ & + (u \leftrightarrow v), \end{aligned} \quad (4.57)$$

where the first two sums are over the same values of k as those in (4.54), and the last two sums are over the solutions of (4.45) with the “+” and “−” signs respectively.

For $p \neq 1$ and $p \neq 0$ one finds that, on all parts of the null boundaries, both $\hat{f}_k^{(p)}$ and $\hat{g}_k^{(p)}$ modes contribute $\delta(0)$ terms to the expectation value of E_+ and E_- . However, when $p = 0$ there is no divergence on the lefthand segments of N_+ and N_- *i.e.* $u = L$ and $v = -L$, respectively. For $p = 1$ there is no divergence from the righthand segments of N_+ and N_- , *i.e.* the lines $v = L$ and $u = -L$, respectively.

4.6 From the Pair of Diamonds to the Infinite Trousers

In this section we provide further evidence that the divergence in energy is located along the past and future lightcones of the singularity by examining the infinite limit of the pair of diamonds. This allows us better to compare the SJ state to scalar QFT in 1+1 Minkowski spacetime. Specifically, we take $L \rightarrow \infty$ in

the pair of diamonds to get two copies of Minkowski spacetime with trousers-type identifications along the positive time axes. We call this double sheeted Lorentzian spacetime the *infinite trousers*. The two planes are labelled A and B in the same way as the pair of diamonds. The conformal compactification of the infinite trousers is the pair of diamonds. The retarded Green function is the same function, $i\Delta_p$ as in the pair of diamonds.

We take an appropriate limit of the eigenfunctions of $i\Delta_p$ and compare them with the usual modes of Minkowski spacetime. Strictly, we are leaving the finite spacetime volume regime in which the SJ formalism is defined. Nevertheless, we can renormalise the modes in order that they have a sensible limiting form and display the usual feature of the passage from a finite box to an infinite spacetime, namely the transition from a countable set of modes to an uncountable, delta-function normalised set.

Consider first the \hat{f}_k copy modes. We define $f_n^L := \frac{L}{\sqrt{\pi k}} \hat{f}_k$ where natural number n labels the eigenvalues in increasing order, in this case via the simple relationship $k = \frac{n\pi}{L}$. For each *real* number $k > 0$ and each value of L , we can find an integer $n_{k,L}$ such that $\lim_{L \rightarrow \infty} \frac{\pi}{L} n_{k,L} = k$. Indeed $n_{k,L} = \lfloor \frac{Lk}{\pi} \rfloor$ will do the job.

Then, in the limit $L \rightarrow \infty$, for each real $k > 0$ we define the infinite trousers copy mode $\tilde{f}_k := \lim_{L \rightarrow \infty} f_{n_{k,L}}^L = \frac{1}{\sqrt{16\pi k}} (e^{-iku} - e^{-ikv})$, where coordinates u and v here are light-cone coordinates on the infinite trousers.

Considering the \hat{g}_k modes, we define $g_n^L := \frac{L}{\sqrt{\pi k}} \hat{g}_k$ where n labels the discrete eigenvalues k_n satisfying $\tan(kL) = 2kL$ in increasing order. Now there is no simple relationship between n and eigenvalues k_n but $k_n \rightarrow (n + \frac{1}{2})\frac{\pi}{L}$ as $n \rightarrow \infty$. So, again, for each real $k > 0$ and all values of L there exist integers $n_{k,L}$ such that $\lim_{L \rightarrow \infty} (n_{k,L} + \frac{1}{2})\frac{\pi}{L} = k$. Then, in the limit $L \rightarrow \infty$, for each real $k > 0$ we define the infinite trousers copy mode $\tilde{g}_k := \lim_{L \rightarrow \infty} g_{n_{k,L}}^L = \frac{1}{\sqrt{16\pi k}} (e^{-iku} + e^{-ikv})$.

4.6.1 The Discontinuous Modes in the Infinite Trousers

The discontinuous modes in the infinite trousers are odd under interchange of the two sheets and, using the same limiting procedure as above applied to the modes $\hat{f}^{(p)}$ and $\hat{g}^{(p)}$ from section 4.4.6, we obtain

$$\begin{aligned} \tilde{f}_k^{(p)}(x) &= \frac{1}{\sqrt{16\pi k}} \sum_{i=1}^8 \left(a_i^f e^{-iku} + b_i^f e^{-ikv} \right) \chi_i(x) \\ \tilde{g}_k^{(p)}(x) &= \frac{1}{\sqrt{16\pi k}} \sum_{i=1}^8 \left(a_i^g e^{-iku} + b_i^g e^{-ikv} \right) \chi_i(x), \end{aligned} \tag{4.58}$$

respectively, where the coefficients are

$$\begin{aligned} a_1^f &= 1, \quad a_2^f = \frac{i+1}{(1+i)p-i} - i, \quad b_1^f = i, \quad b_3^f = \frac{i-1}{(1+i)p-i} + 1 \\ a_1^g &= 1, \quad a_2^g = i + \frac{1+i}{(1+i)p-1}, \quad b_1^g = -i, \quad b_3^g = 1 + \frac{1-i}{(1+i)p-1}. \end{aligned} \quad (4.59)$$

The wave number, $k \in \mathbb{R}$ and $k > 0$.¹

4.6.2 Wightman function

Denoting all the modes collectively as $\tilde{u}_{i,k} = (\tilde{f}_k, \tilde{g}_k, \tilde{f}_k^{(p)}, \tilde{g}_k^{(p)})$, where $i = 1, \dots, 4$ labels the type of mode, the field operator can be expanded as

$$\phi = \sum_{i=1}^4 \int_0^\infty dk (a_{i,k} \tilde{u}_{i,k} + a_{i,k}^\dagger \tilde{u}_{i,k}^*), \quad (4.60)$$

where a_k^\dagger and a_k are creation and annihilation operators respectively. The Wightman function is

$$W_p(x, y) = \sum_{i=1}^4 \int_{k_0}^\infty dk \tilde{u}_{i,k}(x) \tilde{u}_{i,k}^*(y), \quad (4.61)$$

where k_0 is an infrared cutoff, needed because the theory is IR divergent, as is the theory in Minkowski space. In certain regions, this Wightman function equals the Minkowski Wightman function. Specifically, for all values of p , $W_p(x, y)|_{x,y \in R_i} = W_{\text{Mink}}(x, y)$ for $i = 1, 3, 5$ and 7 . The Wightman function differs from W_{Mink} when the arguments lie in regions spacelike to the singularity, or when x and y lie in different regions. It can also be shown that $W_p(x, y) = 0$ if $x \in R_1$ and $y \in R_5$, or $x \in R_3$ and $y \in R_7$: there is no correlation between the two disjoint pieces of the future/past of the singularity.

4.6.3 Energy Density in the SJ State in the Infinite Trousers

The SJ Wightman function in the infinite trousers provides evidence that the energy density is zero everywhere except for the past and future lightcones of the singularity, for any p . Consider x and y in the same region, R_i , and not on the lightcone of x_c . Denote the UV cutoff Wightman function as $W_p^\Lambda(u, v; u', v')$, where

¹In the special case $p = \frac{1}{2}$ the discontinuous modes above, $\{\tilde{f}_k^{(p)}, \tilde{g}_k^{(p)}\}|_{p=\frac{1}{2}}$, are actually linear combinations of the modes that one obtains by performing the limiting procedure directly on the $\hat{f}^{(\frac{1}{2})}$ and $\hat{g}^{(\frac{1}{2})}$ modes in the pair of diamonds from Section 4.4.5.

(u, v) and (u', v') are the lightcone coordinates of x and y respectively, and Λ is a UV cutoff on the k -integral in (4.61). Define the quantity

$$T_p^\Lambda(u, v; u', v') := \frac{1}{2}(\partial_u \partial_{u'} + \partial_v \partial_{v'}) W_p^\Lambda(u, v; u', v') . \quad (4.62)$$

and the corresponding quantity $T_{\text{Mink}}^\Lambda(u, v; u', v')$ for the Minkowski Wightman function, $W_{\text{Mink}}^\Lambda(u, v; u', v')$. The regularised expectation value of the energy density (on a surface of constant time) is then given by

$$\langle 0_{(p)}^\infty | T_{00}(x) | 0_{(p)}^\infty \rangle_{reg} := \lim_{\Lambda \rightarrow \infty} \lim_{y \rightarrow x} (T_p^\Lambda(u, v; u', v') - T_{\text{Mink}}^\Lambda(u, v; u', v')) , \quad (4.63)$$

where $|0_{(p)}^\infty\rangle$ is the SJ state in the infinite trousers. We already know that the difference is zero, before the limits are taken, in regions R_i , $i = 1, 3, 5$ and 7 because the SJ and Minkowski Wightman functions are equal there. It turns out that this difference is zero, before the limits are taken, in the other regions R_i , $i = 2, 4, 6, 8$ as well.

We can also see, at a formal level, that there is a factor of $\delta(0)$ in the energy density on the lightcones from x_c . Consider, without point splitting,

$$\langle 0_{(p)}^\infty | T_{00} | 0_{(p)}^\infty \rangle_{reg} := \langle 0_{(p)}^\infty | T_{00} | 0_{(p)}^\infty \rangle - \langle 0_{\text{Mink}} | T_{00}^{\text{Mink}} | 0_{\text{Mink}} \rangle , \quad (4.64)$$

where

$$\begin{aligned} \langle 0_{(p)}^\infty | T_{00} | 0_{(p)}^\infty \rangle &= \frac{1}{2} \int_0^\Lambda dk \left(\partial_u \tilde{f}_k \partial_u \tilde{f}_k^* + \partial_v \tilde{f}_k \partial_v \tilde{f}_k^* + \partial_u \tilde{g}_k \partial_u \tilde{g}_k^* + \partial_v \tilde{g}_k \partial_v \tilde{g}_k^* \right. \\ &\quad \left. + \partial_u \tilde{f}_k^{(p)} \partial_u \tilde{f}_k^{(p)*} + \partial_v \tilde{g}_k^{(p)} \partial_v \tilde{g}_k^{(p)*} + \partial_u \tilde{g}_k^{(p)} \partial_u \tilde{g}_k^{(p)*} + \partial_v \tilde{f}_k^{(p)} \partial_v \tilde{f}_k^{(p)*} \right) , \end{aligned} \quad (4.65)$$

and the Minkowski vacuum energy is

$$\begin{aligned} \langle 0_{\text{Mink}} | T_{00}^{\text{Mink}} | 0_{\text{Mink}} \rangle &= \frac{1}{2} \int_0^\Lambda dk \partial_u u_k \partial_u u_k^* + \partial_v v_k \partial_v v_k^* \\ &= \frac{1}{2} \int_0^\Lambda dk \frac{k}{2\pi} , \end{aligned} \quad (4.66)$$

where the Klein-Gordon normalised Minkowski space modes are $u_k := \frac{1}{\sqrt{4\pi k}} e^{-iku}$ and $v_k := \frac{1}{\sqrt{4\pi k}} e^{-ikv}$.

Let the point at which we evaluate this quantity have time coordinate less than

zero. In this region the modes $\tilde{f}_k^{(p)}$ and $\tilde{g}_k^{(p)}$ take the form

$$\tilde{f}_k^{(p)} = \frac{1}{\sqrt{16\pi k}} \left(\left(-a_1^f \Theta(u) + a_2^f \Theta(-u) \right) e^{-iku} + \left(b_1^f \Theta(v) - b_3^f \Theta(-v) \right) e^{-ikv} \right) \quad (4.67)$$

$$\tilde{g}_k^{(p)} = \frac{1}{\sqrt{16\pi k}} \left(\left(-a_1^g \Theta(u) + a_2^g \Theta(-u) \right) e^{-iku} + \left(b_1^g \Theta(v) - b_3^g \Theta(-v) \right) e^{-ikv} \right), \quad (4.68)$$

resulting in

$$\begin{aligned} \langle 0_{(p)}^\infty | T_{00} | 0_{(p)}^\infty \rangle_{reg} &= \frac{1}{2} \int_0^\Lambda dk \left\{ \frac{k}{4\pi} + \frac{1}{8\pi k} \left[k^2 (\Theta(u)^2 + \Theta(-u)^2 + \Theta(v)^2 + \Theta(-v)^2) \right. \right. \\ &\quad \left. \left. + \frac{4}{1+2p(p-1)} (p^2 \delta(u)^2 + (1-p)^2 \delta(v)^2) \right] - \frac{k}{2\pi} \right\}. \end{aligned} \quad (4.69)$$

Integrating this over a segment of a constant time surface that does not intersect $u = 0$ or $v = 0$ gives 0. However, if the surface intersects the $u = 0$ ($v = 0$) line then the result diverges unless $p = 0$ ($p = 1$).

For all p , the SJ state has divergent energy on both the past and future lightcones of the singularity. This is a consequence of the time reversal symmetry of the infinite trousers which is respected by the SJ state.

4.7 Propagation and Nonunitarity

4.7.1 Propagation

Returning to the pair of diamonds, we can ask what “propagation law” the Green function corresponds to, in order to compare with previous work in [64]. We recall the usual evolution of initial data with a retarded Green function. Given a solution $f(x)$ of the field equation and its derivative on a spacelike hypersurface Σ and a retarded Green function $G(x, y)$, the forward-propagated solution at a point x in the future domain of dependence, $D^+(\Sigma)$, is

$$f(x) = \int_\Sigma d\Sigma_y^\mu [f(y) \nabla_\mu^y G(x, y) - G(x, y) \nabla_\mu^y f(y)]. \quad (4.70)$$

Consider now the pair of diamonds and retarded Green function $G_p(x, y)$. Take Σ to be a spacelike surface that is a union of two disjoint pieces, $\Sigma = \Sigma_A \cup \Sigma_B$,

where Σ_A (Σ_B) goes from the left to right corners of diamond A (B) and passes under the singularity: Σ is as close as possible to a Cauchy surface. Using (4.70) we can propagate continuous initial data on Σ to any point in its future. Given a solution on and to the past of Σ we call the *completely propagated solution* that which is generated by propagating to every point to the future of Σ in this way. For discontinuous initial data, the propagation law is not well defined, as it would involve derivatives of the discontinuous function multiplied by the discontinuous Green function.

If the initial data is continuous and even under the exchange $A \leftrightarrow B$, the completely propagated solution is also even under the exchange. To see this, we first show that initial data corresponding to the \hat{f}_k and \hat{g}_k modes will propagate to the \hat{f}_k and \hat{g}_k modes respectively everywhere. The result then follows because any solution that is even under the exchange is a linear combination of the \hat{f}_k and \hat{g}_k modes.

To see how initial data corresponding to an \hat{f}_k or \hat{g}_k mode propagates it suffices to consider the propagation of plane waves. Let us denote by $u_k^A(x)$ the function whose initial data is a right-moving plane wave on Σ_A and which is zero on Σ_B , i.e. $u_k^A(y) = e^{-iku} \chi_{2,3,4}(x)$. (4.70) evolves u_k^A to $+p$ for $x \in R_1$ and to $e^{-iku} - p$ for $x \in R_5$.

We can also specify the initial data on Σ for the following plane waves: $u_k^B(x) = e^{-iku} \chi_{6,7,8}(x)$, $v_k^A(x) = e^{-ikv} \chi_{2,3,4}(x)$ and $v_k^B(x) = e^{-ikv} \chi_{6,7,8}(x)$. $u_k^B(x)$ and $v_k^B(x)$ are zero on Σ_A , and $v_k^A(x)$ is zero on Σ_B . Their corresponding completely propagated solutions are:

$$\begin{aligned} u_k^A(x) &= e^{-iku} \chi_{2,3,4,5}(x) + p [\chi_5(x) - \chi_1(x)] \\ u_k^B(x) &= e^{-iku} \chi_{1,6,7,8}(x) + p [\chi_1(x) - \chi_5(x)] , \end{aligned} \quad (4.71)$$

and

$$\begin{aligned} v_k^A(x) &= e^{-ikv} \chi_{1,2,3,4}(x) + (1-p) [\chi_5(x) - \chi_1(x)] \\ v_k^B(x) &= e^{-ikv} \chi_{5,6,7,8}(x) + (1-p) [\chi_1(x) - \chi_5(x)] . \end{aligned} \quad (4.72)$$

Taking linear combinations of the above modes, one can verify that the \hat{f}_k and \hat{g}_k modes “propagate into themselves” in the sense described above.

To compare this to the results in [64] we recall how the pair of diamonds was cut out from the trousers. The modes on the pair of diamonds corresponding to the natural “right-moving plane waves in the trunk” from [64] with periodic boundary conditions take the form $u_k^A(x) + (-1)^n u_k^B(x)$ with $k = \sqrt{2}n\pi/\lambda$ in our conventions (the factor of $\sqrt{2}$ here arises from our definition of the light-cone coordinates). For even n , the constant terms in (4.71) cancel. For odd n , they add up, leading to opposite constant terms $\pm 2p$ in the causal futures of the singularity in the left/right legs. Similar statements apply to left-moving incoming modes. This corresponds

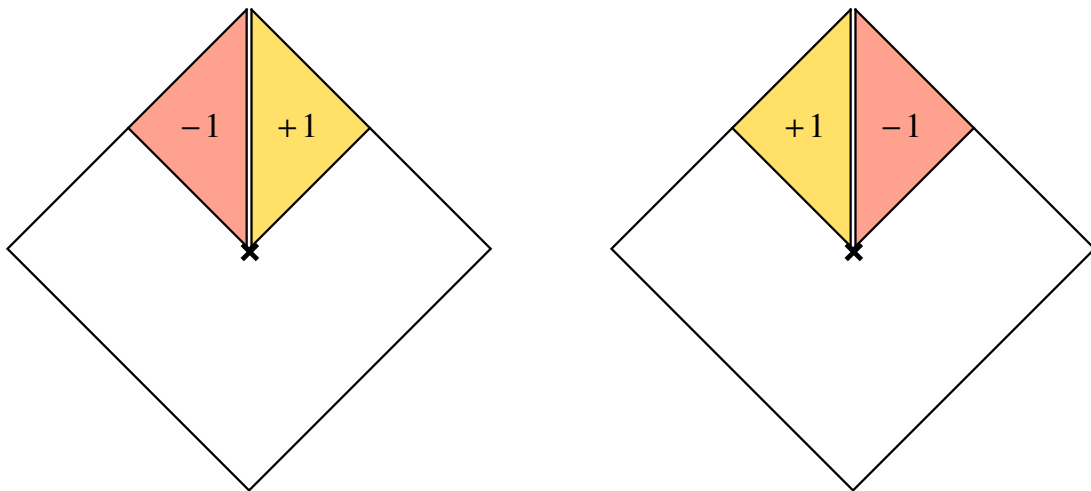


Figure 4.12: Illustration of the $\Gamma_0(x)$ function. The function is zero in the white regions.

precisely to the one-parameter family of propagation laws found in [64], which the authors arrived at by demanding the conservation of what they call the “Klein-Gordon inner product” under the evolution past the singularity. Our parameter p is related to the parameter A in [64] via $p = \frac{1}{2}(1 + A)$.

At the end of [64] the authors mention certain discontinuous functions, which they call $\gamma_0(x)$ and $\gamma(x)$, that violate the propagation rule, and ask whether they are required to form a complete set of modes. The analogous functions in \mathcal{M} are $\Gamma_0(x) = \chi_1(x) - \chi_5(x)$ and $\Gamma(x) = \chi_3(x) - \chi_7(x)$ as illustrated in Figure 4.12 and 4.13 respectively. Each function satisfies the requirements for a solution, and so is expressible as a linear combination of the SJ modes and this means that in the pair of diamonds the notion of “propagation” becomes ill-defined. Solutions $f(x)$ and $f(x) + \lambda\Gamma_0(x)$, where λ is a constant, share the same initial data. Similarly, $f(x)$ and $f(x) + \lambda\Gamma(x)$ have the same final data.

4.7.2 Nonunitarity

The ambiguity in the notion of propagation indicates that the theory in the pair of diamonds is nonunitary. We will see that this can be expressed as the algebra of observables, \mathfrak{A}_- , associated to the past null boundary, N_- , being a strict subset of the algebra of observables, \mathfrak{A} , for the full spacetime.

Let the vertices of the pair of diamonds be labelled z_1, z_2, \dots, z_8 in clockwise order starting from z_1 which is the top vertex of region R_1 , as shown in Figure 4.14 and 4.15. $z_i \in R_i$ for all i . Given any point x not in the causal future of the singularity, x_c , the

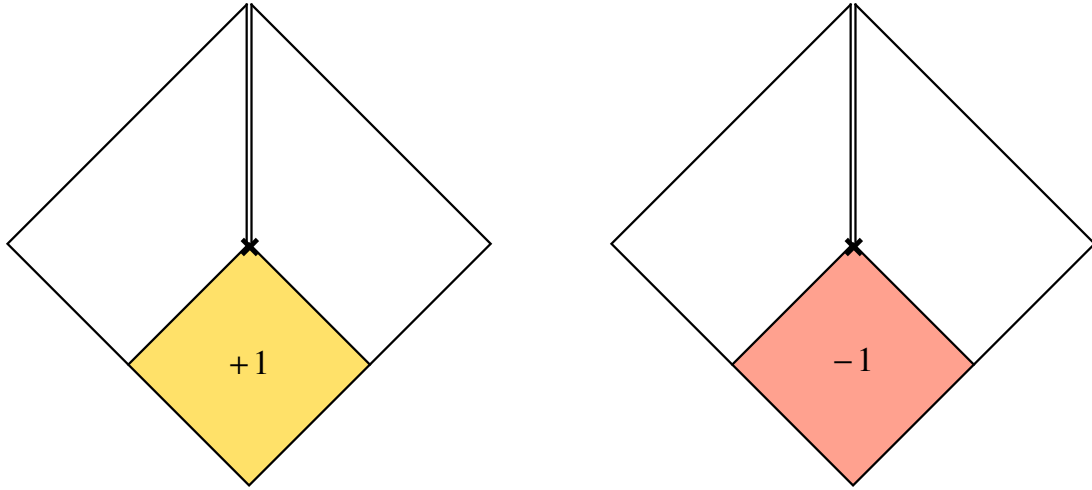


Figure 4.13: Illustration of the $\Gamma(x)$ function. The function is zero in the white regions.

equation of motion (4.25) for a diamond with x at its top vertex and the other three vertices on the past null boundary N_- shows that $\phi(x)$ is determined by values of ϕ on N_- . However, if $y \in R_1$ then $\phi(y)$ is not specified by the initial data on N_- since, using equation of motion (4.26) for the double diamond shown in Figure 4.14,

$$\phi(y) = \phi(y_2) - \phi(z_3) + \phi(z_4) - \phi(z_5) + \phi(z_6) - \phi(z_7) + \phi(y_8), \quad (4.73)$$

where $y_2 \in R_2 \cap N_-$ and $y_8 \in R_8 \cap N_-$ are the points shown in Figure 4.14 and $z_5 \notin N_-$.

Similarly, if $y \in R_5$, then the double diamond in Figure 4.15 gives

$$\phi(y) = \phi(y_6) - \phi(z_7) + \phi(z_8) - \phi(z_1) + \phi(z_2) - \phi(z_3) + \phi(y_4), \quad (4.74)$$

where $y_4 \in R_4 \cap N_-$ and $y_6 \in R_6 \cap N_-$ are the points shown in Figure 4.15 and $z_1 \notin N_-$. In both cases $\phi(y)$ is not specified by data on N_- . However, the extra data needed is not $\phi(z_1)$ and $\phi(z_5)$ since, the equation of motion from the double diamond that is the whole pair of diamonds implies their sum is specified by data on N_- :

$$\phi(z_1) + \phi(z_5) = \phi(z_2) - \phi(z_3) + \phi(z_4) + \phi(z_6) - \phi(z_7) + \phi(z_8). \quad (4.75)$$

Therefore, only $\Phi_+ := \phi(z_1) - \phi(z_5)$ is needed to complement ϕ on N_- .

Similarly, a solution ϕ is specified by data on the future null boundary, N_+ , together with $\Phi_- := \phi(z_3) - \phi(z_7)$.

Thus, Φ_+ (Φ_-) and all operators generated from it are missing from the algebra

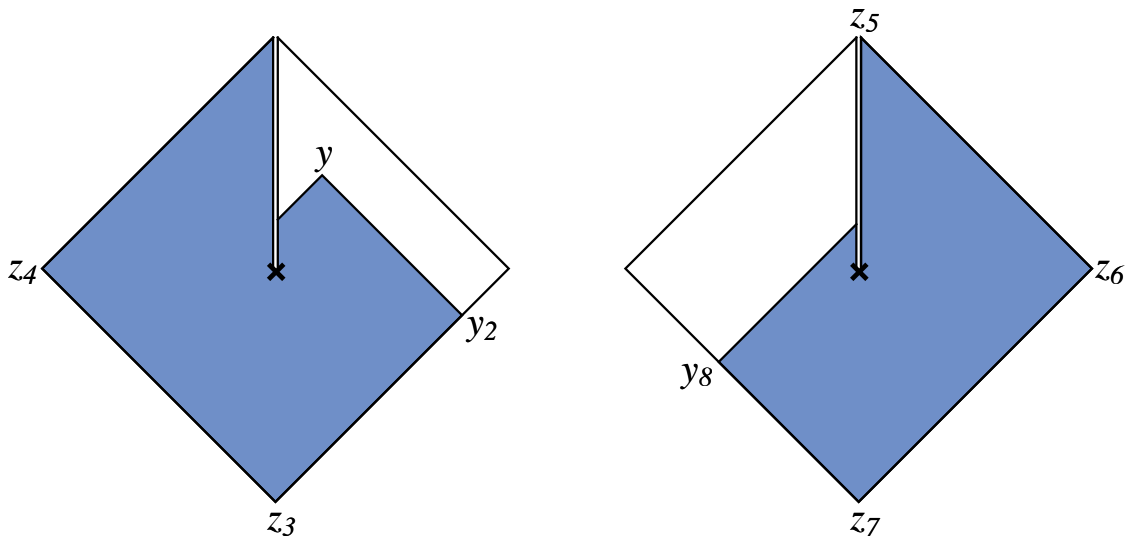


Figure 4.14: The double diamond for equation (4.73).

\mathfrak{A}_- (\mathfrak{A}_+). The structural relationship between \mathfrak{A}_- , \mathfrak{A}_+ and \mathfrak{A} remains to be worked out. Here we just note that

$$\begin{aligned}
 [\Phi_+, \Phi_-] &= [\phi(z_1), \phi(z_3)] - [\phi(z_5), \phi(z_3)] - [\phi(z_1), \phi(z_7)] + [\phi(z_5), \phi(z_7)] \\
 &= i(\Delta(z_1, z_3) - \Delta(z_5, z_3) - \Delta(z_1, z_7) + \Delta(z_5, z_7)) \\
 &= i(1 - 2p) ,
 \end{aligned} \tag{4.76}$$

so the operators commute for $p = \frac{1}{2}$.

4.8 Summary

Trying to make sense of quantum field theory on a topology changing background not only advances the study of topology change but requires us to think afresh about QFT and its foundations. As the SJ formalism for free quantum field theory depends only on spacetime causal order and the retarded Green function, it is straightforward, at least in principle, to apply it to the pair of diamonds, a topology changing spacetime. The surprise was that the SJ modes could be found, and the Wightman function constructed, explicitly. Some of these modes are discontinuous across the future and past lightcones of the singularity and this discontinuity gives rise to a divergence in the energy density on these null lines, confirming the expectation arising from past work by Anderson and DeWitt and by Copeland et al. A similar conclusion was reached by examining the limiting case of the infinite trousers. As

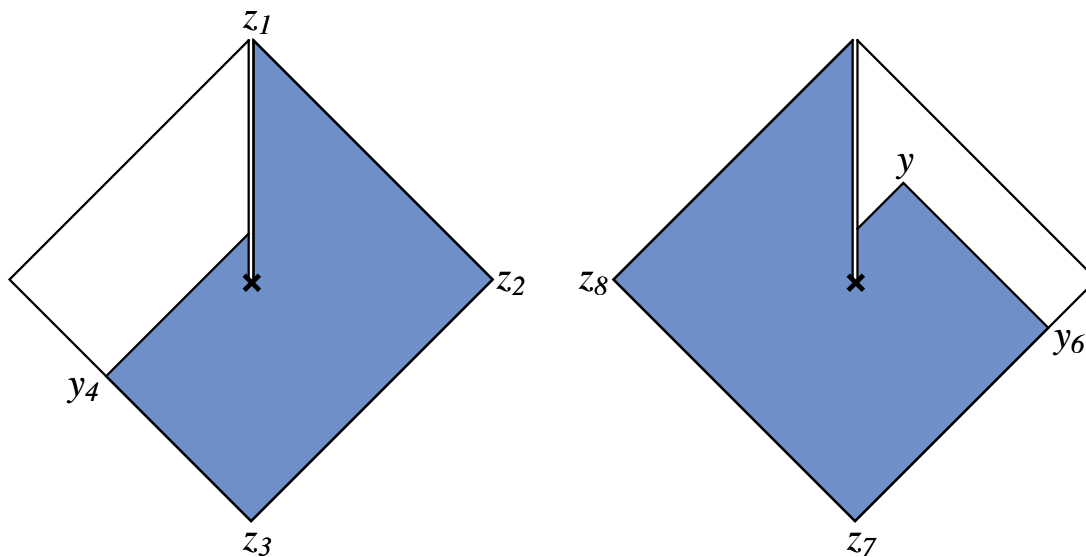


Figure 4.15: The double diamond for equation (4.74).

the SJ state is time reversal symmetric, the divergences appear on both the past and future lightcones of the singularity in contrast to previous work. We have also found a relation between the SJ framework based on the Green function and previous work by Copeland et al. by analysing the concept of propagation forward in time. In a unitary theory, if spacetime region X is in the domain of dependence of region Y then then the corresponding algebras of observables are related by $\mathfrak{A}_X \subseteq \mathfrak{A}_Y$. However we have seen that this fails in the pair of diamonds: the future boundary, N_+ , is in the domain of dependence of the past boundary, N_- , but the corresponding algebra \mathfrak{A}_+ contains an operator that is not in \mathfrak{A}_- .

How should these results be viewed by those who believe that topology change should be part of full quantum gravity? One could argue that since topology change is expected to be a quantum gravity effect we should study it in the context of a background spacetime with no structure at the Planck scale, for example a causal set and this would be interesting to do. It is possible, though, that these results and the previous work are telling us that topology-change of the trousers type is disallowed whilst leaving the question of other types of topology-change very much open. The transition in the trousers belongs to the class of topology-changes in which the spacetime exhibits “causal discontinuity” [70, 75] where the causal past or future of a point changes discontinuously as the point moves across the past or future lightcones of the singularity. The authors of [76] found evidence that causally discontinuous topology changing processes in $1 + 1$ dimensions are suppressed in a sum-over-histories, while causally continuous ones are enhanced. Such observations lend support to Sorkin’s conjecture that the pathology of infinite energy production

occurs in a topology-changing spacetime if and only if it is causally discontinuous.

It would be very interesting therefore to study the type of topology change in 3+1 dimensions with a singularity with Morse signature $(+ + --)$ which is causally continuous. This type of topology change is particularly interesting in 3+1 dimensions because, given any two closed connected 3-manifolds, there exists a cobordism between them which admits a Lorentzian metric with only these types of singularity. It would be interesting to study the SJ theory of a scalar field in such a spacetime. If it can be shown that the SJ Wightman function is well behaved in a case like this, it would be strong evidence that the pathology of divergent energy production is associated only with the trousers.

Chapter 5

Conclusions and Future Directions

In this thesis we have investigated certain questions pertaining to the problem of quantum gravity, and we have made progress by utilising the spacetime causal structure. We began by discussing the quantum gravity path integral, and its discrete alternative found in Causal Set Theory — a theory of quantum gravity that is intimately tied to spacetime causal structure.

In Chapter 2 the gravitational action that enters into the continuum path integral was investigated, and the necessary boundary terms were derived for all signatures of the spacetime boundary. This was done using the tetrad formalism, in which the derivation of the boundary terms is significantly simplified. Using the gauge non-invariance of the tetrad formalism we were able to derive, in a suitable limit, the joint contribution to the action for an intersection of two boundary components.

Chapter 3 saw our attention turn to the action of a causal set, specifically its boundary terms. There we derived a family of causal set expressions for an analogue of the spacelike Gibbons-Hawking-York boundary term in the continuum, which was derived in Chapter 2. Other causal set expressions were also obtained that encapsulated more of continuum boundary geometry. In the process of determining these causal set expressions we also derived a continuum result for the volume of a small causal cone. The fluctuations (due to the sprinkling process) of the different causal set expressions were then investigated numerically, and interestingly the fluctuations of the spacelike boundary terms decreased with sprinkling size in 4D. We extended the different causal set expressions to include a scalar field defined on the causal set, which enabled us to encode continuum objects relating to the normal derivative of a scalar field on the causal set. Finally, the bulk causal set action, or BDG action, was investigated. Specifically we looked at whether it already contained any boundary terms when the spacetime is taken to be a flat interval. We found that the bulk action gave the area of the joint between the top and bottom lightcones of

the interval, which might indicate that the bulk action contains an analogue of the continuum null boundary term and/or the joint contribution.

We then left the causal set action and returned to the continuum path integral in Chapter 4, where we explored the question of whether spacetimes exhibiting spatial topology change are prohibited in the quantum gravity path integral. To attempt to answer this question we looked at one of the simplest topology changing spacetimes — the trousers spacetime — and asked whether one could define a pathology free quantum field theory on that spacetime; the idea being that any pathologies would likely suppress such a topology change in a path integral including a sum over fields as well as spacetimes. The non-globally hyperbolic nature of the trousers spacetime forced us to extend the usual framework of quantum field theory, and our extension resulted in a one parameter family of different quantum field theories that could be defined on the trousers spacetime, all of which contained a pathological infinite energy burst. Our treatment of the quantum field theory using the novel Sorkin-Johnston formalism was more complete than previous works on the trousers spacetime, in the sense that we were able to construct a complete set of basis functions on the space of solutions.

The topics covered in this thesis have been somewhat broad, and hence there are a variety of future directions. That being said, the possible future avenues are all motivated by the same underlying goal — to understand Quantum Gravity.

Take the continuum action derived in Chapter 2. As was discussed in Chapter 2 we do not yet have a complete treatment of the continuum action. Our treatment, for example, did not account for certain boundaries that tend from spacelike/timelike to null at a join, and we did not argue whether codimension-3 meetings of joins contribute to the action. The question of the role of the gravitational action in a quantum theory of gravity is still unclear. The final action proposed in Chapter 2 only contains first order derivatives of the metric, unlike the Einstein-Hilbert action, but it is also not reparameterisation invariant when one considers null boundaries. If one believes that the double path integral is the correct way to formulate a quantum theory, and not a single path integral, then this is no longer an issue, since the parameter dependence drops out when a difference of two actions is taken in the double path integral. Of course one might argue that this gravitational action is only an effective description of a deeper underlying theory, such as String Theory or Causal Set Theory, in which case the issues arising from a continuum gravitational path integral can simply be ignored. The aforementioned concerns aside, it was nonetheless interesting to find that the problems of the gravitational action (its non-reparameterisation invariance) disappeared when considering the more physical

equations of motion, and the arguably more physical double path integral.

There is still much we do not understand about the full causal set action. We have formulated an analogue of the spacelike boundary terms but we do not yet know how to incorporate the timelike or null cases. The bulk causal set action itself is divergent when one considers timelike boundaries, and more work is needed to control this divergence. The bulk causal set action has also been investigated in Monte Carlo simulations of the “Euclidianised” causal set path integral [77, 78], and in those simulations the causal set expression for the spacelike boundary term was not included. Recently some work has been done to include the causal set boundary term in these simulations, and the preliminary results suggest that the boundary term dominates over the bulk term. This is most likely due to the fact that the simulations use the 2D form of the bulk and boundary causal set action, and in 2D the fluctuations of the boundary term grow as the number of causal set points increases. The fluctuations of the 2D bulk term are dampened with the inclusion of an additional non-locality scale, and hence one can only see the effects of the boundary term when studying the two simultaneously. To solve this issue one would need to introduce a non-locality scale (possibly the same scale used in the bulk action) into the causal set boundary action to control its fluctuations in 2D. Alternatively, one could study Monte Carlo simulations using higher dimensional versions of the causal set bulk and boundary actions. The fluctuations of the boundary term do not increase with increasing causal set size in higher dimensions, and hence the boundary term would most likely not dominate the bulk term in higher dimensions. As alluded to in 3.6 the continuum formula for the small causal cone could be useful for deriving the Einstein equations in a similar manner to how Jacobson derives them with the small interval volume formula and the 2nd law of thermodynamics. Or perhaps one could use the small cone formula to formulate an approximate Hamiltonian dynamics on causal sets, akin to the sequential growth models. Both of these avenues should be explored.

Perhaps the most interesting future direction, in the author’s opinion, involves extending the work of Chapter 4. The Sorkin-Johnston formalism ensures one has a complete description of the solution space, and hence a more complete understanding of the corresponding quantum field theory. The formalism is also powerful enough to deal with topology changing spacetimes such as the trousers spacetime, which makes it a promising tool for dealing with higher dimensional spacetimes with topology change. Another useful feature of the formalism is how it can be easily adapted to a discrete spacetime lattice or causal set. This opens up the possibility of a numerical investigation into higher dimensional topology changing spacetimes, where one could

use a lattice or causal set to approximate a continuum spacetime. It would be interesting to see whether the higher dimensional cases come with same pathological infinite energy burst seen in the trousers spacetime. Sorkin has conjectured that this pathology is due to the trousers spacetime being *causally discontinuous*, and that one should see similar pathologies in other causally discontinuous topology changes in higher dimensions. The Sorkin-Johnston formalism offers us a way to test this conjecture, numerically and/or analytically. Even more tantalising is the possibility of finding a type of topology change that does not fall victim to the same pathology, but if Sorkin's conjecture is correct then this cannot happen in 3D where all the relevant topology changes are causally discontinuous. In 4D we get our first glimpse at a spacetime that is *causally continuous* — the spacetime with Morse signature $(+ + - -)$ mentioned in 4.8. If this topology change does not produce an infinite energy burst in the quantum field theory then it has more of a chance of not being suppressed in the quantum gravity path integral. Interestingly, this very topology change occurs in the process of black hole pair production.

Bibliography

- [1] I. Jubb, J. Samuel, R. Sorkin, and S. Surya, “Boundary and Corner Terms in the Action for General Relativity,” *Class. Quant. Grav.* **34** no. 6, (2017) 065006, [arXiv:1612.00149 \[gr-qc\]](#).
- [2] M. Buck, F. Dowker, I. Jubb, and S. Surya, “Boundary Terms for Causal Sets,” *Class. Quant. Grav.* **32** no. 20, (2015) 205004, [arXiv:1502.05388 \[gr-qc\]](#).
- [3] I. Jubb, “The Geometry of Small Causal Cones,” *Class. Quant. Grav.* **34** no. 9, (2017) 094005, [arXiv:1611.00785 \[gr-qc\]](#).
- [4] M. Buck, F. Dowker, I. Jubb, and R. Sorkin, “The SorkinJohnston state in a patch of the trousers spacetime,” *Class. Quant. Grav.* **34** no. 5, (2017) 055002, [arXiv:1609.03573 \[gr-qc\]](#).
- [5] S. W. Hawking, “Breakdown of Predictability in Gravitational Collapse,” *Phys. Rev.* **D14** (1976) 2460–2473.
- [6] L. Susskind and L. Thorlacius, “Gedanken experiments involving black holes,” *Phys. Rev.* **D49** (1994) 966–974, [arXiv:hep-th/9308100 \[hep-th\]](#).
- [7] A. Almheiri, D. Marolf, J. Polchinski, and J. Sully, “Black Holes: Complementarity or Firewalls?,” *JHEP* **02** (2013) 062, [arXiv:1207.3123 \[hep-th\]](#).
- [8] D. P. Rideout and R. D. Sorkin, “A Classical sequential growth dynamics for causal sets,” *Phys. Rev.* **D61** (2000) 024002, [arXiv:gr-qc/9904062 \[gr-qc\]](#).
- [9] D. M. Benincasa and F. Dowker, “The Scalar Curvature of a Causal Set,” *Phys.Rev.Lett.* **104** (2010) 181301, [arXiv:1001.2725 \[gr-qc\]](#).
- [10] F. Dowker and L. Glaser, “Causal set d’Alembertians for various dimensions,” *Class.Quant.Grav.* **30** (2013) 195016, [arXiv:1305.2588 \[gr-qc\]](#).

- [11] L. Glaser, “A closed form expression for the causal set d’Alembertian,” *Class.Quant.Grav.* **31** (2014) 095007, arXiv:1311.1701 [math-ph].
- [12] L. Bombelli, R. K. Koul, J. Lee, and R. D. Sorkin, “A Quantum Source of Entropy for Black Holes,” *Phys. Rev.* **D34** (1986) 373–383.
- [13] D. B. Malament, “The class of continuous timelike curves determines the topology of spacetime,” *Journal of Mathematical Physics* **18** no. 7, (1977) 1399–1404, <http://dx.doi.org/10.1063/1.523436>.
- [14] A. Levichev, “Prescribing the conformal geometry of a lorentz manifold by means of its causal structure,” in *Soviet Math. Dokl.*, vol. 35, p. 133. 1987.
- [15] S. W. Hawking, A. R. King, and P. J. McCarthy, “A New Topology for Curved Space-Time Which Incorporates the Causal, Differential, and Conformal Structures,” *J. Math. Phys.* **17** (1976) 174–181.
- [16] E. Minguzzi and M. Sanchez, “The Causal hierarchy of spacetimes,” in *Recent Developments in pseudo-Riemannian geometry*, ed. by H. Baum and D. Alekseevsky. Zurich, EMS Pub.House, 2008, p.299-358, pp. 299–358. 2006. arXiv:gr-qc/0609119 [gr-qc].
- [17] J. W. York, Jr., “Role of conformal three geometry in the dynamics of gravitation,” *Phys. Rev. Lett.* **28** (1972) 1082–1085.
- [18] G. W. Gibbons and S. W. Hawking, “Action integrals and partition functions in quantum gravity,” *Phys. Rev. D* **15** (May, 1977) 2752–2756.
- [19] R. Wald, *General Relativity*. University of Chicago Press, 1984. <https://books.google.co.uk/books?id=FQgAmQEACAAJ>.
- [20] E. Poisson, *A Relativist’s Toolkit: The Mathematics of Black-Hole Mechanics*. Cambridge University Press, 2004. https://books.google.co.uk/books?id=bk2XEgz_ML4C.
- [21] A. Einstein, “Notiz zu E. Schrödingers Arbeit “Die Energiekomponenten des Gravitationsfeldes”,” *Physikalische Zeitschrift* **19** (1918) .
- [22] R. Sorkin, “Time-evolution problem in regge calculus,” *Phys. Rev. D* **12** (Jul, 1975) 385–396.
- [23] J. B. Hartle and R. Sorkin, “Boundary terms in the action for the regge calculus,” *General Relativity and Gravitation* **13** no. 6, (Jun, 1981) 541–549.

- [24] G. Hayward, “Gravitational action for spacetimes with nonsmooth boundaries,” *Phys. Rev. D* **47** (Apr, 1993) 3275–3280.
- [25] D. Brill and G. Hayward, “Is the gravitational action additive?,” *Phys. Rev. D* **50** (1994) 4914–4919, [arXiv:gr-qc/9403018](#) [gr-qc].
- [26] K. Parattu, S. Chakraborty, B. R. Majhi, and T. Padmanabhan, “A Boundary Term for the Gravitational Action with Null Boundaries,” *Gen. Rel. Grav.* **48** no. 7, (2016) 94, [arXiv:1501.01053](#) [gr-qc].
- [27] K. Parattu, S. Chakraborty, and T. Padmanabhan, “Variational principle for gravity with null and non-null boundaries: a unified boundary counter-term,” *The European Physical Journal C* **76** no. 3, (Mar, 2016) 129.
- [28] Y. Neiman, “On-shell actions with lightlike boundary data,” [arXiv:1212.2922](#) [hep-th].
- [29] Y. Neiman, “The imaginary part of the gravity action and black hole entropy,” *JHEP* **04** (2013) 071, [arXiv:1301.7041](#) [gr-qc].
- [30] Y. Neiman, “Action and entanglement in gravity and field theory,” *Phys. Rev. Lett.* **111** no. 26, (2013) 261302, [arXiv:1310.1839](#) [hep-th].
- [31] Y. Neiman, “Imaginary part of the gravitational action at asymptotic boundaries and horizons,” *Phys. Rev. D* **88** no. 2, (2013) 024037, [arXiv:1305.2207](#) [gr-qc].
- [32] R. J. Epp, “The Symplectic structure of general relativity in the double null (2+2) formalism,” [arXiv:gr-qc/9511060](#) [gr-qc].
- [33] L. Lehner, R. C. Myers, E. Poisson, and R. D. Sorkin, “Gravitational action with null boundaries,” *Phys. Rev. D* **94** no. 8, (2016) 084046, [arXiv:1609.00207](#) [hep-th].
- [34] C. Krishnan and A. Raju, “A Neumann Boundary Term for Gravity,” *Mod. Phys. Lett. A* **32** no. 14, (2017) 1750077, [arXiv:1605.01603](#) [hep-th].
- [35] J. Louko and R. D. Sorkin, “Complex actions in two-dimensional topology change,” *Classical and Quantum Gravity* **14** no. 1, (1997) 179.
- [36] L. Bombelli, J. Lee, D. Meyer, and R. Sorkin, “Space-Time as a Causal Set,” *Phys.Rev.Lett.* **59** (1987) 521–524.

- [37] J. York, “Role of conformal three-geometry in the dynamics of gravitation,” *Phys. Rev. Lett.* **28** (1972) 1082.
- [38] G. Gibbons and S. Hawking, “Action Integrals and Partition Functions in Quantum Gravity,” *Phys.Rev.* **D15** (1977) 2752–2756.
- [39] R. D. Sorkin, “Causal sets: Discrete gravity (notes for the valdivia summer school),” in *Lectures on Quantum Gravity, Proceedings of the Valdivia Summer School, Valdivia, Chile, January 2002*, A. Gomberoff and D. Marolf, eds. Plenum, 2005. [gr-qc/0309009](#).
- [40] G. W. Gibbons and S. N. Solodukhin, “The Geometry of small causal diamonds,” *Phys. Lett.* **B649** (2007) 317–324, [arXiv:hep-th/0703098](#) [[hep-th](#)].
- [41] T. Jacobson, “Entanglement Equilibrium and the Einstein Equation,” *Phys. Rev. Lett.* **116** no. 20, (2016) 201101, [arXiv:1505.04753](#) [[gr-qc](#)].
- [42] D. M. T. Benincasa and F. Dowker, “The Scalar Curvature of a Causal Set,” *Phys. Rev. Lett.* **104** (2010) 181301, [arXiv:1001.2725](#) [[gr-qc](#)].
- [43] F. Dowker and L. Glaser, “Causal set d’Alembertians for various dimensions,” *Class. Quant. Grav.* **30** (2013) 195016, [arXiv:1305.2588](#) [[gr-qc](#)].
- [44] S. Khetrpal and S. Surya, “Boundary Term Contribution to the Volume of a Small Causal Diamond,” *Class. Quant. Grav.* **30** (2013) 065005, [arXiv:1212.0629](#) [[gr-qc](#)].
- [45] M. Roy, D. Sinha, and S. Surya, “Discrete geometry of a small causal diamond,” *Phys. Rev.* **D87** no. 4, (2013) 044046, [arXiv:1212.0631](#) [[gr-qc](#)].
- [46] J. Myrheim, “Statistical geometry,” 1978. CERN preprint TH-2538.
- [47] S. Surya, “Directions in Causal Set Quantum Gravity,” [arXiv:1103.6272](#) [[gr-qc](#)].
- [48] S. Khetrpal and S. Surya, “Boundary Term Contribution to the Volume of a Small Causal Diamond,” *Class. Quant. Grav.* **30** (2013) 065005, [arXiv:1212.0629](#) [[gr-qc](#)].
- [49] E. Poisson, *A Relativist’s Toolkit: The Mathematics of Black-Hole Mechanics*. Cambridge University Press, 2004.
<https://books.google.co.uk/books?id=FKg3mAEACAAJ>.

- [50] R. D. Sorkin, “Does locality fail at intermediate length-scales?,” in *Approaches to Quantum Gravity: Towards a New Understanding of Space and Time*, D. Oriti, ed. Cambridge University Press, 2006. arXiv:gr-qc/0703099.
- [51] A. Belenchia, D. M. T. Benincasa, and F. Dowker, “The continuum limit of a 4-dimensional causal set scalar d’Alembertian,” arXiv:1510.04656 [gr-qc].
- [52] D. M. Benincasa, F. Dowker, and B. Schmitzer, “The Random Discrete Action for 2-Dimensional Spacetime,” *Class.Quant.Grav.* **28** (2011) 105018, arXiv:1011.5191 [gr-qc].
- [53] L. Glaser and S. Surya, “Towards a Definition of Locality in a Manifoldlike Causal Set,” *Phys.Rev.* **D88** (2013) 124026, arXiv:1309.3403 [gr-qc].
- [54] R. D. Sorkin, “Forks in the road, on the way to quantum gravity,” *Int.J.Theor.Phys.* **36** (1997) 2759–2781, arXiv:gr-qc/9706002 [gr-qc].
- [55] R. Sorkin, “Introduction to topological geons,” in *Topological Properties and Global Structure of Space-Time*, P. Bergmann and V. De Sabbata, eds., NATO ASI Series, pp. 249–270. Springer US, 1986.
http://dx.doi.org/10.1007/978-1-4899-3626-4_19.
- [56] R. D. Sorkin and S. Surya, “An Analysis of the representations of the mapping class group of a multi - geon three manifold,” *Int.J.Mod.Phys.* **A13** (1998) 3749–3790, arXiv:gr-qc/9605050 [gr-qc].
- [57] R. Sorkin, “Consequences of Spacetime Topology,” in *3rd Canadian Conference on General Relativity and Relativistic Astrophysics*, A. A. Coley, F. Cooperstock, and B. O. J. Tupper, eds., p. 137. 1990.
- [58] H. F. Dowker and R. D. Sorkin, “A Spin statistics theorem for certain topological geons,” *Class. Quant. Grav.* **15** (1998) 1153–1167, arXiv:gr-qc/9609064 [gr-qc].
- [59] R. P. Geroch, “Topology in general relativity,” *J.Math.Phys.* **8** (1967) 782–786.
- [60] K. S. Thome, “Closed timelike curves,” in *General Relativity and Gravitation 1992, Proceedings of the Thirteenth INT Conference on General Relativity and Gravitation, held at Cordoba, Argentina, 28 June-July 4 1992*, p. 295, CRC Press. 1993.
- [61] T. Dray, C. Manogue, and R. Tucker, “Particle production from signature change,” *Gen.Rel.Grav.* **23** (1991) 967–971.

- [62] G. Gibbons, “Topology change in classical and quantum gravity,” [arXiv:1110.0611 \[gr-qc\]](#).
- [63] A. Anderson and B. S. DeWitt, “Does the Topology of Space Fluctuate?,” *Found.Phys.* **16** (1986) 91–105.
- [64] C. Manogue, E. Copeland, and T. Dray, “The trousers problem revisited,” *Pramana* **30** no. 4, (1988) 279–292.
- [65] R. D. Sorkin, “Scalar Field Theory on a Causal Set in Histories Form,” *J. Phys. Conf. Ser.* **306** (2011) 012017, [arXiv:1107.0698 \[gr-qc\]](#).
- [66] N. Afshordi, S. Aslanbeigi, and R. D. Sorkin, “A Distinguished Vacuum State for a Quantum Field in a Curved Spacetime: Formalism, Features, and Cosmology,” [arXiv:1205.1296 \[hep-th\]](#).
- [67] S. Johnston, “Feynman Propagator for a Free Scalar Field on a Causal Set,” *Phys.Rev.Lett.* **103** (2009) 180401, [arXiv:0909.0944 \[hep-th\]](#).
- [68] M. Reed and B. Simon, *Methods of Modern Mathematical Physics — Volume 1: Functional Analysis*. Gulf Professional Publishing, 1980.
- [69] N. Afshordi, M. Buck, F. Dowker, D. Rideout, R. D. Sorkin, and Y. K. Yazdi, “A Ground State for the Causal Diamond in 2 Dimensions,” *JHEP* **1210** (2012) 088, [arXiv:1207.7101 \[hep-th\]](#).
- [70] F. Dowker and S. Surya, “Topology change and causal continuity,” *Phys.Rev.* **D58** (1998) 124019, [arXiv:gr-qc/9711070 \[gr-qc\]](#).
- [71] S. P. Johnston, *Quantum Fields on Causal Sets*. PhD thesis, Imperial College, 2010. [arXiv:1010.5514 \[hep-th\]](#).
- [72] C. J. Fewster and R. Verch, “On a Recent Construction of “Vacuum-like” Quantum Field States in Curved Spacetime,” [arXiv:1206.1562 \[math-ph\]](#).
- [73] Y. K. Yazdi *Private Communication*. .
- [74] M. Brum and K. Fredenhagen, “Vacuum-like Hadamard states for quantum fields on curved spacetimes,” *Class.Quant.Grav.* **31** (2014) 025024, [arXiv:1307.0482 \[gr-qc\]](#).
- [75] H. F. Dowker, R. S. Garcia, and S. Surya, “Morse index and causal continuity: A criterion for topology change in quantum gravity,” *Class. Quant. Grav.* **17** (2000) 697–712, [gr-qc/9910034](#).

-
- [76] J. Louko and R. D. Sorkin, “Complex actions in two-dimensional topology change,” *Class.Quant.Grav.* **14** (1997) 179–204, arXiv:gr-qc/9511023 [gr-qc].
- [77] S. Surya, “Evidence for the continuum in 2d causal set quantum gravity,” *Classical and Quantum Gravity* **29** no. 13, (2012) 132001.
- [78] L. Glaser and S. Surya, “The hartlehawking wave function in 2d causal set quantum gravity,” *Classical and Quantum Gravity* **33** no. 6, (2016) 065003.
- [79] M. Spiegel, “The summation of series involving roots of transcendental equations and related applications,” *Journal of Applied Physics* **24** no. 9, (1953) 1103–1106.

Appendix A

A.1 Zero Eigenvalue Eigenfunctions Are Not Solutions

We first derive a simple formula that must be satisfied by a zero eigenvalue eigenfunction (ZEE).

Consider x in diamond A with coordinates (L, v') with $v' < 0$. For a function f , $i\Delta_p f = 0$ implies $\int_{-L}^{v'} dv \int_{-L}^L du f(u, v) = 0$. Differentiating this expression with respect to v' implies $\int_{-L}^L du f(u, v') = 0$, for all $v' < 0$. Similarly, all integrals of f along lines of constant u vanish. So,

$$\int_{-L}^L du f(u, v') = 0 \quad \text{and} \quad \int_{-L}^L dv f(u', v) = 0 \quad \forall u', v' \neq 0. \quad (\text{A.1})$$

We say a nonzero function f is a ZEE if it satisfies (A.1). We say an element of $L^2(M)$ is a ZEE if it has a nonzero representative which satisfies (A.1).

Claim: If $[f] \in L^2(M)$ is both a ZEE and a solution, then it has a representative function that is both a ZEE and a solution.

Proof: It suffices to show that a representative function of $[f]$ which is a solution, and which we might as well call f , can be changed on a set of measure zero, so that it satisfies (A.1), whilst remaining a solution. Recall the conditions for a function to be a solution are $\mathfrak{E}^D f = 0$ for every diamond, D , that doesn't contain x_c and $\mathfrak{E}^{DD} f = 0$ for every double diamond, DD , that contains x_c .

The function $f(x)$ can only fail (A.1) on a set of lines of measure zero, since $[f]$ is a ZEE. On one such null line the integral of $f(x)$ will be some non-zero real number, η . We can alter $f(x)$ by subtracting from it the function that is $\frac{\eta}{2L}$ along that null line and zero everywhere else. The resulting function, $\tilde{f}(x)$, now satisfies (A.1) on that particular null line and $\tilde{f}(x)$ still satisfies the conditions for it to be a solution. We can continue to adjust the function in this way for all of the null lines on which $f(x)$ failed (A.1). The resulting function will be both a solution and a ZEE.

Claim: $[h] \in L^2(M)$ cannot be both a ZEE and a solution.

Proof: Let $[h] \in L^2(M)$ be both a ZEE and a solution and let the representative, h , be both a ZEE and a solution. We will prove that $h \sim 0$, the zero function.

$h(x)$ satisfies $\mathfrak{C}^D h = 0$ for all diamonds D that do not contain x_c . Take such a D in diamond A with corners x_1, x_2, x_3 and x_4 that have light-cone coordinates $(u, v), (-L, v), (-L, -L)$ and $(u, -L)$ respectively, where $u \in [-L, L]$ and $v \in [-L, 0)$. With these coordinates the equation $\mathfrak{C}^D h = 0$ becomes

$$h(u, v) - h(-L, v) + h(-L, -L) - h(u, -L) = 0. \quad (\text{A.2})$$

Integrating this along u , and using $\int_{-L}^L du h(u, v) = 0$ for all $v \neq 0$ gives $h(-L, v) = h(-L, -L)$. This is true for all $v < 0$ and so $h(x)$ is constant along the line of $u = -L$ for $v < 0$. The same reasoning shows that on the line of $v = -L$ for $u < 0$ the function must equal the same constant, which we call C .

Using this in (A.2) implies that $h(u, v) = C$ if $u, v < 0$ in diamond A , *i.e.* in region R_3 . Similar reasoning shows that $h(x)$ is constant in the interior of each region R_i for $i = 1, \dots, 8$. Given that $h(x)$ is a ZEE it must satisfy (A.1) which implies the constants must be equal in magnitude in each region with alternating signs as one traverses the regions R_1 to R_8 in order. Therefore $h(x) = C \sum_{i=1}^8 (-1)^{i-1} \chi_i(x)$. The equation of motion, $\mathfrak{C}^{DD} h = 0$, then implies that $C = 0$.

A.2 Sum of Squares of Eigenvalues

A.2.1 $p \neq \frac{1}{2}$

The sum over all the positive and negative eigenvalues is

$$\sum_{\text{all modes}} \lambda_k^2 = \sum_{\text{cont.}} \lambda_k^2 + \sum_{\text{discont.}} \lambda_k^2, \quad (\text{A.3})$$

where the first sum on the right is over the continuous copy modes (\hat{f}_k, \hat{g}_k and their complex conjugates), and the second sum is over the discontinuous modes ($\hat{f}_k^{(p)}, \hat{g}_k^{(p)}$ and their complex conjugates). The sum over the continuous modes equals $2L^4$ [71]. As the eigenvalues come in positive and negative pairs the second sum equals twice

the sum over just the positive eigenvalues. Then

$$\sum_{\text{all modes}} \lambda_k^2 = 2L^4 + 2 \sum_{\substack{\text{pos.} \\ \text{discont.}}} \lambda_k^2 = 2L^4 + 2L^2 \left(\sum_{\substack{\text{pos.} \\ +}} k^{-2} + \sum_{\substack{\text{pos.} \\ -}} k^{-2} \right), \quad (\text{A.4})$$

where the last expression uses $\lambda_k = \frac{L}{k}$, and the sum over the positive eigenvalues of the discontinuous modes is split into two sums over $k > 0$ satisfying (4.45) with the “+” and “−” signs respectively.

The “+” sign in (4.45) gives the following transcendental equation for k :

$$((kL)^2 + 2) \cos(kL) + kL(2 + kL(1 - 2p)) \sin(kL) - 2 = 0. \quad (\text{A.5})$$

For $p \neq \frac{1}{2}$, equation (A.5) has both positive and negative roots with no degeneracy. One can verify that the set of negative roots of (A.5) is equal to the set of positive roots of (4.45) with the “−” sign chosen. This means that the last two sums in (A.4) can be written as a single sum over all roots (positive and negative) of (A.5), which we write as $\sum_i k_i^{-2}$.

Taylor expanding $\cos(kL)$ and $\sin(kL)$ about $k = 0$ in (A.5) gives

$$2(kL)^2 + (1 - 2p)(kL)^3 - \frac{3}{4}(kL)^4 + \mathcal{O}(k^5) = 0. \quad (\text{A.6})$$

We can think of (A.6) as an infinite degree polynomial, if we imagine continuing the expansion forever. We want to evaluate a sum over a particular power of the roots of this infinite polynomial. To do this we require a result from finite degree polynomials.

Expressing a polynomial of finite degree in terms of its roots,

$$\alpha_n x^n + \alpha_{n-1} x^{n-1} + \dots + \alpha_1 x + \alpha_0 = \alpha_n (x - x_1)(x - x_2) \dots (x - x_n), \quad (\text{A.7})$$

one can verify Vieta’s formulae. From these it is straightforward to show that

$$\left(-\frac{\alpha_1}{\alpha_0} \right)^2 - 2 \frac{\alpha_2}{\alpha_0} = \frac{1}{x_1^2} + \frac{1}{x_2^2} + \dots + \frac{1}{x_n^2}. \quad (\text{A.8})$$

Such formulae are extended in [79] to infinite polynomials such as (A.5). Dividing (A.6) by $(kL)^2$ gives

$$2 + (1 - 2p)kL - \frac{3}{4}(kL)^2 + \mathcal{O}(k^3) = 0, \quad (\text{A.9})$$

so that $\alpha_0 = 2$, $\alpha_1 = (1-2p)L$, and $\alpha_2 = -\frac{3L^2}{4}$, which gives $\sum_i k_i^{-2} = L^2(1-p(1-p))$. The sum of the squares of all the positive and negative eigenvalues of $i\Delta_p$ is then

$$\sum_{\text{all modes}} \lambda_k^2 = 2L^4 + 2L^4(1-p(1-p)) = 2L^4(2-p(1-p)) . \quad (\text{A.10})$$

This agrees with (4.34), which means that we have all the eigenfunctions of $i\Delta_p$.

A.2.2 $p = \frac{1}{2}$

The sum over the eigenvalues is again split into sums over the continuous and discontinuous modes. The sum over the continuous modes gives $2L^4$, as before, and the sum over the discontinuous modes can be written as twice the sum over the positive eigenvalues. Then,

$$\sum_{\text{all modes}} \lambda_k^2 = 2L^4 + 2 \sum_{\substack{\text{pos.} \\ \text{discont.}}} \lambda_k^2 = 2L^4 + 2L^2 \left(\sum_{\substack{\text{pos.} \\ f}} k^{-2} + \sum_{\substack{\text{pos.} \\ g}} k^{-2} \right) , \quad (\text{A.11})$$

where, in the last two sums, we have used $\lambda_k = \frac{L}{k}$ with $k > 0$ satisfying (4.40). The sum over the discontinuous modes is split into two sums over the eigenvalues of the $\hat{f}_k^{(\frac{1}{2})}$ and $\hat{g}_k^{(\frac{1}{2})}$ modes respectively.

Since the transcendental equation (4.40) for k is the same for the two sets of modes $\hat{f}_k^{(\frac{1}{2})}$ and $\hat{g}_k^{(\frac{1}{2})}$, the last two sums in (A.11) are equal. The transcendental equation is

$$(2 + (kL)^2) \cos(kL) + 2kL \sin(kL) - 2 = 0 . \quad (\text{A.12})$$

The roots of this equation come in positive/negative pairs of the same absolute value, and so the sum over the positive roots will be equal to half the sum over all the roots. Hence the last term in brackets in (A.11) is equal to a sum over all the roots of (A.12), which we write as $\sum_i k_i^{-2}$.

The Taylor expansion of (A.12) around $k = 0$ is

$$2(kL)^2 - \frac{3}{4}(kL)^4 + \mathcal{O}(k^6) = 0 . \quad (\text{A.13})$$

Dividing by $(kL)^2$ we find $\alpha_0 = 2$, $\alpha_1 = 0$ and $\alpha_2 = -\frac{3L^2}{4}$ and hence $\sum_i k_i^{-2} = \frac{3L^2}{4}$.

The sum over all the eigenvalues is then

$$\sum_{\text{all modes}} \lambda_k^2 = 2L^4 + 2L^2 \left(\sum_{\substack{\text{pos.} \\ f}} k^{-2} + \sum_{\substack{\text{pos.} \\ g}} k^{-2} \right) = 2L^4 + 2L^2 \sum_i k_i^{-2} = \frac{7L^4}{2}, \quad (\text{A.14})$$

which is equal to the right hand side of (4.34) with $p = \frac{1}{2}$.